FINGERPRINT RECOGNITION: A HISTOGRAM ANALYSIS BASED FUZZY C-MEANS MULTILEVEL STRUCTURAL APPROACH

Mohamed Ahmed Wahby Shalaby

A Thesis

in

The Department

of

Electrical and Computer Engineering

Presented in Partial Fulfillment of the Requirements

for the Degree of Doctor of Philosophy at

Concordia University

Montreal, Quebec, Canada

March 2012

CONCORDIA UNIVERSITY

SCHOOL OF GRADUATE STUDIES

This is to certify that the thesis prepared

By: Mohamed Ahmed Wahby Shalaby

Entitled: Fingerprint Recognition: A Histogram Analysis Based Fuzzy C-Means Multilevel Structural Approach

and submitted in partial fulfillment of the requirements for the degree of

DOCTOR OF PHILOSOPHY (Electrical & Computer Engineering)

complies with the regulations of the University and meets the accepted standards with respect to originality and quality.

Signed by the final examining committee:

_____ Chair
Dr. M. Elektorowicz

_____ External Examiner
Dr. D. Zhang

_____ External to Program
Dr. R. Ganesan

_____ Examiner
Dr. W.E. Lynch

_____ Examiner
Dr. M.N.S. Swamy

_____ Examiner
Dr. W-P. Zhu

_____ Supervisor
Dr. M.O. Ahmad

Approved by _____
Dr. J.X. Zhang, Graduate Program Director

April 20, 2012 _____
Dr. Robin A.L. Drew, Dean
Faculty of Engineering & Computer Science

ABSTRACT

Fingerprint Recognition: A Histogram Analysis Based Fuzzy C-Means Multilevel Structural Approach

Mohamed Ahmed Wahby Shalaby, Ph. D.

Concordia University, 2012.

In order to fight identity fraud, the use of a reliable personal identifier has become a necessity. Fingerprints are considered one of the best biometric measurements and are used as a universal personal identifier. There are two main phases in the recognition of personal identity using fingerprints: 1) extraction of suitable features of fingerprints, and 2) fingerprint matching making use of the extracted features to find the correspondence and similarity between the fingerprint images. Use of global features in minutia-based fingerprint recognition schemes enhances their recognition capability but at the expense of a substantially increased complexity. The recognition accuracies of most of the fingerprint recognition schemes, which rely on some sort of crisp clustering of the fingerprint features, are adversely affected due to the problems associated with the behavioral and anatomical characteristics of the fingerprints. The objective of this research is to develop efficient and cost-effective techniques for fingerprint recognition, that can meet the challenges arising from using both the local and global features of the fingerprints as well as effectively deal with the problems resulting from the crisp clustering of the fingerprint features. To this end, the structural information of local and global features of fingerprints are used for their decomposition, representation and

matching in a multilevel hierarchical framework. The problems associated with the crisp clustering of the fingerprint features are addressed by incorporating the ideas of fuzzy logic in developing the various stages of the proposed fingerprint recognition scheme.

In the first part of this thesis, a novel low-complexity multilevel structural scheme for fingerprint recognition (MSFR) is proposed by first decomposing fingerprint images into regions based on crisp partitioning of some global features of the fingerprints. Then, multilevel feature vectors representing the structural information of the fingerprints are formulated by employing both the global and local features, and a fast multilevel matching algorithm using this representation is devised.

Inspired by the ability of fuzzy-based clustering techniques in dealing more effectively with the natural patterns, in the second part of the thesis, a new fuzzy based clustering technique that can deal with the partitioning problem of the fingerprint having the behavioral and anatomical characteristics is proposed and then used to develop a fuzzy based multilevel structural fingerprint recognition scheme. First, a histogram analysis fuzzy c-means (HA-FCM) clustering technique is devised for the partitioning of the fingerprints. The parameters of this partitioning technique, i.e., the number of clusters and the set of initial cluster centers, are determined in an automated manner by employing the histogram of the fingerprint orientation field. The development of the HA-FCM partitioning scheme is further pursued to devise an enhanced HA-FCM (EAH-FCM) algorithm. In this algorithm, the smoothness of the fingerprint partitioning is improved through a regularization of the fingerprint orientation field, and the computational complexity is reduced by decreasing the number of operations and by increasing the convergence rate of the underlying iterative process of the HA-FCM

technique. Finally, a new fuzzy based fingerprint recognition scheme (FMSFR), based on the EHA-FCM partitioning scheme and the basic ideas used in the development of the MSFR scheme, is proposed.

Extensive experiments are conducted throughout this thesis using a number of challenging benchmark databases. These databases are selected from the FVC2002, FVC2004 and FVC2006 competitions containing a wide variety of challenges for fingerprint recognition. Simulation results demonstrate not only the effectiveness of the proposed techniques and schemes but also their superiority over some of the state-of-the-art techniques, in terms of the recognition accuracy and the computational complexity.

ACKNOWLEDGEMENTS

It is my pleasure to express my deep gratitude and thanks to my thesis supervisor Professor M.O. Ahmad for his continuous guidance and support throughout the course of this research. His valuable suggestions and positive responses have been very useful, and were among the major reasons that enabled me to pursue my research. I consider my experience with him, as my supervisor, a very rich one, from which I have learned a lot, and I would like to thank him especially for that.

Special thanks to my dear parents, who are the first inspiration for me in the field of research work. I am grateful for what they taught me about hard work and perseverance which are particularly essential in conducting research. I am grateful for their continuous support and prayers for me, which eased a lot of the hardships that faced. I would like to dedicate this thesis to the soul of my dear father who passed away months before finishing this work.

Special thanks are due to my dear wife and my dear kids for their patience and encouragement. I am also grateful for their continuous support and prayers for me. Actually, without their unlimited support I would not be able to pursue my work. Dear wife, there are no enough words to describe my appreciation for you.

I would like also to thank all my other family members, my friends and my colleagues who supported me and were always available in times of need.

I would like to thank the Egyptian government for their partial financial support of this research.

TABLE OF CONTENTS

List of Figures

List of Tables

List of Symbols

c	Number of clusters
c'	Pre-initial number of clusters
D	Set of effective sub-ranges of the orientation values
d_l	l^{th} effective sub-range
$FCOF$	Set of fuzzy clustered orientation field
FMR	False match rate
$FMFV$	Fuzzy-based multilevel feature vector
$FNMR$	False non-match rate
$FV1$	First- level feature vector, i.e., global features
$FV2$	Second-level feature vector, i.e., neighborhood features
$FV3$	Third-level feature vector, i.e., local features
HOF	Histogram of orientation field
I	Input template for recognition
$I_{\Re_j}$	j^{th} plain region of I^{th} fingerprint template
MFV	Multilevel feature vector
$Minu_i$	Minutiae set of i^{th} plain region
n	Number of data items (i.e., number of patterns)
$\mathbf{O}$	Orientation field matrix
$\mathbf{O}_q$	Quantized orientation field matrix
$\Re$	Set of decomposed regions
$\Re_i$	Multilevel feature vector of i^{th} plain region

$\Re_P$	Plain region
$\Re_{P\_Center}$	Geometrical center of a plain region
$\Re_S$	Singular region
S	Set of segments of orientation values
s_m	m^{th} segment of orientation values
T	Reference (i.e., stored) fingerprint template of a person
$T_{\Re_i}$	i^{th} plain region of fingerprint template T
U	Membership matrix of size $n \times c$
u_{ij}	Membership degree for pattern i with respect to cluster j
V	Set of cluster centers
v_j	Center of j^{th} cluster
$V(0)$	Initial set of cluster centers
$V'(0)$	Pre-initial set of cluster centers
X	Pattern vector of size n
x_i	i^{th} data item (pattern)
$\overline{X}$	Regularized data set
$\widetilde{X}$	Reduced data set
$\bar{x}_i$	Regularized data item
$\widetilde{x}_l$	l^{th} distinct orientation value in data set $\widetilde{X}$
Δ	Quantization step
Δ_l	Fuzzy-clustering step of the l^{th} plain region

ε_n Adaptive threshold parameter used in the stopping criteria of the iterative EHA-FCM algorithm.

ϕ_i Curvature of a i^{th} plain region

λ_l Number of blocks in an image having orientation value equal to $\widetilde{x}_l$

θ_{Core} Average orientation of the core region $\Re_{S_1}$

θ_i Orientation of i^{th} plain region

θ_{ij} Relative orientation of j^{th} plain region with respect to that of given i^{th} plain region

θ_{P-Core} Perpendicular orientation to θ_{Core}

θ_R Dominant direction of the fingerprint ridges contained in the image block

$\theta_{\Re-Core}$ Relative orientation of a region with respect to θ_{Core}

ρ_{ij} Relative position of geometrical center of j^{th} plain region with respect to that of given i^{th} plain region

ω_l Degree of belonging of the l^{th} plain region to its associated cluster

ξ Type and position of a region

ψ_r Belonging degree of r^{th} minutia to a plain region under consideration

List of Abbreviations

2D	Two dimensional
AFIS	Automatic fingerprint identification system
AFVS	Automatic fingerprint verification system
DORIC	Differences of the orientation values along a circle
EHA-FCM	Enhanced histogram analysis fuzzy c-means
ERR	Equal error rate
FAR	False acceptance rate
FCM	Fuzzy c-means
FCOF	Fuzzy clustered orientation field
FCOI	Fuzzy clustered orientation images
FCP	Fuzzy-based clustering problems
FCR	Fingerprint correct rate
FMC	Fuzzy-based measure of the correctness
FMFV	Fuzzy-based multilevel feature vector
FMLM	Fuzzy-based multilevel matching
FMR	False match rate
FMSFR	Fuzzy-based multilevel structural fingerprint recognition
FN	False negative
FNMR	False non-match rate
FP	False positive
FRR	False rejection rate
FVC	Fingerprint verification competition

HA	Histogram analysis
HA-FCM	Histogram analysis fuzzy c-means
ID	Identification
MFV	Multilevel feature vector
MLM	Multilevel matching
MR	Magnetic resonance
MSFR	Multilevel structural fingerprint recognition
OF	Orientation field
OMC	Oriented minutia code
PIN	Personal identification number
RDRHA-FCM	Reduced-data regularized histogram analysis fuzzy c-means
RHA-FCM	Regularized histogram analysis fuzzy c-means
ROC	Receiver operating characteristic
SP	Singular point
SVM	Support vector machine
TP	True positive

CHAPTER 1

Introduction

In recent years, the use of personal identification/authentication to fight identity fraud has become one of the most important problems to be solved using automated systems. It is quite important to make the computer to be able to achieve successful answers to the questions "Who is she/he?" or "Does this person have the claimed identity?". Personal identity could be verified using different methods such as username and password, personal identification number (PIN), personal cards with photos (e.g. medical card and driving license) and biometric (body) measurements such as, face, iris, signature, and fingerprints. The personal identities that do not depend on the body measurements may be stolen or shared. Moreover, it is very unlikely and theoretically impossible that two persons would have the same body measurements.

The biometric measurements have been used for criminal investigations and personal identification for quite some time. Among all the known body measurements, human fingerprints have been found to be one of the most distinctive personal identifiers [1]. This fact shows the importance of using human fingerprints as a universal identifier.

1.1 Fingerprint Based Biometric Systems

A *biometric recognition system* makes use of the *anatomical* characteristics, e.g. fingerprints, face, and palmprint of a human being, or the *behavioral* characteristics, e.g. handwriting, signature, and voice, for manually or automatically recognizing individuals.

These characteristics are called *biometric identifiers*, or simply biometrics. Figure 1.1 shows a few typical examples of biometrics. In Figure 1.1(a), two examples of anatomical characteristics have been shown, which are a fingerprint and palmprint. In addition, Figure 1.1(b) shows two examples of behavioral characteristics, which are a signature and voice. Some of the biometrics may be considered as a combination of anatomical and behavioral characteristics. For example, even though a fingerprint is considered as an anatomical characteristic in nature, the usage of the input device to capture it (e.g., how a user presents a finger to the fingerprint scanner) depends on the person's behavior.

(a) (b)

Figure 1.1: Examples of the biometrics (a) anatomical (fingerprint and palmprint) and (b) behavioral biometrics (signature and voice) [1, 2].

In order for a biometric measurement to be chosen as an identifier, it should satisfy the following requirements: universality, distinctiveness, permanence and ease of collectability. A biometric system to be considered as a practical recognition system, there are a number of issues that should be addressed [1]:

- *Performance;* It refers to the achievable recognition accuracy, the response time, and the resource requirements. It is noted that the operational and the environmental factors affect the performance metrics.

- *Acceptability*; It indicates the extent to which individuals are willing to accept a particular biometric identifier in their daily lives.
- *Circumvention;* It refers to the simplicity to deceive the system by fraudulent methods.

The fingerprint, which is a graphical ridge/valley pattern of a human finger, has been found to be the most suitable biometric for the personal identification applications. This has been supported by a comparative study of different human biometric measurements with respect to the above requirements [1]. This study shows that among the various human biometric measures, fingerprint is the one that has a good compromise among all the desirable features:

- *Universality;* The majority of the population has legible fingerprints.
- *Distinctiveness;* It has been found that, each person has his/her own distinctive fingerprint. Even the identical twins can be identified successfully based on their fingerprints; meanwhile some other biometrics such as the face would fail.
- *Permanence;* Fingerprints are formed during the fetal stage and remain structurally unchanged throughout the life of a person.
- *Collectability*; Fingerprint can be collected easily and measured quantitatively.
- *High Performance*; The fingerprint recognition systems are able to achieve a higher accuracy compared to other biometric systems.

Since the fingerprint recognition system can be viewed as a pattern recognition system, the system should be designed to be capable of extracting salient features from fingerprints and matching them in a robust way [1]. Based on the application, a

fingerprint recognition system may be classified as either an automatic fingerprint *verification* system (AFVS) or an automatic fingerprint *identification* system (AFIS). The AFVS conducts a one-to-one comparison to verify the claimed identity, whereas the AFIS conducts one-to-many comparisons to establish the identity of the individual. Fingerprint representation, i.e., the feature extraction and template formulation, and fingerprint matching are considered to be the core modules of an automated fingerprint recognition (verification/identification) system. These two modules are the most expensive parts, in terms of the computational complexity, within the system. Therefore, these two modules need to be designed as simple as possible in order to achieve the required accuracy at a reasonable cost. Based on the information (features) associated with the fingerprint's ridge/valley pattern of a human finger, a template could be formulated to represent the fingerprint. These features are traditionally categorized as the global features, such as ridge orientations, and the local features, such as minutiae and pores [1, 3–8]. It has been found that the local features (minutiae) provide highly distinctive information about the fingerprint. Therefore, they have been traditionally used for fingerprint representation and matching [1]. On the other hand, the global features have been used generally for the fingerprint image enhancement at the preprocessing stage [9], for classification (indexing) of fingerprints [10–13] and for fingerprint image partitioning [14].

1.2 Challenges in Fingerprint Recognition

Despite decades of a research work in the fingerprint recognition problem, it is still considered as a challenging and important pattern recognition problem to be solved [1]. In order to have the best and accurate results (especially for criminal cases), we still have

to depend on the opinion of a human expert, which makes the process rather expensive. Hence, there is still a compelling need to have an efficient and inexpensive automated fingerprint recognition system with acceptable recognition accuracy.

As mentioned earlier, a fingerprint is considered to have a combination of the anatomical and behavioral characteristics of the person in a question. Even though the ridge/valley structure and minutiae distribution are the unique identifier of a person, the extraction of this information, and therefore the recognition/identification becomes challenging, since the fingerprints of the person are affected due to his/her anatomical and behavioral characteristics. Furthermore, the requirements (e.g. the accuracy and the time limit) and the working conditions (e.g. the scanner capability and the storage limit) of the fingerprint applications pose additional challenges. For example, a door lock system should be able to provide a very high accuracy with a short response time, while using a small area scanner with a limited space of the storage.

The challenges in fingerprint recognition could be categorized as follows:

1) **Challenges due to behavioral characteristics**
   a) **Incomplete and rotated fingerprint images:** This situation arises due to the person's lack of experience in using fingerprint scanners; or from the fingerprint images received from the crime scenes.
   b) **Poor quality fingerprint image:** The fingerprint images with low quality are mainly due to the capability of the input device, the pressure of the fingertip on the input device or the condition of the skin.
   c) **Deformation of the fingerprint ridges**: The fingerprint images of the same person may have some differences in their ridge thicknesses or shapes, which is

mainly due to different forces by the same person's finger against the input device.

Due to the above mentioned behavioral-based problems, the fingerprint images taken from the same finger may sometimes look quite different, which is known as intra-class variability. Figure 1.2 contains six images represent the same fingerprint with different qualities, rotation angels and portions of this finger. It is seen from this figure that it is very difficult to decide whether all these images represent the same finger or not.

Figure 1.2: Six images represent the same fingerprint with different qualities, rotation angels and portions of this fingerprint.

2) Challenges due to anatomical characteristics

a) Distortion of the fingerprint ridges: Some changes of the fingerprint ridges shapes due to some natural life events, such as cuts and burns.

b) **Inter-class similarity:** The fingerprints from different fingers may appear naturally quite similar.

3) **Challenges due to application requirements**

a) **Fingerprint template size:** Some fingerprint applications, such as door lock, have a limitation on the storage space. Accordingly, it is a challenge to formulate a suitable template to represent the fingerprint image within the determined size.

b) **Response time:** The response time of a fingerprint recognition system consists mainly of scanning of the image, pre-processing, representation and matching modules. Some recent fingerprint applications to be accepted by the customers, such as banking systems, require a very short response time.

1.3 Existing Schemes of Fingerprint Recognition: A Literature Review

Over the last forty years, the majority of fingerprint recognition schemes have been developed based on the matching of the local features of the extracted minutiae. Despite the highly distinctive feature and storage efficiency of minutiae, it is extremely difficult to extract and represent them accurately. This difficulty which arises mainly due to the anatomical and behavioral-based challenges mentioned in Section 1.2, affects on the overall performance of the fingerprint recognition scheme. In order to overcome the problem of the effect of the inaccurate minutia extraction on the fingerprint recognition accuracy, a number of fingerprint recognition schemes have recently been proposed. These techniques can be classified into two broad categories: 1) the techniques that are based on the local and global features of minutiae, and 2) those that are based on the global structure of the fingerprint ridge pattern and the local minutiae features.

1.3.1 Techniques based on the local and global features of minutiae

Originally, the minutiae-based fingerprint recognition schemes used only the local attributes of the minutiae (i.e., position, direction, and type) for fingerprint representation and matching. In view of the above mentioned anatomical and behavioral-based challenges, the use of these local minutiae attributes is not reliable enough. Therefore, the main idea in the first category is in devising a minutia descriptor in which the local minutiae attributes are combined with some global minutiae features. Accordingly, the fingerprint representation based on this descriptor should be more immune than the traditional minutia descriptors against some of the above mentioned challenges. In the following, some of the recently developed schemes based on this idea are reviewed.

a) Willis and Myers [15] investigated the development of a robust algorithm allowing a good recognition of low-quality fingerprints with inexpensive hardware. They proposed a new approach called a *wedge ring overlay minutia* detector that is particularly robust to imperfections. The main drawbacks for this scheme are: 1) The fingerprint images have to be enhanced prior to the representation. 2) There is a high degree of computational complexity associated with their feature extraction algorithm.

b) Ceguerra and Koprinska [16] proposed a new approach for combining minutia's local and global features by using the matched local features as the reference axis for generating shape signature as a global feature. The dependence on minutiae to generate a shape signature is the main weakness of the approach.

c) Tico and Kuosmannen [17] proposed a new representation for the fingerprint minutiae, which consisted of the local minutiae attributes and a local orientation-based minutia descriptor. The proposed minutiae descriptor matching fails when two minutiae

are close to each other, since their descriptors in this case would be very similar. In addition, this technique has a high computational complexity especially when the number of minutiae is large.

d) Qi et al. [18] modified the minutia descriptor proposed in [17] by using the curvature map instead of using the orientation field in constructing the minutia descriptor. They have shown that their scheme provides a higher accuracy than that provided by the scheme of [17]. However, this scheme has even higher computational complexity resulting from the curvature map construction.

e) Jea and Venu [19] presented an approach that uses localized secondary features derived from the relative minutiae information. Due to the nature of minutiae distribution inside the fingerprint images, this secondary feature might misinform the matcher.

f) Jia *et al.* [20] proposed an improved fingerprint matching technique using both the weighting method and the support vector machine (SVM). A new weighting feature based on the distance between minutiae is introduced to supplement the minutiae information. A pre-processing stage of image enhancement to reduce the possibility of detecting the false minutiae is required. Therefore, the proposed technique requires a high computational complexity.

g) Feng [21] has proposed a combination of two different minutiae descriptors. The two descriptors that have been used are a texture-based descriptor and a minutiae-based descriptor, to provide more accurate matching results. In [22] a genetic algorithm for fingerprint matching has been developed based on the modification of these

descriptors. Both the schemes require a high computational complexity for fingerprint representation.

From the above review it is seen that the fingerprint recognition schemes, which are based on the use of a minutia descriptor in which the local minutiae attributes are combined with some global minutiae features, were always able to achieve a higher accuracy than that provided by the traditional only minutiae-based schemes. The main drawback of the algorithms in this category is that since the fingerprint recognition schemes are totally dependent on the extracted minutiae, a false extraction of a minutia (i.e., spurious minutia) may greatly affect the recognition accuracy. Consequently, some of these schemes have used a pre-processing stage of image enhancement to reduce the possibility of detecting the spurious minutiae [15], [17], [18], [20].

1.3.2 Minutiae features combined with global fingerprint features

Researchers in the fingerprint recognition community have recently started paying attention to the use of some distinct characteristics of the fingerprint global features that traditionally belonged only to the domain of fingerprint classification and indexing [23–35]. The main reasons for looking for some distinguishing features of the fingerprint other than the minutiae are as follows: 1) A reliable detection of minutiae is difficult in poor-quality fingerprint images, especially without the use of a pre-processing step for image enhancement. 2) The formulation of a robust minutia descriptor is a time-consuming process. 3) The use of additional information gathered from the global features in conjunction with the local minutiae features might increase the recognition accuracy and robustness. Even though the global features of the fingerprint ridge pattern, such as ridge orientation and frequency, ridge shape, and texture information, may be

extracted more reliably than minutiae, their distinctiveness is generally lower than the minutiae attributes. Accordingly in the second category of fingerprint recognition schemes, fingerprint recognition is carried out based on the use of both the local minutiae features and the global features for fingerprint representation and matching. In the following, some of these schemes are reviewed.

a) Jain *et al*. [23] proposed a filter-based algorithm that uses a bank of Gabor filters to capture both local and global details in a fingerprint as a compact fixed-length FingerCode [13]. This technique is suitable for matching as well as storage on a smartcard. They have shown that the matching performance can be improved by combining the decisions of the matchers based on complementary (minutiae-based and filter-based) fingerprint information. This technique has some limitations, such as, the reference point localization and the recourse to the fingerprint pre-alignment stage. Accordingly, it is not suitable for poor quality and incomplete fingerprint images.

b) Ross *et al.* [24, 25] have developed a hybrid fingerprint matching scheme that uses both the minutiae and a ridge texture map. First of all a set of local minutiae features are extracted from the fingerprint image. This minutiae feature vector is used for estimating the transformation parameters, which are required to align the ridge feature maps of the two fingerprint images. Therefore, in order to avoid the effect of spurious minutiae, a fingerprint enhancement step is necessary, thus adding to the processing time. Unfortunately, the proposed technique has not been tested using a benchmark database.

c) Krivec *et al.* [26] proposed a method, which due to its compressibility, can be applied in memory constrained environments. This is important for applications, such as smartcards and independent identification modules, which have recently gained

popularity. The hybrid fingerprint matchers are well known as a powerful tool for high-security applications, where the reliability of a single fingerprint characteristic is not high enough for intended applications. The proposed method uses minutia point matcher as the first stage of matching and after successfully completing this stage, a second stage of matching is carried out based on the homogeneity of the direction map of the reference image. The direction map is compressed using a quad tree. However since, the method depends on the minutiae features as a first stage of matching, so it fails if many false minutiae have been detected.

d) Jinwei et al. [27] have proposed the use of a model-based fingerprint orientation field, as a global feature, in combination with the extracted minutiae set for the matching purpose. For the global feature, two different model-based orientation fields have been used. The first one is suitable when the singular point is detected. The second one, which is a modified model, is more useful in situations when there is a difficulty in detecting the singular points. Unfortunately, the latter one does not perform as well as the former one at the regions around the singular points. In either case, the final matching score is obtained by combining results from the local and global matchers. The results have been presented to show that the use of the two matchers provides higher recognition accuracy. However, the scheme suffers from a high computational complexity, due to the use of model-based orientation field, and the need of performing a pre-alignment step before the matching step.

e) Shi *et al.* [28] proposed a fingerprint representation, in which the information about the singular point has been combined with its neighborhood minutiae. In this scheme, the computational complexity of the matching has been reduced since the

number of candidate minutiae required for identification has been decreased. This approach assumes the existence of singular points (especially the core point), thus it is not suitable for fingerprint images without a detected core pint.

f) Nanni and Lumini [29] have presented a hybrid wavelet-based fingerprint matcher, with the need to perform an enhancement step before the extraction of minutiae set, and to do a pre-alignment step before applying a 2D wavelet transform on the image's sub-windows. Since the method depends on an accurate extraction of the minutiae set to perform a pre-alignment step, it would fail in the cases of poor-quality or incomplete fingerprint images.

g) Benhammadi *et al*. [30], based on the reuse of the FingerCode technique [13], have proposed a new hybrid fingerprint matching technique, which depends on the minutiae texture maps. This method has essentially three drawbacks: (i) This approach consumes more time in the enrolment and matching processes. (ii) Since each minutia has its own oriented minutia code (OMC) feature vector, this requires a large template size compared with the original FingerCode method. (iii) The recognition accuracy of this method is affected by the presence of spurious minutiae.

It is seen from the above review that the idea of combining local feature (minutiae) with the global fingerprint features is a promising methodology and helpful to overcome the problems associated with the minutia-based techniques. Furthermore, it is also seen from this review that the choice of the global feature(s) is crucial and has a significant impact on the overall performance of the fingerprint recognition scheme [23–34]. This has also been supported by a comparative study of the impact of combining multiple features on the recognition accuracy [35]. This study has concluded that a larger

improvement can usually be obtained as more features are combined; however, a combination of more than four features results only in a marginal performance improvement [35].

1.4 Research Objectives and Approach

The use of both the local and global features of a fingerprint in a technique of the either category described above for fingerprint recognition is quite useful in solving the problems that arise from the behavioral and anatomical characteristics such as ridge pattern deformation, translation and/or rotation, incomplete fingerprint, etc., of fingerprints. However, there is set of other problems that arise from the basic idea of using both the local and global features of a fingerprint in fingerprint recognition techniques: 1) The usage of fingerprint's global and local features necessitates a larger template to represent a fingerprint, especially for techniques using complicated minutia descriptor. 2) The extraction and usage of the global features makes the overall computational complexity of the technique high. 3) Most of these techniques require a step of pre-alignment, which depends mainly on the minutiae, prior to carrying out the matching process. Thus, a technique requiring such a pre-alignment suffers from the effect of the spurious minutiae. Further, most of the fingerprint recognition schemes rely on some sort of crisp clustering of the fingerprint features. The recognition accuracies of such schemes are adversely affected for fingerprints with behavioral or anatomical characteristics.

The objective of this research is to develop efficient and cost-effective techniques for fingerprint recognition that can meet not only the challenges arising from using both the local and global features of the fingerprints but also deal effectively with the

problems resulting from the crisp clustering of the features when the fingerprints are marred with the behavioral or anatomical characteristics. To this end, the structural information of local and global features of fingerprints are used for their decomposition, representation and matching in a multilevel hierarchical framework. The problems associated with the crisp clustering of the fingerprint features are also addressed in this thesis by incorporating the ideas of fuzzy logic in developing the various stages of the proposed fingerprint recognition scheme.

1.5 Organization of the Thesis

The thesis is organized as follows.

In Chapter 2, the background material necessary for the work undertaken in this thesis is presented. The main parts of the fingerprint recognition systems, the performance metrics, and the benchmark databases used for examining the performance of fingerprint recognition systems are discussed. The fuzzy clustering techniques and their important role in the pattern recognition field are also briefly discussed.

In Chapter 3, the first stage of the proposed multilevel structural approach for fingerprint recognition, i.e., the decomposition of the fingerprint image into regions using the global features, is developed. In this chapter, the traditional crisp techniques for both singular point detection and partitioning of the orientation field are used. The proposed multilevel structural scheme for fingerprint representation and matching is then presented in Chapter 4. A multilevel feature vector is first formulated by employing the structural information of the local and global features of each region with a view of obtaining a fingerprint representation that is less variant to the displacement, rotation and deformation of the fingerprint ridges. Next, a fast multilevel matching algorithm, in

which the correspondence problem is dealt with by making use of the global features and the similarity problem is taken care by employing both the global and local features, is devised.

In Chapter 5, the idea of fuzzy logic to cluster the fingerprint features is introduced in order to overcome the limitation of crisp clustering in effectively dealing with the problems arising from the behavioral and anatomical characteristics of fingerprints. A new fingerprint partitioning scheme based on the fuzzy c-means clustering technique is developed. In this technique, the number of clusters and the set of the initial cluster centers are determined in a rational and automated manner through an analysis of the orientation field histogram. Moreover, by using this fuzzy-based partitioning scheme, a new technique for detecting the singular points of the fingerprint is developed. In this technique, singular points are determined by certain cluster distributions that characterize different types of singular points. In Chapter 6, the fuzzy-based partitioning scheme is further modified in order to enhance the smoothness of the fingerprint partitions and to reduce the computational complexity. In Chapter 7, this enhanced partitioning scheme is then used to develop a fuzzy-based fingerprint recognition scheme relying on the basic ideas of the multilevel structural scheme presented in Chapters 3 and 4. Finally, Chapter 8 concludes the thesis by summarizing the research work undertaken in this thesis and highlighting the contributions made.

CHAPTER 2

Background Material

2.1 Introduction

In this chapter, the required background material for the work undertaken in this thesis is presented. In Section 2.2, the different types of fingerprint recognition systems are first described. In Section 2.3, the main modules of these recognition systems, namely fingerprint representation and matching, are discussed in details. In Section 2.4, the most important metrics to measure the performance of fingerprint recognition systems are presented. In order to examine and compare the performance of a fingerprint recognition system there is a need to use a benchmark fingerprint database; in Section 2.5 some of the benchmark fingerprint databases, used in the literature, are reviewed. Finally, in Section 2.6, the fuzzy clustering techniques and their important role in the pattern recognition field are briefly discussed.

2.2 Automated Fingerprint Verification/Identification Systems

As mentioned in chapter 1, a fingerprint recognition system may be classified as either an automatic fingerprint *verification* system (AFVS) or an automatic fingerprint *identification* system (AFIS) as specified below:

(i) The *verification* system (AFVS) authenticates a person's identity by comparing the captured biometric characteristic with the person's own biometric template(s), which are pre-stored in the system. AFVS conducts a one-to-one comparison to

determine whether the identity claimed by the individual is true. Accordingly, a verification system accepts the person's request as a genuine template, or rejects it as an imposter template.

(ii) The *identification* system (AFIS) recognizes an individual by searching the entire templates database for a match. Therefore, AFIS conducts one-to-many comparisons to establish the identity of the individual. Accordingly, the identification system accepts the person's request as a genuine template if a match has been found; otherwise the request will be rejected as an imposter template.

For either system there is an important common operational mode:

- Enrollment mode: to insert a new identity template for a new person in the system's database as shown in Figure 2.1(a). This enrollment mode is required once at the time of system installation (e.g. Airport security check) or once for each new identity registration (e.g. Bank system).

The verification task is responsible for verifying individuals at the point of access. During the operation phase the personal ID is required to be entered. As shown in Figure 2.1(a, b), an automatic fingerprint verification system (AFVS) consists mainly of four modules:

- Data Acquisition: By which the fingerprint image is acquired in a digital format using a biometric sensor, such as a scanner.
- Pre-processing: Sometimes it is required to apply some pre-processing algorithms (e.g. noise rejection, edge enhancement). In fact, the need for this step depends mainly on the quality of the acquired fingerprint images; which

is affected by the scanning process and the surrounding working environment. Therefore, some AFVS dose not need the pre-processing step.

- Feature Extraction: to extract the required salient features from a fingerprint image, and to formulate the template (to enroll or to verify).
- Matching: to compare the extracted fingerprint template against the reference template retrieved from the system database based on the entered personal ID. Accordingly, it makes a final decision (matched or non-matched).

Although, an automatic fingerprint identification system (AFIS) also consists of the same four modules mentioned above, the difference between AFIS and AFVS is in the matching module. In the identification task, no personal ID is provided and the system compares the extracted fingerprint template against all reference templates of the personal identities enrolled in the system database. Therefore, the AFIS matching module conducts a one-to-many comparison to establish the identity of the individual, as shown in Figure 2.1(c). In the case of the identification systems with large databases, the AFIS matching module is computationally expensive. Thus, the fingerprint classification and indexing techniques are often deployed to limit the number of templates that have to be matched against the input [1].

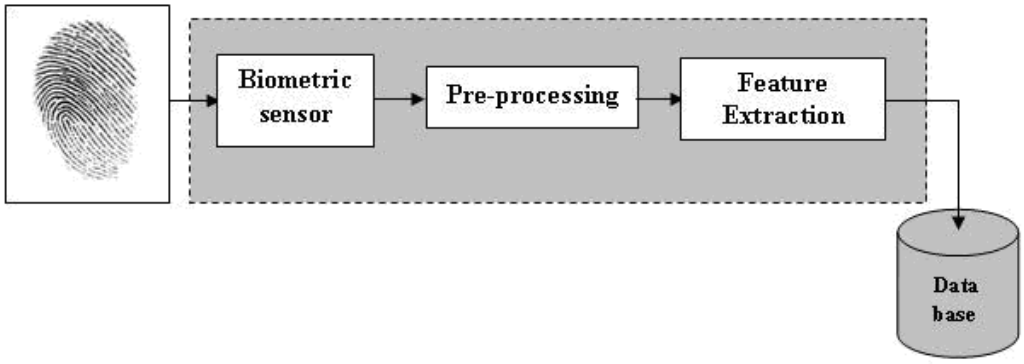

(a)

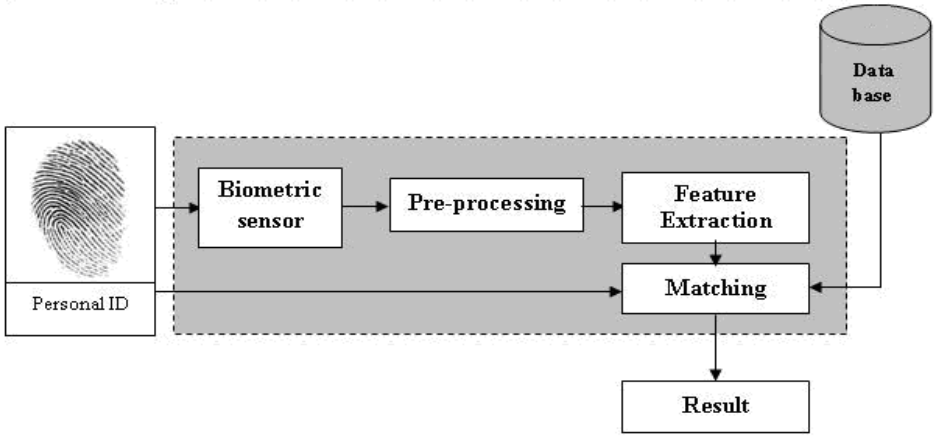

(b)

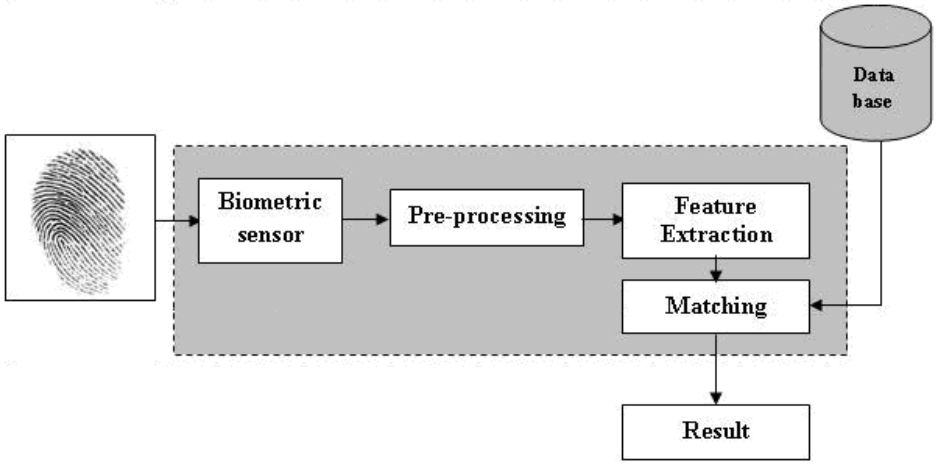

(c)

Figure 2.1: General architecture for the main parts of the fingerprint recognition system (a) Enrollment operation, (b) Verification operation, and (c) Identification operation.

2.3 Fingerprint Representation and Matching

Fingerprint representation, i.e. the features extraction and template formulation, and fingerprint matching are considered the core modules of the automated fingerprint recognition (verification/identification) systems. Since these two modules are the most complicated parts within the system, they have to be designed as perfect as possible in order to meet the performance requirements of an automatic fingerprint recognition system.

2.3.1 Fingerprint representation

The importance of the fingerprint representation module arises from two facts: First, the original fingerprint images can not be saved directly in the system database, since it requires a large amount of storage space. Second, the objective in devising a suitable fingerprint representation is to provide a high accuracy in fingerprint recognition with a reasonable complexity, i.e. the fingerprint matching module could be simplified without affecting the accuracy of the matching results based on a suitable method to represent a fingerprint image in the system database. Thus, the problem of fingerprint representation is to determine a measurement (feature) space, in which fingerprint images taken from a specific finger form a compact cluster different from those of other fingers from the stand point of these features.

The fingerprints are the graphical ridge/valley patterns of human fingers; hence a fingerprint is mainly represented by using the information (features) associated with its ridges. These features are traditionally categorized as the global features and the local features. Normally, for these features (known as the feature vector) to be considered as a suitable representation of a fingerprint, they need to satisfy the following requirements:

1. *Saliency:* the feature vector should represent distinctive information about the fingerprint.
2. *Extractability:* these features can be easily detected.
3. *Compactness:* the feature vector could be stored in a compact form (to save the storage space)
4. *Usefulness:* the feature vector should to be formulated such that it becomes useful for the matching step.

- ***Global Features***

The global features represent the overall ridges pattern. As shown in Figure 2.2, the pattern of the ridges flow of the fingerprint has a smooth curvature everywhere, except nearby some regions which are called singular regions. In addition, the density of the ridges varies based on their locations with respect to theses singular regions. Based on these different characteristics of the ridge pattern, many global features have been defined to be used for fingerprint recognition systems as follows:

1. **Singular points**, called loop and delta, are a sort of control (reference) points around which the ridge lines are wrapped [1]. It has been found that, the human fingerprint has at most four singular points (i.e. two loops and two deltas), as shown in Figure 2.2, or at least one singular point which is the upper loop (the core). Since there are many different fingerprints that contain the same singular points topology, this feature is not sufficient for verification or identification purposes. Nevertheless, this feature is helpful as it is used to prealign fingerprint images that need to be matched. In fact, most of the matching algorithms need a pre-alignment step. Usually, the pre-alignment

depends on the core point as a center reference point. Another popular use of fingerprints' singular points is to determine the fingerprint category (i.e. fingerprint classes) as shown in Figure 2.3.

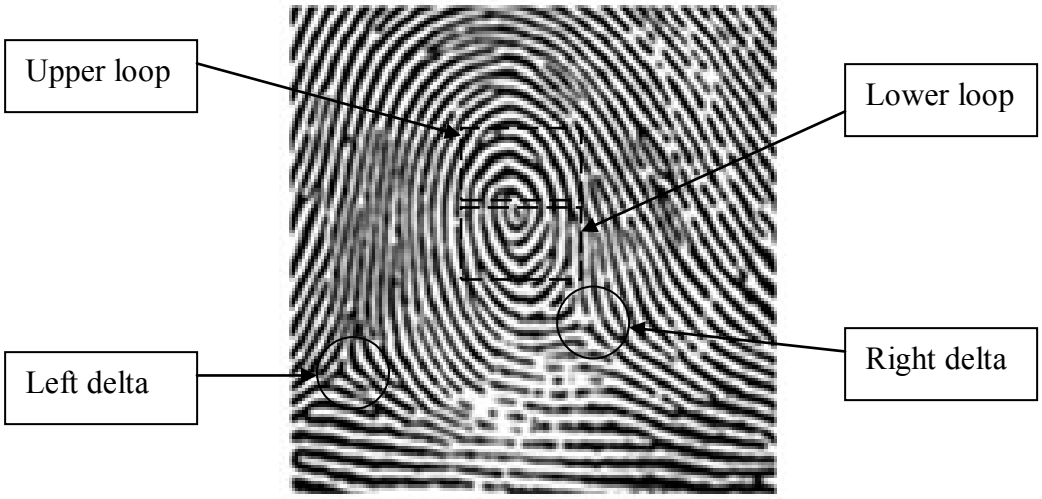

Figure 2.2: Fingerprint image shows the different global features.

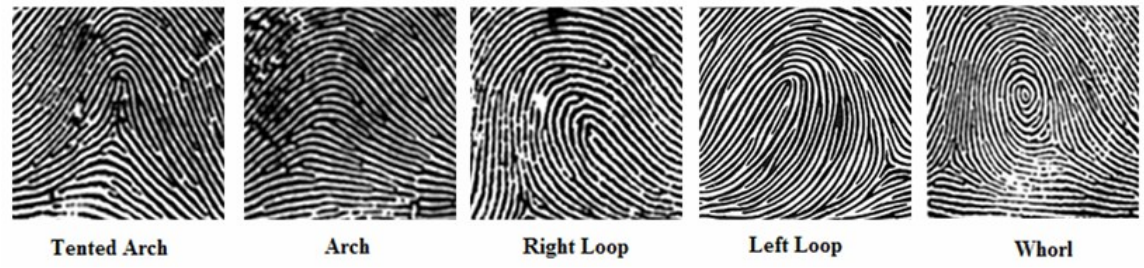

(a) (b) (c) (d) (e)

Figure 2.3: Fingerprint patterns as they appear at a coarse level: (a) tented arch, (b) arch, (c) right loop, (d) left loop, and (e) whorl.

2. **Local ridge orientation**, which is known as the orientation field or the directional image of the fingerprint (Figure 2.4). There are many techniques have been proposed to calculate the local ridge orientation [1]. The most natural approach for estimating the local ridge orientation is based on the computation of gradients in the fingerprint image [36]. In practical, a ridge orientation value is calculated for each block of size $N \times N$. Each block is

assigned an orientation value θ_R in the interval [0,π) that corresponds to the most dominant direction of the ridges contained therein. The orientation values are calculated with respect to the horizontal border of the image (2.1). The orientation field **O** can then be considered as a matrix whose $(k,l)^{\text{th}}$ element represents the orientation value of the $(k,l)^{\text{th}}$ block.

$$\theta_R = \frac{1}{2}\tan^{-1}\left(\frac{\sum_{i=1}^{N}\sum_{j=1}^{N} 2\, G_x(i,j)\, G_y(i,j)}{\sum_{i=1}^{N}\sum_{j=1}^{N}(G_x(i,j)^2 - G_y(i,j)^2)}\right) \tag{2.1}$$

where $G_x(i,j)$ and $G_y(i,j)$ are the values of the gradients at pixel (i,j) in the x and y directions, respectively, using 3×3 Sobel mask.

3. **Local ridge frequency,** which is known as the frequency image or the ridge density map of the fingerprint (Figure 2.5) [9, 37]. The local ridge frequency of the $(k,l)^{\text{th}}$ block is defined as the number of the ridges per unit length along a segment orthogonal to the local ridge orientation θ_R [1]. It has been noticed that, the ridge density varies across different parts of the same fingerprint (Figure 2.5). In addition, different fingerprints have been found to have naturally different ridge density maps [1].
4. **Local ridge curvature,** which is known as the curvature map of the fingerprint (Figure 2.6). Qi et al [18, 38] have been proposed the use of the orientation field of the fingerprint image to construct the curvature map. The curvature of the $(k,l)^{\text{th}}$ block is defined as the half of the difference between

the orientations of the two neighboring blocks to which the direction of the $(k,l)^{\text{th}}$ block.

The global features of the fingerprint, especially the first three global features, have been traditionally used for image enhancement at a preprocessing stage [9], for classification (indexing) of fingerprint [10–13], for fingerprint image partitioning [14], and for singular points detection [39–40]. Even though, the global features of the fingerprint are not considered as a completely distinctiveness features, they might be used with the local features to enhance the accuracy of the fingerprint matching, as mentioned in Section 1.3.

Figure 2.4: Fingerprint and its orientation image.

Figure 2.5: Fingerprint and its frequency image [37].

Figure 2.6: Fingerprint and its curvature map and the orientation image [18, 38].

- ***Local Features***

The local features represent the small details of the ridges, which normally can not be seen by the human eyes. These features have been reported as the highest distinctiveness characteristics of the fingerprint [1]. Traditionally, the local ridge characteristics, called minute details (shortly called *minutiae*), are widely used for the fingerprint representation and matching. These small details are found to remain in the fingerprint pattern unchanged over an individual's lifetime [1]. The two most prominent *minutiae* are: *ridge ending* and *ridge bifurcation* (see Figure 2.7). A ridge ending is defined as the ridge point where a ridge ends abruptly. A ridge bifurcation is defined as the ridge point where a ridge forks or diverges into branch ridges. The FBI minutiae coordinate model considers only termination and bifurcations: each minutia is denoted by its type, the x and y coordinates and the angle between the tangent to the ridge line at the minutia position and the horizontal axis [1]. The minutiae can be extracted, in general, either through a binarization process of the fingerprint ridges or directly from the gray-scale fingerprint image [1].

Figure 2.7: Minutiae types: Ridge endings and ridge bifurcations.

2.3.2 Fingerprint matching

The process of fingerprint matching is to compare the fingerprint templates by using a set of similarity measures of the corresponding features in these templates. And thus the matching scheme returns a score between 0 and 1 representing the degree of similarity between the two fingerprint images, or a binary score of 0 or 1 indicating whether or not the fingerprint under consideration is the same as the reference fingerprint. The accuracy of the final decision and the response time are the two main concerns of a matching scheme. However, the requirements on the degree of accuracy and the response time of a matching scheme vary from one application to another. Although this matching process seems easy to do, it is an extremely difficult problem to solve due to the challenges associated with the behavioral and anatomical characteristics of fingerprints.

2.4 Performance Metrics

Each fingerprint application has its own requirement. Examples of such requirements are the degree of accuracy required, and the speed of the system's response. Thus, practical

performance requirements of a biometric system are very much application dependent. Three main factors are used in evaluating the performance of a fingerprint recognition system:

1- Fingerprint system's decision accuracy, i.e., the recognition accuracy.

2- The computational complexity of the feature extraction, template formulation and matching modules.

3- The size of the resultant features vector (i.e., template), and whether this template has a fixed or variable size.

In order to measure the decision accuracy of the fingerprint recognition system, the fingerprint verification problem is defined as follows [1]. Let the stored fingerprint template of a person be represented with T, and the acquired input for recognition be represented with I. Then the null and alternate hypotheses are:

$H_0 : I \neq T$, input I is not from the same person as the original template.

$H_1 : I = T$, input I is from the same person as the original template.

The associated decisions are:

D_0 : The person is not who she/he claims to be.

D_1 : The person is who she/he claims to be.

The verification involves matching T and I using a similarity measure $S(T, I)$. If the matching score is less than the system threshold t, then decide D_0, else decide D_1. Accordingly, the testing formulation inherently contains two types of errors:

Type A: false match (D_1 is decided when H_0 is true);

Type B: false non-match (D_0 is decided when H_1 is true).

False match rate (FMR) is the probability of type A error (also called *false acceptance rate* (FAR)); and false non-match rate (FNMR) is the probability of type B error (also called *false rejection rate* (FRR)):

$$FMR = p(D_1 \mid H_0 = true) \tag{2.2}$$

$$FNMR = p(D_0 \mid H_1 = true) \tag{2.3}$$

In order to evaluate the accuracy of a biometric system, scores generated from a number of fingerprint pairs from the same finger are to be collected (the distribution $p(s \mid H_1 = true)$ of such scores is traditionally called *genuine distribution*). In addition, scores generated from a number of fingerprint pairs from different fingers also need to be collected (the distribution $p(s \mid H_0 = true)$ of such scores is traditionally called *impostor distribution*). Figure 2.8 graphically illustrates the computation of FMR and FNMR over genuine and impostor distributions. From the drawing, it is evident that FMR is the percentage of impostor pairs whose matching score is greater than or equal to the threshold t, and FNMR is the percentage of genuine pairs whose matching score is less than t [1]. Another important error measure of the system performance is the *equal error rate* (ERR), which is defined as the error rate at the threshold t at which FAR = FRR. The most common used measurements are: *false acceptance rate* (FAR), *false rejection rate* (FRR) and the *equal error rate* (ERR). It is also recommended to report the system performance at all operating points (threshold t), by plotting FRR(t) against FAR(t) as a receiver operating characteristic (ROC) curve [1].

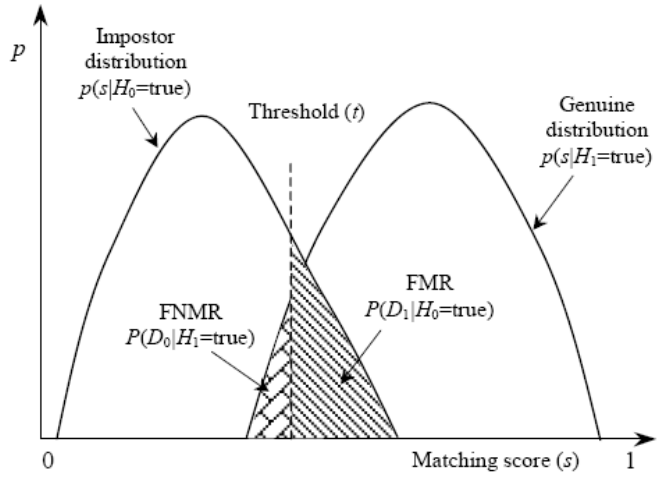

Figure 2.8: FMR and FNMR, for a given threshold t, are displayed over the genuine and impostor score distributions [1].

The computational complexity of a fingerprint recognition scheme is measured, in general, by reporting the CPU times of the different modules of the system. There are mainly two time measures to be reported: the enrollment time and the matching time. The enrollment time is defined as the time needed for fingerprint representation module, which includes pre-processing step, features extraction and template formulation (Figure 2.1(a)). The matching time represents mainly the time needed for comparing two different templates (reference template vs. input template). Finally, the size of the formulated template in bytes, which is called a model size [41], is another important performance metric to be reported.

2.5 Fingerprint Benchmark Databases

With the increase in the number of commercial systems for fingerprint-based recognition, proper evaluation protocols are needed. So, testing of all the algorithms should be carried out on one common database, to know the best feature extraction/matching technique

satisfying an application's requirements. Recently, the first fingerprint verification competition (FVC2000) was a good start in establishing such protocols with new dataset well suited for the evaluation of algorithms with live-scan images [42].

Our main concern in choosing a fingerprint database for experimentation is to ensure that the fingerprint images contained therein represent the real life situations, meaning that the images have been collected under unsupervised conditions and without a quality check. The public domain databases from Fingerprint Verification Competitions (FVC), i.e., FVC2000 [43], FVC2002 [44], FVC2004 [41], and FVC2006 [45, 46] satisfy that concern. Each of these FVCs contains four different benchmark databases, namely, DB1, DB2, DB3, and DB4. The first three databases consist of real-life fingerprints and they have been acquired by using different types of sensors. The fourth one has been created by using a synthetic fingerprint generator (SFinGe). In the first three FVCs, each database contains 8 impressions of a finger with different qualities of the image and may contain the images of a finger even only partially. Each database contains 110 fingers, i.e., a total of 880 fingerprints. The fingers numbered 101 to 110 (set B) have been selected for training and estimating the parameter values, and the rest of the fingers, numbered 1 to 100 (set A), are used for testing. In FVC2006, each database contains 150 fingers with 12 impressions of each, i.e. a total of 1800 fingerprints. The fingers numbered 141 to 150 (set B) have been selected for training and estimating the parameter values, and the rest of the fingers, numbered 1 to 140 (set A), are used for testing. Tables 2.1, 2.2, 2.3 and 2.4 provides a summary in terms of the fingerprint size, resolution and the source of acquisition of the benchmark FVC databases [41–46].

Table 2.1: Summary of the benchmark FVC2000 databases [42–43]

	DB1	DB2	DB3	DB4
Sensor type	Optical	Capacitive	Optical	SFinGe
Image size (pixels)	300x300	256x364	448x478	240x320
Resolution (dpi)	500	500	500	~ 500

Table 2.2: Summary of the benchmark FVC2002 databases [44]

	DB1	DB2	DB3	DB4
Sensor type	Optical	Optical	Capacitive	SFinGe v2.51
Image size (pixels)	388x374	296x560	300x300	288x384
Resolution (dpi)	500	569	500	~ 500

Table 2.3: Summary of the benchmark FVC2004 databases [41]

	DB1	DB2	DB3	DB4
Sensor type	Optical	Optical	Thermal sweeping	SFinGe v3.0
Image size (pixels)	640x480	328x364	300x480	288x384
Resolution (dpi)	500	500	512	~ 500

Table 2.4: Summary of the benchmark FVC2006 databases [45, 46]

	DB1	DB2	DB3	DB4
Sensor type	Electrical field	Optical	Thermal sweeping	SFinGe v3.0
Image size (pixels)	96x96	400x560	400x500	288x384
Resolution (dpi)	250	569	500	~ 500

2.6 A Fuzzy-based Clustering Technique

Because of to the nature of many problems in pattern recognition and image processing fields, the use of fuzzy-based techniques has been shown to be capable of achieving better results [47]. Among these techniques, the fuzzy-based clustering problems (FCP) represent important area in pattern recognition and image processing fields. In general, the clustering problems are based on the notion of unsupervised learning and consist in assembling patterns or entities in restricted classes. In the crisp clustering, each pattern is classified in a single cluster, assuming well-defined class boundaries. However, the boundaries in the real life situations between natural classes may be overlapping. Thus, a

certain input pattern may be not completely belong to a single class, but partially belong to the other classes too. Therefore, the use of the crisp clustering models to solve real life problems should be limited. On the other hand, the FCP have been proposed to deal with the real life problems more effectively. The beginning of fuzzy clustering can be traced to early works of Bellman et al. [48] and Ruspini [49]. The fuzzy clustering methods give us more information than the crisp ones about the degree of membership of a pattern. The FCP consist of assigning a set of patterns to a given number of clusters such that each of them may belong to more than one cluster with different degrees of membership. In general, FCP can be classified into three categories: (i) fuzzy clustering based on fuzzy relation, (ii) fuzzy clustering based on fuzzy rule learning, and (iii) fuzzy clustering based on the optimization of an objective function [50, 51].

The most popular heuristic for solving FCP based on the optimization of an objective function is the so called fuzzy c-means method (FCM) [51]. It has been successfully applied in a large number of areas such as chemistry, biology, and medical diagnosis [47, 50]. The FCM has been also widely used in image segmentation [52–59]. The fuzzy clustering with an objective function (FCM) is similar to the well-known k-means heuristic used for crisp clustering. The FCM alternatively, which depends on the fuzzy sets theory [47, 51, 60, 61], assigns membership degrees of a set of patterns to a given number of clusters until there is no more improvement in the objective function value.

2.6.1 Standard FCM algorithm

In order to classify n patterns into c clusters, the problem of FCM clustering could be formulated as follows: First, given n patterns in d-dimensional space, where the pattern

vector is represented as $X = \{x_1, x_2, ..., x_n\}, x_i = (x_{i1}, x_{i2}, ..., x_{id}), i = 1,2,...,n$ Therefore, the x_{ik} represents the k^{th} attribute (or feature) associated with pattern i. Second, let c denotes a known number of clusters. Accordingly, let U be a matrix of size $n \times c$, where its item u_{ij} denotes the membership degree for pattern i with respect to cluster j, with the following two constraints:

$$\sum_{j=1}^{c} u_{ij} = 1, \forall i = 1,2,...,n \tag{2.4}$$

$$0 \le u_{ij} \le 1, \forall i = 1,2,...,n; \forall j = 1,2,...,c \tag{2.5}$$

Finally, the FCM algorithm is an iterative optimization that minimizes the objective function defined as follows [50].

$$J_m = \sum_{j=1}^{c} \sum_{i=1}^{N} u_{ij}^{m} \left\| x_i - v_j \right\|^2 \tag{2.6}$$

where:

- m is a tuning parameter which controls the degree of fuzziness in the clustering process. The FCM iterative algorithm works under condition that $m > 1$, and usually $m = 2$.
- $V = \{v_1, v_2, ..., v_c\}$ is a set of the centers of the clusters, where $v_j = (v_{j1}, v_{j2}, ..., v_{jd})$ is the center of the j^{th} class.
- $\| \bullet \|$ is the Euclidean distance defined on R^d.

Then the optimal fuzzy clustering structure of set X is obtained as a solution of the non-linear programming problem (P) in variables (U,V). By fixing U the problem (P) reduces to finding V and we also find U by fixing V.

For this objective function Eq. 2.4, there exist one global optimum solution and a number of other possible local optimum solutions. Based on the initial set of the centers of the clusters V^0, the FCM algorithm has been proved to converge to one of theses optimum solutions (local or global) [62]. Normally, finding the global optimum appears to be very difficult, since the initial set of the centers of the clusters V^0 is usually unknown. Therefore, in many cases, the initial set of the centers of the clusters V^0 is randomly initialized.

2.6.2 An illustrative numerical example

In this section, we are presenting the solutions of a numerical example (Table 2.5) obtained by the different crisp and FCM clustering techniques. In addition to the above mentioned FCM clustering technique, we are using two crisp techniques:

1- The quantization method: under the assumption of knowing the possible range of the values of the data items, a group of crisp sets with their centers could be defined. Accordingly each pattern is assigned to one of these crisp sets. This technique is much simpler than the k-Means heuristic.

2- The well known k-means heuristic, which depends mainly on the given pattern vector to provide the centers of the clusters. Similar to the FCM, the k-Means heuristic depends on the initialization step and also converges to one of the local optimum solutions.

In this example, the pattern vector contains fifteen data items, i.e. $n = 15$, such that each data item represents the age of a person. Then, by using the three clustering techniques, these patterns are to be classified into three clusters, i.e. $c = 3$. These clusters representing: (1) the younger people, (2) the middle-age people and (3) the elderly people.

Table 2.5: A given set of ages of different persons in the illustrative numerical example.

P#	1	2	3	4	5	6	7	8	9	10	11	12	13	14	15
Age	30.5	18.9	19.5	68.5	30.7	4	15.8	69	37.8	86	85	60	49	89	82

1- By assuming that the minimum age is equal to zero and the maximum possible age is one hundred, then we can define three crisp sets as follows:

i. The younger people's age $Y = \{y_i \mid 0 \le y_i < 33.5\}$

ii. The middle-age people $M = \{m_i \mid 33.5 \le m_i < 67\}$

iii. The elderly people $E = \{e_i \mid 67 \le e_i \le 100\}$

And thus, the set of cluster centers, based on the quantization technique, is V = [16.66, 50, 83.33]. Accordingly, the clustering solution of the given pattern vector is obtained as listed in Table 2.6.

Table 2.6: The clustering solution obtained using the quantization technique.

P#	1	2	3	4	5	6	7	8	9	10	11	12	13	14	15
Cluster#	1	1	1	3	1	1	1	3	2	3	3	2	2	3	3

2- By using the k-Means technique, one of the possible set of cluster centers to this problem is V = [14.55, 37, 77.07]. Accordingly, the clustering solution of the given pattern vector is obtained as listed in Table 2.7.

Table 2.7: The clustering solution obtained using the K-means technique.

P#	1	2	3	4	5	6	7	8	9	10	11	12	13	14	15
Cluster#	2	1	1	3	2	1	1	3	2	3	3	3	2	3	3

3- By using the FCM technique, one of the possible set of cluster centers to this problem is V = [20.69, 59.06, 84.77]. Accordingly, the clustering solution of the given pattern vector is obtained as listed in Table 2.8. By using the FCM technique, the patterns are classified such that each pattern belongs to all clusters with different membership degrees as seen from Table 2.8.

Table 2.8: The clustering solution obtained using the FCM technique.

P#	u_{i1}	u_{i2}	u_{i3}
1	0.8691	0.10251	0.028392
2	0.99728	0.0019815	0.00073661
3	0.99876	0.00090401	0.00033212
4	0.028328	0.72718	0.24449
5	0.86296	0.10747	0.02957
6	0.88139	0.080978	0.037632
7	0.98251	0.012553	0.004939
8	0.029396	0.69488	0.27573
9	0.56176	0.36371	0.074529
10	0.00035163	0.0020672	0.99758
11	1.2367e-005	7.6033e-005	0.99991
12	0.00056613	0.99801	0.0014254
13	0.10483	0.82952	0.065647
14	0.0037388	0.019467	0.97679
15	0.0020134	0.014386	0.9836

It is seen from Tables 2.6, 2.7, and 2.8, that the solutions achieved by the crisp techniques are quite near to each others, i.e., 12 patterns out of 15 have been classified to

belong to similar clusters. On the other hand, the FCM technique provides a different manner of the clustering solution. For example: pattern number 9 {37.8} has been assigned to cluster number 2 using both crisp techniques which means it belongs to the middle age group, whereas the FCM technique assigns the same pattern to the first and second clusters with the largest membership to the first cluster, which means this pattern is more likely to be considered as the younger people group. Another example: pattern number 11 {85} which is almost equal to the center of the third cluster, and therefore its membership is almost equal to one under the third cluster.

2.7 Summary

The purpose of this chapter has been to present the background material necessary for the development of the work undertaken in this thesis. The fingerprint recognition systems are classified as an automatic fingerprint verification system or an automatic fingerprint identification system. In this chapter, these systems have been first discussed and their different operational modes described. Next, the main modules of these systems, namely, the fingerprint representation and matching, have been discussed in details. Then, to measure the performance of the fingerprint recognition systems in terms of the accuracy and complexity, the most commonly used performance metrics in the area of fingerprint recognition have been presented. Benchmark databases are used in order to examine and compare the performances of fingerprint recognition systems. In this chapter, some of the most challenging databases containing a variety of fingerprint difficulties are also described.

Since one of the objectives of the work undertaken in this thesis to address the problems arising from a crisp partitioning of the features by exploring the possibility of

employing a fuzzy based partitioning, finally, different types of the fuzzy-based clustering techniques have been reviewed. The most popular heuristic for solving fuzzy clustering problems, i.e. fuzzy c-means method, has been described in this chapter. It has been shown through a numerical example that the use of the fuzzy c-means technique provides a smoother clustering solution in comparison to that provided by crisp clustering techniques.

CHAPTER 3

Fingerprint Decomposition

3.1 Introduction

In fingerprint recognition problem, the global features of the fingerprint image represent mainly the structural information of the fingerprint ridges. In comparison to the local features (minutiae) of the fingerprint, the global features can be determined more reliably. Therefore, the idea of combining the global features with the local features of a fingerprint could provide a promising methodology to achieve recognition accuracy higher than that achieved by minutia-based techniques.

Considering that the fingerprint recognition is a complex problem, it is proposed to simplify it by using a strategy of divide-and-conquer for developing a multilevel structural fingerprint recognition (MSFR) scheme. As a first phase of this scheme, in this chapter, a low-complexity algorithm for decomposing a fingerprint image into regions (sub-images) is developed by using more than one of its global features [63]. In Section 3.2, a comparative study of the different global features of fingerprint images is first undertaken, in order to choose the most effective ones in terms of their extraction reliability and their importance in solving the fingerprint recognition problem. In Section 3.3, the idea of partitioning a fingerprint image based on the global features is discussed and the previous work done in this area is reviewed. Finally, a new technique for decomposing fingerprint images using global features selected based on the conclusion drawn in Sections 3.2 and 3.3 is presented in Section 3.4.

3.2 The Global Features of the Fingerprint: A Comparative Study

As mentioned in Chapter 2, the global features of the fingerprint are: the singular points, the orientation field, the ridge frequency map, and the curvature map. Based on the characteristics of these global features, the main differences between them could be summarized as follows:

- The ridge density map is considered as a raw feature of the ridges of the fingerprint, since it is calculated directly from these ridges. Even though, different fingerprints have been found to have naturally different ridge density maps, these maps are affected by the person's behavioral characteristics. During the acquisition process of the fingerprint image, different pressures on the fingertip against input device lead to different ridges densities. Hence, the values of the resulting ridge density maps of same finger are affected. Accordingly, this feature could be considered as a behavioral and an anatomical characteristic. Therefore, the ridge density map may be useful for the fingerprint recognition only under certain circumstances, such as the acquisition process of the fingerprint images has been done under supervision.

- The orientation field is considered also as a raw feature of the ridges of the fingerprint. There are mainly two behavioral characteristics of a person which may affect on the values of the ridges orientations. First, the possibility of having different rotations of the fingertip during the image acquisition, which is a tolerable effect by finding a reference orientation among different fingerprint images [1]. Second, the possibility of having some amount of deformation of the ridges due to different pressures on the fingertip during the acquisition process, which is also a tolerable effect by smoothing the original orientation field [39] or by devising a deformable model [64, 65]. Therefore, the

orientation field could be considered as an anatomical characteristic, since the effect of the person's behavioral characteristics on the values of the orientation field is limited. In addition, the orientation field provides, to some extent, discriminatory information other than that provided by the traditionally and widely used minutiae points. It has some special characteristics: (i) The ridge orientations are almost continuous and smooth everywhere, except for the regions near the singular points, which makes the process of extraction of the orientation field robust and less sensitive to noise. (ii) Compared to the local features, it is more immune to ridge pattern deformation and rotation or translation.

- The curvature map is calculated based on the orientation field. Even though, this feature carries another kind of useful information [18, 38], it is solely depend on the orientation field. Accordingly, it does not actually present a new feature compared with the orientation field, meanwhile its formulation requires an additional computational cost compared with the previous two global features.

- The singular points (cores and deltas) are detected based also on the orientation field. These features could be considered as anatomical characteristics, since they are not affected by the behavioral characteristics of a person. Actually, the singular points represent a special ridge shapes within the fingerprint image. Therefore, it carries very important information as well as the orientation field.

In figure 3.1, two fingerprint images scanned from the same finger are presented [44] with their orientation fields and their ridge density maps. The first image, Figure 3.1(a), represents a complete fingerprint image with a good quality. Whereas, the second image, Figure 3.1(b), represents a lower quality incomplete fingerprint image with a certain amount of rotation and deformation of the ridges. Figures 3.1(b) and (c) show the

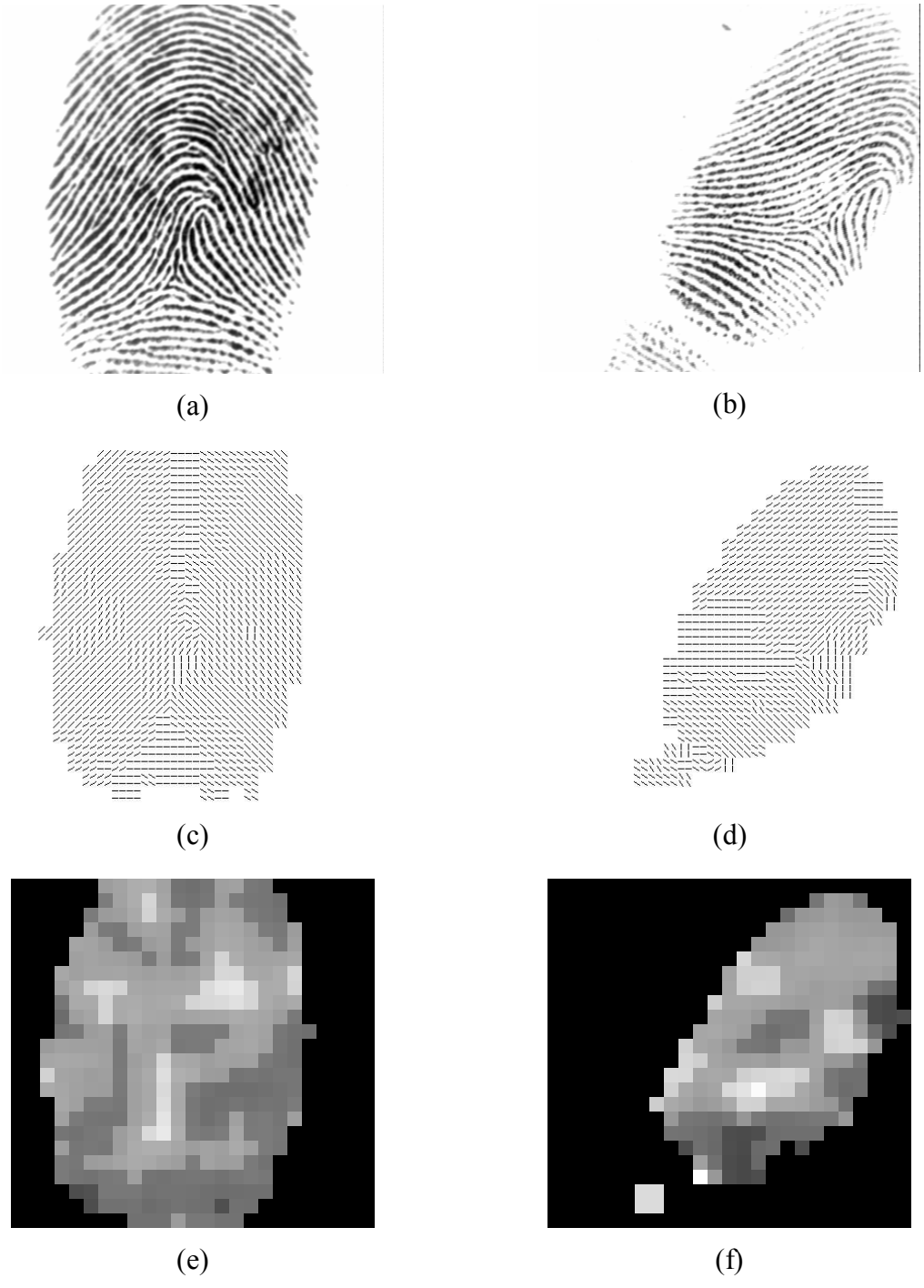

Figure 3.1: Two fingerprint images taken for the same finger (a, b) with their orientation fields (c, d) and their ridge density maps (e, f).

orientation fields of both images, which have been obtained by using a gradient based method similar to that proposed by Ratha *et al.* [36]. Finally, the ridge density maps of the fingerprint images, Figures 3.1(d) and (e), have been obtained by using the method proposed by Hong *et al.* [9]. In their method, the local ridge density is determined as the inverse of the average number of the pixels between two consecutive peaks of gray-levels (i.e., ridges) along the direction normal to the local ridge orientation. Therefore, the higher ridge density areas are represented by the brighter areas in the Figures 3.1(d) and (e) and vice versa.

It is seen from Figures 3.1(b) and (c) that the ridge orientations of the correspondent areas of the images have almost similar orientations after rotating the second one to be aligned vertically with the first one. On the other hand, Figures 3.1(d) and (e) show that there are differences between the ridge densities of the correspondent areas of the fingerprint images. One can conclude from this example that the orientation field is, in general, a more reliable global feature than the ridge frequency map.

Finally, Table 3.1 summarizes the above comparisons between the different global features in terms of: (i) the feature type, if it is a raw or dependent feature, (ii) the biometric characteristic of the feature, (iii) the reliability of extracting the feature from the fingerprint image, and (iv) the importance of using the feature for fingerprint recognition field. It is seen from this table the singular points and the orientation field are the most important characteristics that can be used as global features of a fingerprint or to be used to extract other features.

Table 3.1: The attributes of the global features of the fingerprint.

	Feature type	Biometric characteristic	Reliability	Importance
Ridge density map	Raw	Anatomical/behavioral	Low	High
Orientation field	Raw	Anatomical	High	High
Curvature map	Dependent	Anatomical	High	Low
Singular points	Dependent	Anatomical	High	High

3.3 Fingerprint Image Partitioning Schemes

Over the last decade, the idea of partitioning the fingerprint image into different areas has been used for fingerprint classification [10–13], recognition purposes [23, 32] or for detecting singular points [66, 67]. Even though there are many global features of the fingerprint have been defined, most of the proposed partitioning schemes have used only the singular points or the orientation field. Therefore, the partitioning schemes in the literature could be categorized into two groups: 1) The partitioning schemes which based on the singular points, and 2) orientation field-based partitioning schemes. In this section, the previous work that has been done in this area is reviewed.

3.3.1 Partitioning schemes based on the singular points

As mentioned in Chapter 2, the singular points are classified as core and deltas. Naturally, any fingerprint has at least one singular point which is the core point (i.e. the upper loop) accordingly the core point plays a very important role in the fingerprint recognition field. That was the main motivation for some researchers to use the core point as a center point for partitioning the fingerprint image. In [14], Bazen and Gerez have proposed an intrinsic coordinate system for fingerprint matching by partitioning the fingerprint image mainly into four regular regions based on the locations and orientations

of the singular points (i.e. both the core and deltas). Some other researchers have proposed the idea of fingerprint image tessellation around the core point to partition the image [13, 23, 32]. In [13], Anil *et al* have been proposed a multi-channel approach to fingerprint classification. In this approach a fingerprint representation, based on the circular image tessellation around the core point, has been formulated which is called FingerCode [13]. The flow diagram of this approach is depicted in Figure 3.2, which is composed of the following steps:

1. Determine a reference point (i.e. the core) and region of interest for the fingerprint image.
2. Tessellate the region of interest around the reference point in a circular fashion.
3. Filter the region of interest in four different directions using a bank of Gabor filters to capture the global information.
4. Decompose the input image into a set of component images, each of which preserves certain ridge structures.
5. Compute the standard deviation of the component images in each sector to generate the feature vector, which is called FingerCode.
6. Feed the feature vector into a classifier.

In [23], Anil *et al.* have been reused the same idea of circular image tessellation around the core point for fingerprint representation and matching. In order to capture both the global and local features, the region of interest has been filtered in eight (not only four) different directions using a bank of Gabor filters [23]. In [32] a fingerprint recognition scheme has been proposed using tessellated invariant moment features. This

scheme starts by locating a reference point, which represents the maximum curvature in an orientation field image. It has been used to determine a unique reference point for all types of fingerprints. Based on their definition of the reference point in [32], it is in general corresponds to the core point. To minimize the effects of noise and nonlinear distortions, a region of interest centered on the reference point is then determined and tessellated into a predefined number of non overlapping square cells (Figure 3.3) [32].

The main disadvantage associated with the above fingerprint image partitioning schemes is in their dependence on the use only of the singular points. In some cases such as the incomplete fingerprint images or images with low quality, the detection of the singular points is problematic, accordingly, the above image partitioning schemes fail.

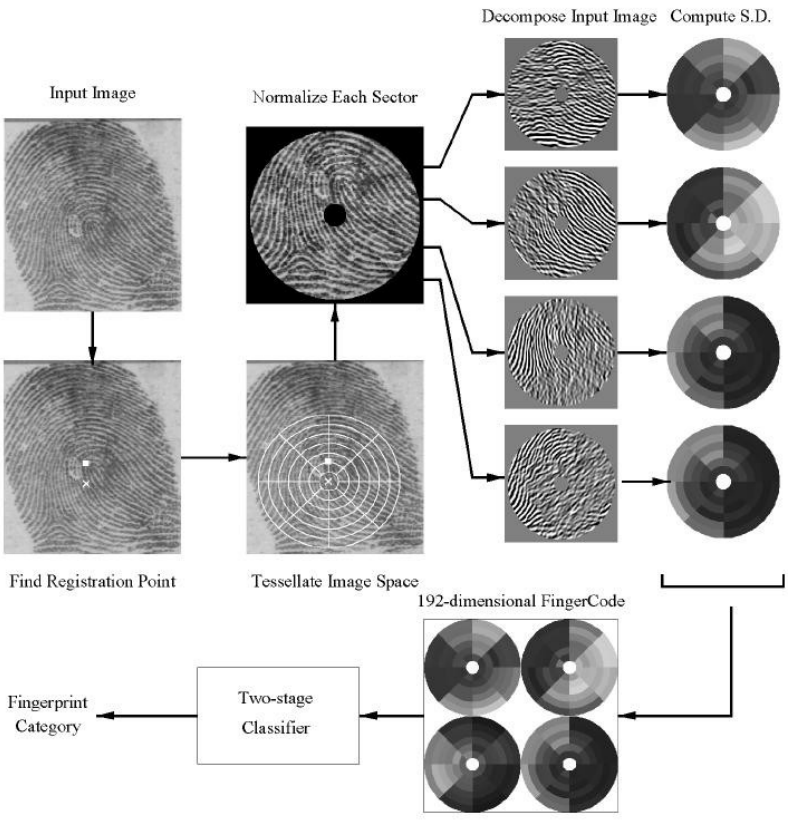

Figure 3.2: Flow diagram of the multi-channel approach to fingerprint classification [13].

Figure 3.3: A fingerprint image tessellated around the core point into a predefined number of non overlapping square cells [32].

3.3.2 Partitioning schemes based on the orientation field

Many researchers have proposed fingerprint image partitioning schemes by using only the orientation field [10–12, 66, 67]. These image partitioning schemes have been used for either fingerprint classification [10–12] or for singular points detection [66, 67]. In [12] by using the orientation field, Maio and Maltoni have proposed an iterative clustering algorithm to partition the fingerprint image into regions characterized by homogeneous orientation values. Due to the nature of the ridge orientations, which are almost continuous and smooth everywhere except for the regions near the singular points, the clustering algorithm proposed in [12] requires a high computational cost. Therefore, Cappelli *et al.* [11] have proposed another approach, which is based on performing a guided clustering with the aim of reducing the degrees of freedom during the partitioning process. In this approach, a set of dynamic masks has been defined directly derived from the most common fingerprint classes, to guide the clustering algorithm [11]. In [10], Yao *et al.* have used the same fingerprint image partitioning scheme proposed in [11] to

represent the fingerprint as a relational graph, in order to know the fingerprint class by using recursive neural networks and support vector machines.

Some authors noted that the partitioning of the fingerprint image using the orientation field into regions characterized by homogeneous orientation implicitly reveals the position of singularities. Hung and Huang [66] and Huang, Liu, and Hung [67] have quantized the orientation field by using a small number of orientation values, such that each orientation value determines a region. By tracing the borderlines between the adjacent regions, which are called fault-lines, they have defined a geometrical method to detect the singular points. This was done by noting that the fault lines converge towards loop singularities (i.e. upper and lower cores) and diverge from deltas.

Contrary to the partitioning schemes based on the singular points, the dependence on the orientation field is more robust since the information on the ridge orientations is always available. The main challenge in the orientation field based partitioning schemes is in clustering the irregularities of the regions containing singular points leads to the requirement of high computational complexity techniques.

3.4 The Proposed Fingerprint Decomposition Algorithm

Based on the discussions made in the previous sections, three main observations could be drawn: 1) the global features of the fingerprint represent quite important information about the structure of the fingerprint ridges. 2) The singular points and the orientation field are the most important characteristics that can be used as global features of a fingerprint or to be used to extract other features. 3) The singular points and the orientation field have been used for various fingerprint partitioning techniques.

Therefore, a new fingerprint image decomposition (partitioning) algorithm by using both the singular points and the orientation field is now developed in this section.

In the proposed algorithm, the fingerprint image is decomposed into regions (sub-images), such that each region has a unique global feature characteristic. Since the ridge orientations are almost continuous and smooth everywhere, except for the regions near the singular points, the fingerprint image is decomposed into singular and non-singular regions. A region is defined to be a singular region, if it contains a core or delta, or a plain region, if it contains only ridges having orientation values within a specified range. This results in lowering the computational complexity of the proposed decomposition scheme compared to that of the schemes in [10–12].

To start with, the orientation field of the fingerprint image is obtained by a method similar to that proposed by Ratha et al. [36]. A ridge orientation value is calculated for each block of size N×N. Each block is assigned an orientation value in the interval $[0,\pi)$ that corresponds to the most dominant direction of the ridges contained therein. The orientation values are calculated with respect to the horizontal border of the image. The orientation field $\mathbf{O}$ can then be considered as a matrix whose $(k,l)^{\text{th}}$ element represents the orientation value of the $(k,l)^{\text{th}}$ block. After the construction of the orientation field, a quantization operation is performed on the elements of the matrix $\mathbf{O}$ to obtain a quantized orientation field $\mathbf{O}_q$ by allowing the elements of $\mathbf{O}_q$ to assume values in range of $[0,\pi)$ at steps of Δ. The use of the quantized orientation field $\mathbf{O}_q$ facilitates the succeeding steps in the fingerprint decomposition scheme. Next, a process of segmentation is carried out for separating the fingerprint foreground and the background areas. Each $N \times N$ block is assigned to the foreground or background area

according to the variance of the gray-levels in a direction orthogonal to the ridge orientation [36]. Detection of singular points is then carried out by a shape analysis technique of the orientation field in the fingerprint image [39]. Through this shape analysis, it is not only possible to detect a singular point but also to determine its type, that is, whether it is an upper or lower core or a left or right delta.

Finally, the fingerprint image is decomposed into different regions and represented as a set $\Re = \{\Re_{S_1}, \Re_{S_2}, \Re_{S_3}, \Re_{P_1}, \Re_{P_2}, ..., \Re_{P_L}\}$, where $\Re_{P_i} = \{B_j^{\theta_i}, j = 1,...,M\}$ is a plain region that contains a group of adjacent image blocks $B_j^{\theta_i}$, all having the same orientation value θ_i which is chosen from the set $\{0,\Delta,2\Delta,\ldots,\pi\text{-}\Delta\}$, and $\Re_{S_i} = \{B_{f,g}, f = 1,...,F, g = 1,...,G\}$, where $B_{f,g}$ is the $(f,g)^{\text{th}}$ image block corresponding to a singular point (i.e. a core or delta). In the proposed method, a singular point region $\Re_{S_i}$ could be only one of three types: the core region $\Re_{S_1}$ (upper and/or lower core), the left delta region $\Re_{S_2}$, and the right delta region $\Re_{S_3}$. Note that if both lower and upper cores exist simultaneously, they are included in the same region $\Re_{S_1}$, since they are located relatively in a closer proximity than left and right deltas do. During the decomposition process, there is a possibility to have abnormal regions: 1) *Isolated region, which is a region that has no adjacent regions, i.e. the image blocks of this region have no neighboring blocks belonging to other regions.* This situation arises due to the presence of noise beyond the fingerprint region or within the region that isolates a part of the fingerprint from the rest of the fingerprint regions. In either case, such an isolated region is removed from $\Re$. In the case of the former, such an isolated region is not useful at all, whereas in the latter case it cannot be used, since it lacks the availability of

neighboring regions. 2) *A small region containing only a few blocks.* This situation arises due mainly to an incomplete fingerprint image, in which some ridges are not complete. A small region does not carry much global information but it may contain some useful local information. Retaining this small region increases the computational complexity of the fingerprint recognition. Consequently such a region is distributed among the neighboring regions based on the orientation values of the ridges within the region under consideration.

The proposed fingerprint image decomposition scheme described in the preceding paragraphs can now be summarized as an algorithm with the following steps.

Algorithm 3.1: Fingerprint decomposition

1- Divide the fingerprint image into $H \times W$ blocks each of size $N \times N$ pixels.

2- For each block $k = 1:H$ and $l = 1:W$

- Compute the dominant ridge (k,l) direction in the current block θ_R by using the equation:

$$\theta_R = \frac{1}{2}\tan^{-1}\left(\frac{\sum_{i=1}^{N}\sum_{j=1}^{N} 2\,G_x(i,j)\,G_y(i,j)}{\sum_{i=1}^{N}\sum_{j=1}^{N}\left(G_x(i,j)^2 - G_y(i,j)^2\right)}\right) \tag{3.1}$$

where $G_x(i,j)$ and $G_y(i,j)$ are the values of the gradients at pixel (i,j) in the x and y directions, respectively, using 3×3 Sobel mask.

- Formulate the orientation field $\mathbf{O}$ as a matrix, where $\mathbf{O}(k,l) = \theta_R$.
- Formulate the quantized orientation field $\mathbf{O}_q$ as a matrix, where $\mathbf{O}_q(k,l) = Quantization(\theta_R, \Delta)$, Δ being the quantization step.

- Compute the variance σ^2 of the gray levels of image pixels within the current image block, in a direction that is perpendicular to θ_R.
- If $\sigma^2 \le \tau$, where τ is an empirically specified threshold, then the current image block belongs to the background, and it has to be removed from the orientation field, therefore, we set $\mathbf{O}(k,l) = -1$ and $\mathbf{O}_q(k,l) = -1$.

3- Detect the location of the upper_core, lower_core, left_delta and right_delta points by applying the shape analysis technique [39] on $\mathbf{O}_q$.

4- Define the singular point regions $\Re_{S_i} = \{B_{f,g}, f = 1,...,F, g = 1,...,G\}$ by choosing the blocks that contain the singular points, then remove these blocks from $\mathbf{O}_q$ by assigning a "–1" value to the items that corresponded to the blocks of this region.

5- Divide the rest of the items of $\mathbf{O}_q$, into $\Omega = \pi / \Delta$ groups. Each group represents the fingerprint image blocks, which have only one orientation value selected from the set $\{0,\Delta,2\Delta,\ldots,\pi-\Delta\}$.

6- For each group n = 1 : Ω

Define the plain regions $\Re_{P_i} = \{B_j^{\theta_i}, j = 1,...,M\}$ by gathering the adjacent blocks into one region. The adjacent blocks are identified using the 8-connetcivity criteria [68].

7- Use the output of steps 4 and 6 to represent the decomposed image as a set of regions $\Re = \{\Re_{S_1}, \Re_{S_2}, \Re_{S_3}, \Re_{P_1}, \Re_{P_2}, ..., \Re_{P_L}\}$.

8- For each plain region i = 1 : L

- If the region is an isolated region, then remove the region from set $\mathfrak{R}$, and remove its blocks from $\mathbf{O}$ and $\mathbf{O}_q$ by assigning a "–1" value to the items that corresponded to the blocks of this region.
- If the region is a very small region (i.e. a region contains a number of blocks ≤ t), then remove the region from set $\mathfrak{R}$, and reassign its blocks to the adjacent regions.

In order to show the usefulness of the proposed decomposition algorithm, two experiments have been conducted. In the first one, two fingerprint images corresponding to the same fingertip have been decomposed using the proposed algorithm. Figure 3.4 contains these two fingerprint images (a and b) with their decomposed images (c and d). In this experiment, the chosen two images contain different parts from the original fingerprint. By comparing the decomposed images, two main observations can be made. First, the singular regions of the two images (i.e. core and left delta) are clearly corresponding to each other. Second, the correspondence between the plain regions of the two images could be easily determined. These two observations show that the images taken from the same finger should have, in general, the same set of decomposed regions.

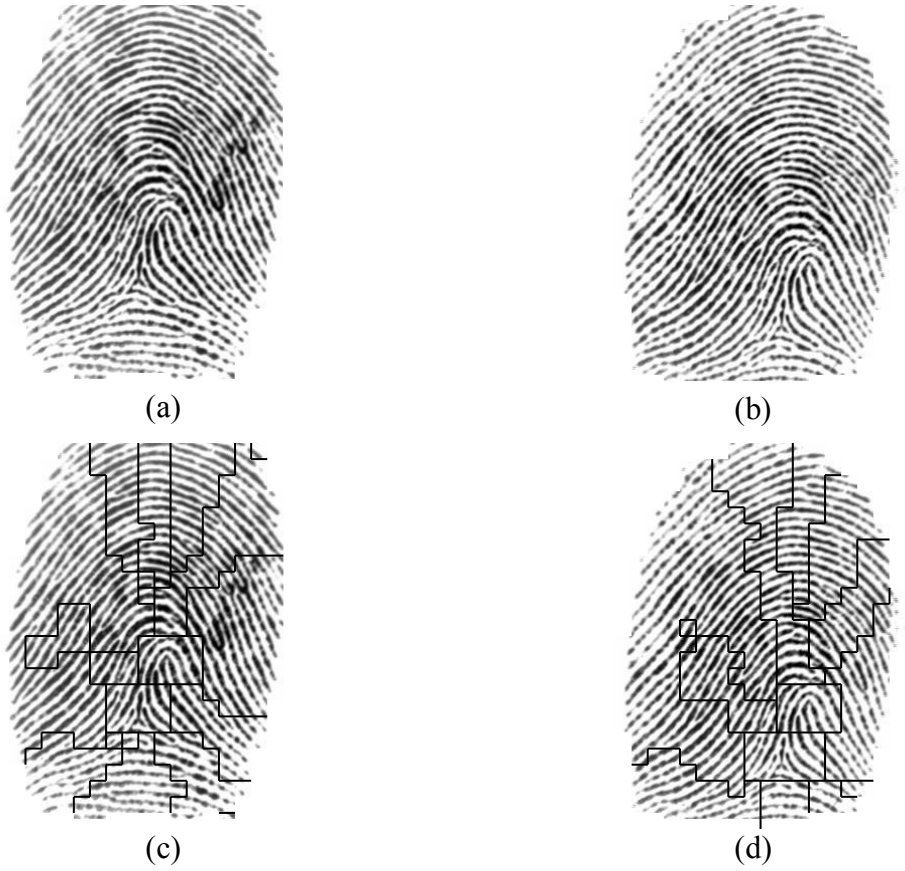

Figure 3.4: An example of two fingerprint images taken from the same finger (a, b), and the resulting decomposed images (c, d).

In the second experiment, two fingerprint images corresponding to different fingertips have been decomposed using the proposed algorithm. As shown in Figures 3.5(a) and (b), these two fingerprint images belong to the right loop fingerprint class, however the second image has only the upper core and the left delta is not presented due to the incomplete scanning of its fingertip. By comparing the decomposed images Figures 3.5(c) and (d), two main observations can be made. First, the singular regions of the two images, in this case only the cores, are corresponding to each other. Second, the correspondence between the plain regions of the two images could not be determined. These two observations show that the images taken from different fingers should have, in

general, different sets of decomposed regions, even though these images belong to the same class. From the two experiments, it is seen that the inter-class similarity problem could be dealt effectively using the proposed decomposition algorithm.

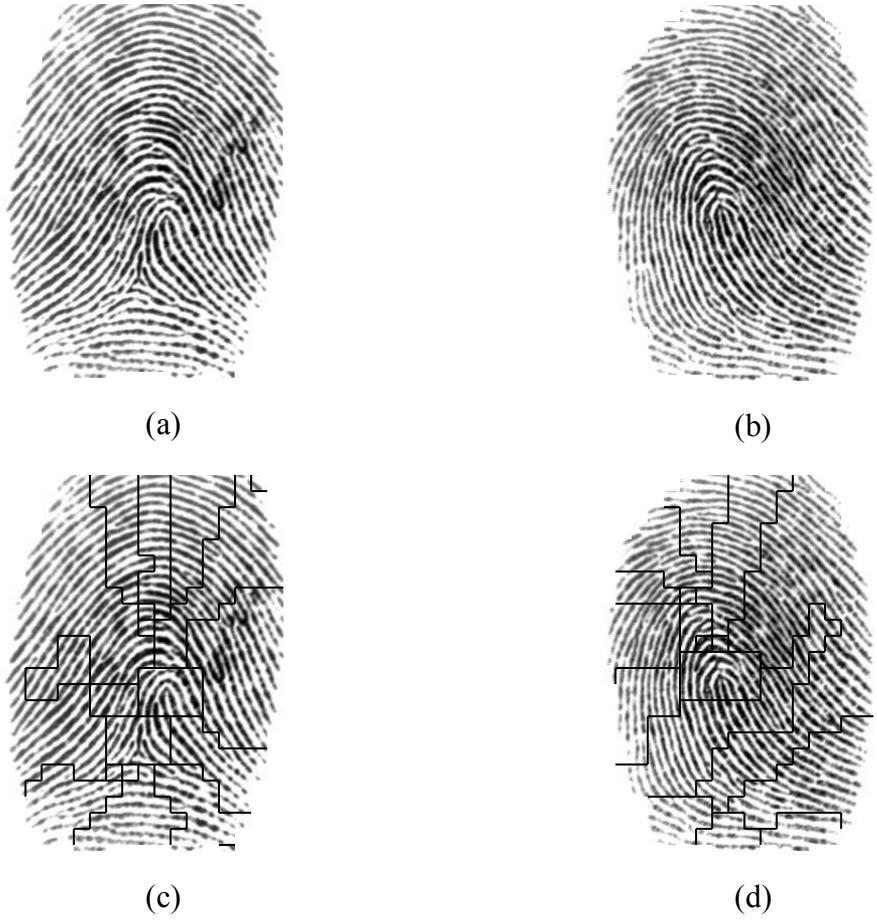

(a) (b)

(c) (d)

Figure 3.5: An example of two fingerprint images taken from different fingers (a, b), and the resulting decomposed images (c, d).

3.5 Summary

The idea of combining the local feature, minutiae, with global features has been shown to be a promising methodology to provide fingerprint recognition accuracy higher than that provided by the techniques using only minutia. In this chapter, a comparative study of the

different global features of the fingerprint image has been first undertaken in order to choose the most suitable ones for fingerprint recognition. It has seen from this study that the orientation field and the singular points are the most important characteristics that can be used as global features of a fingerprint.

Considering that the fingerprint recognition is a complex problem, the proposed scheme by using a strategy of divide-and-conquer simplifies this problem and provides a solution to the original complex problem at a lower complexity. The idea of partitioning the fingerprint images using only global features has been then discussed in detail, and the previous related work reviewed. The partitioning schemes in the literature could be categorized into two groups: 1) the partitioning schemes that are based on the singular points, 2) orientation field-based partitioning schemes. In this chapter, a novel technique has been proposed for decomposing fingerprint image into different regions using both the orientation field and the singular points. The new algorithm for fingerprint decomposition provides a preliminary representation of the fingerprint image as a set of regions based only on singular points and the ridge orientations. In the next chapter, this preliminary representation will be used to formulate a multilevel structural representation for fingerprint images.

CHAPTER 4

A Multilevel Fingerprint Representation and Matching

4.1 Introduction

In the previous chapter, the fingerprint image was decomposed into a set of singular and plain regions by using the fingerprint decomposition technique. In this chapter, by using this set of regions, schemes for fingerprint representation and matching for multilevel structural fingerprint recognition are presented [63]. In Section 4.2, for each region, a multilevel feature vector (MFV) is formulated by employing the structural information of local and global features of the fingerprint, and thus devising a multilevel fingerprint representation. Next, in Section 4.3, a multilevel matching algorithm is developed based on the MFVs in order to find a similarity between two fingerprints. Finally in Section 4.4, extensive experiments are conducted using some challenging benchmark databases, and the results compared with those of some state-of-the-art schemes.

4.2 Multilevel Fingerprint Representation

The problem of fingerprint representation is to determine a measurement (feature) space, in which fingerprint images belonging to a specific finger form a compact cluster different from those of other fingers from the stand point of these features. The objective in devising a suitable fingerprint representation is to provide a high accuracy in fingerprint recognition with a reasonable complexity. In the previous chapter, by using the locations of the singular points and the orientation field, a fingerprint image has been

decomposed and represented as a set of regions $\mathfrak{R}$. This preliminary representation is based only on two of the global features of the fingerprint. In this section, we propose a multilevel structural fingerprint representation that includes information on both the global and local features. Each extracted region resulting from the application of Algorithm 3.1 on a fingerprint image has a distinguishable global feature such as the ridge orientation or whether or not it contains a singular point. In addition, the region might also contain a group of minutiae that belong to the ridges inside the region. In the proposed scheme, a region of the fingerprint is represented using three different levels of fingerprint characteristics.

1) The global features of a region, which represent mainly the global structure of the fingerprint image with respect to the core region.

2) The neighborhood features of a region, which represent the region's characteristics in relation to its adjacent regions. This level of characteristics is especially useful when the fingerprint core point is not detectable; such a situation arises in fingerprint images with poor quality at the core point region.

3) The local characteristics of a region, such as curvature of ridges and minutiae, which vary from region to region.

4.2.1 Formulation of multilevel feature vectors

We now describe the formulation of these three levels of characteristics in a multilevel feature vector (MFV).

(i) Formulation of Global Features (FV1)

In order to capture the global structure of the fingerprint image, we specify three global features: (i) the type of the region, in regard to whether it is a plain or a singular

region, and (ii) its position and (iii) its orientation, both relative to the core point. The first feature is already determined after the application of Algorithm 3.1 on the fingerprint image. To quantify the second and third features, we first introduce a new rectangular coordinate system and split the entire fingerprint image into eight sectors based on the location and orientation of the core point (Figure 4.1). The location of the core point is considered as the origin. The new coordinate system consists of the axes θ_{Core} and θ_{P-Core}, where θ_{Core} is the average orientation of the core region $\Re_{S_1}$, and θ_{P-Core} is perpendicular to θ_{Core}. The orientations of these two axes are calculated using the following formulas:

$$\theta_{Core} = \frac{1}{F.G}\sum_{f=1}^{F}\sum_{g=1}^{G}\theta_R(B_{f,g}) \tag{4.1}$$

$$\theta_{P-Core} = \begin{cases} \theta_{Core} - \dfrac{\pi}{2} & if\ \theta_{Core} \geq \dfrac{\pi}{2} \\ \theta_{Core} + \dfrac{\pi}{2} & if\ \theta_{Core} < \dfrac{\pi}{2} \end{cases} \tag{4.2}$$

Starting from θ_{Core} axis, the entire image is divided into eight sectors, such that each sector covers 45^o of the space around the core point. Sectors are then labeled as 1 to 8. The second feature for each plain region is calculated by finding the sector in which the geometrical center $\Re_{P\_Center}$ of the region is located.

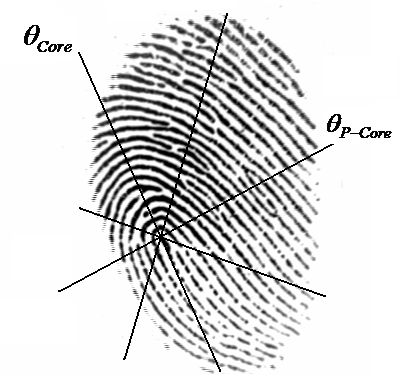

Figure 4.1: Coordinates system defined based on θ_{Core}.

The above three features are used to form the first level (FV1) of a multilevel feature vector using only two components as follows:

a- Type and position of a region (ξ)

In order to reduce the final fingerprint template size, ξ is used to represent both the relative position of a region with respect to the core point region as well as the type of the region. For a plain region $\Re_{P_i}$, ξ represents the relative position, and hence, its value is between 1 and 8, and for singular regions, the core, left delta, and right delta are represented by the digits 9, 10, and 11, respectively.

b- Relative orientation ($\theta_{\Re-Core}$) of a region

By considering θ_{Core} as reference orientation, this feature is used to represent the orientation of a plain region relative to the orientation of the core. For each plain region, this feature is calculated by subtracting θ_{Core} from the orientation θ_k of the ridges of this plain region.

With the formulation of FV1 as carried out above, it is seen that its two components are invariant to displacement and rotation, and thus a pre-alignment step,

commonly employed prior to the matching process of the fingerprint recognition, would not be required.

(ii) Formulation of Neighborhood Features (FV2)

In order to capture the characteristics of a region in relation to its adjacent regions, a pair of features for each adjacent region, the relative position ρ_{ij} and the relative orientation θ_{ij}, is used. The feature ρ_{ij} of region i is defined as the position of the geometrical center of its adjacent region j relative to that of region i. The second feature θ_{ij} is defined as the orientation of the adjacent region j relative to that of region i. In order to evaluate ρ_{ij}, a coordinate system is defined in a manner similar to that defined for the formulation of global features by using the geometrical center $\Re_{P\_Center}$ of region i as the origin and by using its ridge orientation θ_i instead of θ_{Core}. The relative orientation θ_{ij} is calculated by subtracting θ_i from θ_j. The formulation of FV2 is a set of neighborhood features of region i with the number of components equal to the number of adjacent regions.

(iii) Formulation of Local Features (FV3)

The third group of features, FV3, contains two local features: the curvature of the ridges belonging to a region and the set of minutiae contained therein.

a. Curvature of a region (ϕ_i)

   This feature represents the curvature ϕ_i of the ridges of a region i, which is calculated only for the plain regions $\Re_{P_i}$ as $\phi_i = \theta_{i\max} - \theta_{i\min}$, where $\theta_{i\min}$ and $\theta_{i\max}$ are, respectively, the smallest and largest orientation values of the ridges

contained in region i, which are retrieved from the original orientation field $\mathbf{O}$ within $\Re_{P_i}$. Therefore, the value of this feature is in the range $[0, \Delta]$.

b. Minutiae set $Minu_i = \{m_1, m_2, ..., m_L\}$

The traditional minutiae-based approaches represent each minutia l as $m_l = (x_l, y_l, \theta_l, t_l)$, where (x_l, y_l) is the minutia's location, θ_l is the minutia's orientation, and t_l is the minutia's type (i.e. ridge ending or ridge bifurcation). In the proposed representation, a minutia is represented as (x_l, y_l, t_l), since θ_l is already implicitly represented as $\theta_{\Re-Core}$ corresponding to the region. Thus, this minutiae descriptor requires a template size smaller than that used in the traditional minutiae representation.

By using the features formulated as above, the proposed fingerprint representation (i.e. the fingerprint template) is defined as $MFV = \{\Re_{S_1}, \Re_{S_2}, \Re_{S_3}, \Re_1, \Re_2, ..., \Re_k\}$, in which $\Re_{S_i} = \{FV1_{S_i}\}$ corresponding to a singular region S_i and $\Re_i = \{FV1_i, FV2_i, FV3_i\}$ corresponding to a plain region i, where $FV1_i = (\zeta_i, \theta_{\Re_i-Core})$, $FV2_i = \{(\rho_{iq}, \theta_{iq}), q = 1, ..., Q\}$, and $FV3_i = \{\phi_i, Minu_i = \{(x_l, y_l, t_l), l = 1, ..., L\}\}$ contain, respectively, the global, neighborhood and local features for a plain region i. Hence, the size of the proposed MFV varies according to the number of the regions. Finally, one can expect the proposed fingerprint representation to be more accurate and reliable, since two different levels of structural features that are invariant to translation and rotation have been incorporated in the representation.

4.2.2 Core detection using FV2

The fingerprint ridges around a core point have a shape that is like a semi-circle in the case of an upper core, or have a shape that resembles a circle in the case of a whorl fingerprint. In these cases, the ridges on both sides of the core are almost parallel to each other; in other words, the orientations of these ridges are equal to each other. As motioned in the previous section, the detection of singular points (core and deltas) is carried out by analyzing the shapes represented by the orientation field. Unfortunately, this shape analysis technique cannot detect the core point in a situation when the quality of the fingerprint in the core region is poor (see Figure 4.2(a)), or when the location of the core point is very close to the boundary of the fingerprint (see Figure 4.2(b)). This is so, because in the shape analysis technique, the location of the core is determined by searching for a specific shape of the ridges, namely a cap or cup, in the fingerprint image. Thus, in this case (i.e., when the core is not successfully detectable) the formulation of the MFVs, in the proposed technique of fingerprint image decomposition, is carried out by using only the orientation field. Therefore, the resulting MFVs are an incomplete representation of the fingerprint, since it does not contain the information concerning the core region. However, in the proposed technique the FV2 component of the incomplete MFV can be used to detect the presence and the location of the core in a situation when it was not detected by the shape analysis technique. Thus, if the core information is not present in any of the MFVs formulated after the fingerprint decomposition, the relative orientation θ_{ij} of FV2 of the MFVs are checked. If θ_{ij} for a certain FV2 is found to be zero, we conclude that, there exists a core point between the regions i and j. The

corresponding MFV is then modified to reflect this fact. If none of FV2's are detected to have $\theta_{ij} = 0$, the fingerprint image is declared to have no core.

(a) (b)

Figure 4.2: Two examples of fingerprint images (a) Core with undesirable noise. (b) Incomplete core located at the image borders.

4.3 Multilevel Matching

The process of fingerprint matching is to compare the fingerprint templates of two fingerprint images and return a score between 0 and 1 representing the degree of similarity between the two fingerprint images, or a binary score of 0 or 1 indicating whether or not the fingerprint under consideration is the same as the reference fingerprint. The accuracy of the final decision and the response time are the two main concerns of a matching scheme. However, the requirements on the degree of accuracy and the response time of a matching scheme vary from one application to another. In this section, we propose a fingerprint multilevel matching (MLM) scheme using the MFVs formulated in Section 4.2. We denote the MFVs corresponding to the reference fingerprint template

retrieved from the database as $T = \{\Re_{S_1}, \Re_{S_2}, \Re_{S_3}, \Re_1, \Re_2, ..., \Re_M\}$ with M plain regions, and the MFVs corresponding to the template of the input fingerprint to be matched as $I = \{\Re_{S_1}, \Re_{S_2}, \Re_{S_3}, \Re_1, \Re_2, ..., \Re_N\}$ with N plain regions. As explained in the previous section, the formulation of FV1 depends on the presence of core region; therefore, in the case when the core point does not exist or it is undetectable, in the proposed multilevel matching scheme we use only FV2 and FV3 to report the final matching result between T and I.

On the onset, the proposed multilevel matching scheme determines whether or not both T and I belong to the same category. By using $\Re_{S_1}$, $\Re_{S_2}$, and $\Re_{S_3}$ for the templates T and I, the category of the fingerprint is identified as left loop, right loop, whorl, arch, or tended arch. If T and I are found to belong to the same category, then by using FV1 the best corresponding pairs of regions from T and I are found, and the degree of similarity, referred to as elementary similarity measure, between the two fingerprints is estimated. If the value of this elementary measure is equal to zero, then the proposed scheme reports a non-match and stops the matching process. Otherwise, the matching process moves on to the next level of matching, in which the calculations of the so called secondary similarity measure is carried out by using FV2 of T and I. If the value of this secondary estimate is equal to zero, a non-match is reported and further matching of T and I is stopped. Otherwise, the matching scheme moves on to a third level and a tertiary similarity between T and I is estimated by using FV3. Finally, the three degrees of similarities are combined to obtain the final matching result.

We now derive expressions for the three similarity measures of fingerprints, which in turn depend on functions representing the similarity of the regions from the T and I templates, using FV1, FV2, and FV3.

1) Similarity measure based on FV1= $\{\xi, \theta_{\Re-Core}\}$

For a plain region, the value of the first component ξ ranges from 1 to 8; therefore, in order to find the correspondence between two plain regions belonging to T and I, respectively, we first define a spatial distance function between the two plain regions $I_{\Re_j}$ and $T_{\Re_i}$ as

$$SD(\xi(I_{\Re_j}), \xi(T_{\Re_i})) = \min\left(\left| \xi(I_{\Re_j}) - \xi(T_{\Re_i}) \right|, 8 - \left| \xi(I_{\Re_j}) - \xi(T_{\Re_i}) \right| \right) \tag{4.3}$$

where $\xi(I_{\Re_j})$ and $\xi(T_{\Re_i})$ denote the values of the type and position features for the regions $I_{\Re_j}$ and $T_{\Re_i}$, respectively. An optimal similarity function between these two regions is then obtained by using the normalized difference of the orientation values $\theta_{\Re-Core}$ of the regions from T and I as [17], [27]

$$S_1(I_{\Re_j}, T_{\Re_i}) = \begin{cases} \exp\left(-\partial(I_{\Re_j}, T_{\Re_i}) \Big/ \mu \right) & \text{if } SD(\xi(I_{\Re_j}), \xi(T_{\Re_i})) \le 1 \\ 0 & \text{otherwise} \end{cases} \tag{4.4}$$

where $\partial(I_{\Re_j}, T_{\Re_i})$ is the normalized orientation distance [27] between the two regions $I_{\Re_j}$ and $T_{\Re_i}$ evaluated by using the equation

$$\partial(I_{\Re_j}, T_{\Re_i}) = \begin{cases} \dfrac{2}{\pi}\partial_0(I_{\Re_j}, T_{\Re_i}) & \text{if } \partial_0(I_{\Re_j}, T_{\Re_i}) \le \dfrac{\pi}{2} \\ \dfrac{2}{\pi}\left(\pi - \partial_0(I_{\Re_j}, T_{\Re_i})\right) & \text{otherwise} \end{cases} \tag{4.5}$$

with the symbol $\partial_0(I_{\Re_j}, T_{\Re_i})$ representing the orientation distance between the two regions $I_{\Re_j}$ and $T_{\Re_i}$, and evaluated as

$$\partial_0(I_{\Re_j}, T_{\Re_i}) = \begin{cases} \alpha_{ij} & if\ (\theta_{\Re-Core}(I_{\Re_j}).\theta_{\Re-Core}(T_{\Re_i})) \geq 0 \\ \min\left[\beta_{ij}, \pi - \beta_{ij}\right] & otherwise \end{cases} \tag{4.6}$$

where α_{ij} is the absolute difference of $\theta_{\Re-Core}(I_{\Re_j})$ and $\theta_{\Re-Core}(T_{\Re_i})$, and β_{ij} is the sum of their absolute values.

In order to find the best corresponding regions from I and T, the similarity between a region of the template I and a region of the template T is first calculated using (5). Then region $T_{\Re_i}$ is reported as a best corresponding region i.e. mate of $I_{\Re_j}$, if the similarity between them is greater than all other similarities between $I_{\Re_j}$ and the other regions from template T. Hence, for each region $j = 1,...,N$ from template I, its mate from regions from T can be formulated as

$$B(j) = \begin{cases} 0 & if\ S_1(I_{\Re_j}, T_{\Re_i}) = 0, \forall i = 1,...,M \\ k & otherwise \end{cases} \tag{4.7}$$

where k is the index of the region from template T that has maximum similarity with a region j of template I. Thus, a value $B(j) = 0$ implies that a region j in template I is not mated to any region in template T; hence, $S_1(I_{\Re_j}, T_{\Re_{B(j)}}) = 0$. Finally, the expression for the elementary similarity measure between I and T is obtained as

$$FV1(I,T) = \frac{1}{K}\sum_{j=1}^{N} S_1(I_{\Re_j}, T_{\Re_{B(j)}}) \tag{4.8}$$

where K is the number of mated regions.

2) Similarity measure based on FV2 = $\{\rho_{jq}, \theta_{jq}\}$

A plain region j has a group of neighbors $q = \{1,2,...,Q\}$ each having a pair $\{\rho_{jq}, \theta_{jq}\}$ to represent the neighborhood relationship. The spatial distance function $SD(\rho_{jq}(I_{\Re_j}), \rho_{ih}(T_{\Re_i}))$ between two regions h and q representing the neighbor of the region i in T and that j in I, respectively can be calculated using (4.3). In addition, the orientation distance function between these two neighboring regions h and q is defined as

$$\partial_0(\theta_{jq}(I_{\Re_j}), \theta_{ih}(T_{\Re_i})) = \begin{cases} \left|\theta_{jq}(I_{\Re_j}) - \theta_{ih}(T_{\Re_i})\right| & if\ (\theta_{jq}(I_{\Re_j}).\theta_{ih}(T_{\Re_i})) \geq 0 \\ \Delta & otherwise \end{cases} \tag{4.9}$$

By using the two distance measures, $SD(\bullet)$ given by (4.3) and $\partial_0(\bullet)$ given by (4.9), the neighborhood correspondence between a neighbor in T and that in I can be obtained as

$$SR(I_{\Re_j}(q), T_{\Re_i}(h)) = \begin{cases} 1 & if\ SD(\rho_{jq}(I_{\Re_j}), \rho_{ih}(T_{\Re_i})) \leq 1\ and\ \partial_0(\theta_{jq}(I_{\Re_j}), \theta_{ih}(T_{\Re_i})) < \Delta \\ 0 & otherwise \end{cases} \tag{4.10}$$

where Δ is the quantization step as specified in Section 3.4. Then, the overall similarity measure $S_2(I_{\Re_j}, T_{\Re_i})$ between two regions from T and I based on their neighborhood relationships is obtained as

$$S_2(I_{\Re_j}, T_{\Re_i}) = \frac{1}{F}\sum_{q=1}^{Q} \max\left\{SR(I_{\Re_j}(q), T_{\Re_i}(h)), h = 1,...,H\right\} \tag{4.11}$$

where F is the number of mated neighborhood correspondence.

Finally, the expression for the secondary similarity measure between I and T is obtained as

$$FV2(I,T) = \frac{1}{K}\sum_{j=1}^{N} S_2(I_{\Re_j}, T_{\Re_{B(j)}}) \tag{4.12}$$

where K is the number of mated regions.

3) Similarity measure based on FV3 = $\{\phi, \{(x_l, y_l, t_l), l = 1,..., L\}\}$

The similarity function between the two regions $I_{\Re_j}$ and $T_{\Re_i}$ based on the first component ϕ of the feature vector FV3 is defined as

$$CD(\phi(I_{\Re_j}), \phi(T_{\Re_i})) = \begin{cases} 1 & if \ \left|\phi(I_{\Re_j}) - \phi(T_{\Re_i})\right| \le \Delta/2 \\ 0 & otherwise \end{cases} \tag{4.13}$$

where $\phi(I_{\Re_j})$ and $\phi(T_{\Re_i})$ represent the values of the curvature features for the regions $I_{\Re_j}$ and $T_{\Re_i}$, respectively.

As for the second component of FV3, the minutiae set $Minu = \{(x_l, y_l, t_l), l = 1,..., L\}$, we first compare the set in a region of I with that of T to determine the mated minutiae. The two minutiae, $m_l(I_{\Re_j})$ and $m_q(T_{\Re_i})$ having the same type, are considered a mated pair if their Euclidean spatial distance $SD(m_l(I_{\Re_j}), m_q(T_{\Re_i}))$ is smaller than a pre-specified tolerance r_0, that is,

$$MD(m_l(I_{\Re_j}), m_q(T_{\Re_i})) = \begin{cases} 1 & SD(m_l(I_{\Re_j}), m_q(T_{\Re_i})) \le r_0 \ and \ t_l(I_{\Re_j}) = t_q(T_{\Re_i}) \\ 0 & otherwise \end{cases} \tag{4.14}$$

Then, a similarity measure using the minutiae set of FV3 is obtained as

$$SM(Minu(I_{\Re_j}), Minu(T_{\Re_i})) = \frac{1}{L}\sum_{l=1}^{L} \max\left\{ MD(m_l(I_{\Re_j}), m_q(T_{\Re_i})),\ q = 1,..., Q \right\} \tag{4.15}$$

where L is the total number of minutiae in $I_{\Re_j}$. The overall similarity measure $S_3(I_{\Re_i}, T_{\Re_l})$ between two regions based on FV3 can be defined as

$$S_3(I_{\Re_j}, T_{\Re_i}) = 0.5\left(SM(Minu(I_{\Re_j}), Minu(T_{\Re_i})) + CD(I_{\Re_j}(\phi), T_{\Re_i}(\phi))\right) \tag{4.16}$$

The tertiary similarity score between I and T using the K pairs of mated regions, is given by

$$FV3(I,T) = \frac{1}{K}\sum_{j=1}^{N} S_3(I_{\Re_j}, T_{\Re_{B(j)}}) \tag{4.17}$$

The final similarity score between I and T is obtained as a weighted sum of the similarity measures given by (4.8), (4.12) and (4.17) as

$$S(I,T) = w_1 . FV1(I,T) + w_2 . FV2(I,T) + w_3 . FV3(I,T) \tag{4.18}$$

where the values of the weights w_1, w_2 and w_3 can be adjusted depending on the nature of the fingerprint images.

The proposed fingerprint multilevel matching scheme described in the preceding paragraphs can now be summarized as an algorithm.

Algorithm 4.1: Multilevel fingerprint matching

1- For each region $j = 1,...,N$ of template I

   a. For each region $i = 1,...,M$ of template T

      - Compute $Similarity\_matrix(i,j) = S_1(I_{\Re_j}, T_{\Re_i})$ using (4.4).

   b. $mated\_score_1(j) = Max(Similarity\_matrix(1:M, j))$.

   c. Compute $B(j)$ using (4.7).

2- By using the $mated\_score_1$, calculate the elementary similarity measure $FV1(I,T)$ using (4.8). If $FV1(I,T) = 0$, then report a non-match and exit; otherwise go to step 3.

3- For each region $j = 1,...,N$ of template I

   a. Let $i = B(j)$.

   b. Compute $mated\_score_2(j) = S_2(I_{\Re_j}, T_{\Re_i})$ using (4.11).

4- By using the $mated\_score_2$, calculate the secondary similarity measure $FV2(I,T)$ using (4.12). If $FV2(I,T)=0$, then report a non-match and exit; otherwise go to step 5.

5- For each region $j=1,...,N$ of template I

   a. Let $i=B(j)$.

   b. compute $mated\_score_3(j)=S_3(I_{\Re_j},T_{\Re_i})$ using (4.16).

6- By using the $mated\_score_3$, calculate the tertiary similarity measure $FV3(I,T)$ using (4.17).

7- Compute the total similarity score between T and I using (4.18).

As mentioned earlier, in the case when the core point does not exist or it is undetectable, we use only FV2 and FV3. In such a case, FV2 is used to find the mated pairs of regions instead of using FV1. Thus, $S_1(I_{\Re_j},T_{\Re_i})$ is replaced by $S_2(I_{\Re_j},T_{\Re_i})$ in (4.7) for finding the list of mated regions, B.

In the case of traditional minutiae-based matching schemes, the matching decision depends on the comparison results of all the minutiae from the two fingerprint templates. This implies that a large number of comparisons are required. In addition, the majority of the minutiae-based matching schemes require a pre-alignment step [1]. However, the proposed multilevel matching algorithm requires comparisons of the minutiae only from the corresponding regions. Hence, the number of comparisons is much smaller than that required by the traditional techniques. As an example, consider two fingerprint templates each with 40 minutiae. A traditional minutiae-based matching scheme with an absolute pre-alignment technique [1] requires 40×40 = 1600 comparisons. On the other hand, for

the proposed matching scheme with the fingerprints assumed to be decomposed into 10 regions, each on the average having 4 minutiae, only 10×10 = 100 comparisons are required to find the mated regions. Since another (4×4) comparisons would be required to find the mated minutiae for each region, the total number of comparisons required for the proposed scheme is 100 + 10 (4×4) = 260. Thus, for this example, the required number of comparisons in the proposed method is only 16% of that required by a traditional method. The reduction in the number of comparisons enhances the overall performance especially for the AFIS, since it conducts one-to-many comparisons to establish the identity of an individual. Finally, it is to be noted that the proposed method does not require a pre-alignment step prior to the fingerprint matching, since it is possible to determine the correspondence between different parts of the fingerprint images by using the formulated fingerprint representation without any alignment. Therefore, the proposed matching algorithm has a lower computational complexity compared to the minutiae-based matching schemes.

4.4 Experimental Results and Comparisons

In this section, we first discuss the choice of the databases and suitability of their use for a critical examination of the proposed fingerprint recognition scheme. Next with the chosen databases, the performance of the proposed multilevel structural fingerprint recognition scheme is studied and compared with that of some of the recently proposed algorithms.

4.4.1 Databases

Our main concern in choosing a fingerprint database for experimentation is to ensure that the fingerprint images contained therein represent the real life situations, meaning that the images have been collected under unsupervised conditions and without a quality check. The public domain databases from Fingerprint Verification Competitions (FVC), i.e., FVC2000 [43], FVC2002 [44], FVC2004 [41], and FVC2006 [45, 46] satisfy that concern. Each of these FVCs contains four different benchmark databases, namely, DB1, DB2, DB3, and DB4. The first three databases consist of real-life fingerprints and they have been acquired by using different types of sensors. The fourth one has been created by using a synthetic fingerprint generator (SFinGe). In the first three FVCs, each database contains 8 impressions of a finger with different qualities of the image and may contain the images of a finger even only partially. Each database contains 110 fingers, i.e., a total of 880 fingerprints. The fingers numbered 101 to 110 (set B) have been selected for training and estimating the parameter values, and the rest of the fingers, numbered 1 to 100 (set A), are used for testing. In FVC2006, each database contains 150 fingers with 12 impressions of each, i.e. a total of 1800 fingerprints, which have been also divided into sets A and B.

Since the proposed scheme uses both the global features of fingerprint (i.e. singular points and ridge orientations) and the local features (i.e. minutiae), in order to test the efficacy of our scheme, we must make sure to choose databases in which the fingerprints are not necessarily biased in favor of these features. The fingerprint images in FVC2002 (DB1 and DB2) have been designed using large-area touch sensors with a wide variations in the amount of rotation and translation; therefore, they have significant

bearing on the global features and to a certain extent on the local features as well. On the other hand, the fingerprint images of FVC2002 (DB3 and DB4) have been designed using smaller-area touch sensors and the images in these databases frequently consist of partial fingerprints. Thus, these fingerprints significantly affect the local features and to a lesser extent the global features as well. The fingerprint images of FVC2004 databases have been designed using large-area touch sensor (DB1), medium- and small-area touch sensors (DB2 and DB4), and a sweep sensor (DB3), and the fingerprints in all these databases have the main characteristic of plastic distortion [1]. Therefore, the fingerprints in these databases affect almost invariably the global features even when a fingerprint does not have a translation or rotation. Finally, the fingerprint images of FVC2006 databases have been designed using small-area touch sensor (DB1), large- and medium-area touch sensors (DB2 and DB4), and a sweep sensor (DB3). It is noted that FVC2006 DB1 has been classified as a database with a high degree of difficulty [1]. Based on the above consideration of possible distortions in fingerprints that affect their global and local features, we chose the databases FVC2002 (DB1, DB3, and DB4), FVC2004 (DB1 and DB2) and FVC2006 (DB1) to evaluate the proposed fingerprint recognition scheme. Table 4.1 provides a summary in terms of the fingerprint size, resolution and the source of acquisition of the selected databases [41, 44–46]. In our tests, we follow the experimental protocols proposed in [40]

Table 4.1: Summary of the databases selected for experimentation

	FVC2002			FVC2004		FVC2006
	DB1	DB3	DB4	DB1	DB2	DB1
Sensor type	Optical sensor	Capacitive sensor	SFinGe v2.51	Optical sensor	Optical sensor	Electric field sensor
Image size	388x374	300x300	288x384	640x480	328x364	96x96
Resolution	500 dpi	500 dpi	~ 500 dpi	500 dpi	500 dpi	250 dpi

4.4.2 Parameters Selection and Performance

First, sets B of the databases selected are used to find the best values of the parameters needed for the implementation of the proposed scheme. For the proposed fingerprint decomposition algorithm, the most reasonable block size N is selected as two times the ridge width of a fingerprint to provide a compromised performance between the recognition accuracy and complexity. In order to generate the quantized orientation field $\mathbf{O}_q$, three different quantization levels were tested on the orientation field. By using a 4-level quantization, the quantized orientation field becomes too crude which affects the recognition accuracy. On the other hand, a 16-level quantization has an adverse effect on the computational complexity of the algorithm. In view of these considerations, an 8-level quantization (i.e., a quantization step $\Delta = 22.5$) is chosen to generate $\mathbf{O}_q$. Accordingly, the maximum number of plain regions extracted by the proposed decomposition algorithm is sixteen. The value of the parameter μ used in the matching algorithm is empirically (based on the training set) fixed to be $1/6$ for calculating the similarity measure $S_1(I_{\Re_j}, T_{\Re_i})$. The values assigned to the weights w_1, w_2 and w_3 are based on the following consideration. The weights w_1 and w_2 are associated with the global features, and w_3 with the local features of the fingerprint. Since minutia is the most important feature in the fingerprint recognition, we provide the largest weight to w_3, with the remainder of the total weight being divided between w_1 and w_2, which are associated with the global features based on the core point(s) and the neighborhood relations of the ridges, respectively. However, this remainder of the total weight is completely assigned to w_2, if the core does not exist. When the fingerprint images are

captured using small- or medium-area sensors, it is quite likely that some or many of the images are only partial. In such a case, the number of minutiae in an image is smaller. Consequently, for the databases designed using small- or medium-area sensors, the value of weight assigned to w_3 can be reduced and that to w_1 correspondingly increased. The reason for assigning more weight to w_1 is that in case of partial fingerprint images, the global features based on the core point is more reliable than the one based on the neighborhood relations, since the available information on the ridges is now less. Table 4.2 gives a summary on the values assigned to the weights w_1, w_2 and w_3 for the various databases.

Table 4.2: The values of the weights used for the selected databases

Weight	FVC 2002						FVC 2004				FVC 2006	
	DB1		DB3		DB4		DB1		DB2		DB1	
	With core	w/o core	With core	w/o core	With core	w/o core	With core	w/o core	With core	w/o core	With core	w/o core
w_1	0.2	0	0.25	0	0.25	0	0.2	0	0.25	0	0.25	0
w_2	0.2	0.4	0.2	0.45	0.2	0.45	0.2	0.4	0.2	0.45	0.2	0.45
w_3	0.6		0.55		0.55		0.6		0.55		0.55	

In order to study the performance of the proposed MSFR scheme, the algorithms for the fingerprint representation and matching are implemented on a machine with a 1.8 GHz CPU and 512 MB RAM. The average enrollment (fingerprint representation) time is found to be 0.23 s for the fingerprint images of the six selected databases. Table 4.3 shows the performance of the proposed scheme in terms of equal error rate (EER) [1], and the average CPU times for the fingerprint decomposition and the template formulation components of the fingerprint representation and the average CPU time of the matching, using the six selected databases. It is seen from this table that the proposed scheme for the fingerprint decomposition and the formulation of the template together

require on the average only 22% of the average enrollment time. In addition, the proposed MLM scheme provides a very short matching decision time (i.e. only a few milliseconds). Accordingly, the proposed MLM scheme yields a very good performance for large scale database applications.

Table 4.3: The performance of the MSFR on the selected databases

	FVC 2002			FVC 2004		FVC 2006
	DB1	DB3	DB4	DB1	DB2	DB1
EER (%)	2.57 %	6 %	2.81 %	2 %	3.2 %	5.21%
Fingerprint decomposition (ms)	30	25	25	34	35	37
Template formulation (ms)	20	18.5	16.5	27	24	8.6
Matching (ms)	6.2	3.9	3.6	6.24	5.3	2.5

4.4.3 Comparisons with Previous Works

The proposed scheme is compared in terms of ROC (false rejection rate (FRR) versus false acceptance rate (FAR)) curves, EER and template size with four representative works, which adopt some global features, namely the orientation field and/or the core point, in conjunction with the local feature minutiae into the formulation of the fingerprint template and matching. The first scheme proposed by Tico et al. [17] uses an orientation-based minutia descriptor that comprises information about the orientation field in a broad region around a minutia point. The second scheme, due to Qi et al. [18], proposed the use of a curvature-based minutia descriptor that uses the orientation field to calculate the curvature of the ridges around the minutia point. These two schemes can be categorized as minutiae based matching schemes, in which a large number of samples around the minutia are required in order to formulate each minutia descriptor; accordingly the template formulation has a large computational complexity. Compared

with these two schemes, the proposed MSFR scheme formulates the fingerprint template by using a simpler minutia descriptor, in addition to the global features, as explained in Section 4.2. Figure 4.3 depicts the ROC curves for FVC2002 DB1 obtained by using the proposed scheme as well as the schemes of [17] and [18]. It is seen from this figure that the accuracy of the proposed MSFR scheme is better than that of Tico et al. The accuracy of the proposed scheme is also better than that of Qi et al. except for the region FAR< 0.1% when the accuracy of the latter becomes slightly better. This slight improvement in the accuracy of the scheme of Qi et al. is achieved at the expense of a larger computational complexity associated with their minutiae descriptor. However, our proposed scheme provides a lower EER (2.5%) compared to that provided by Qi et al. (3.4%) or Tico et al. (4.5%).

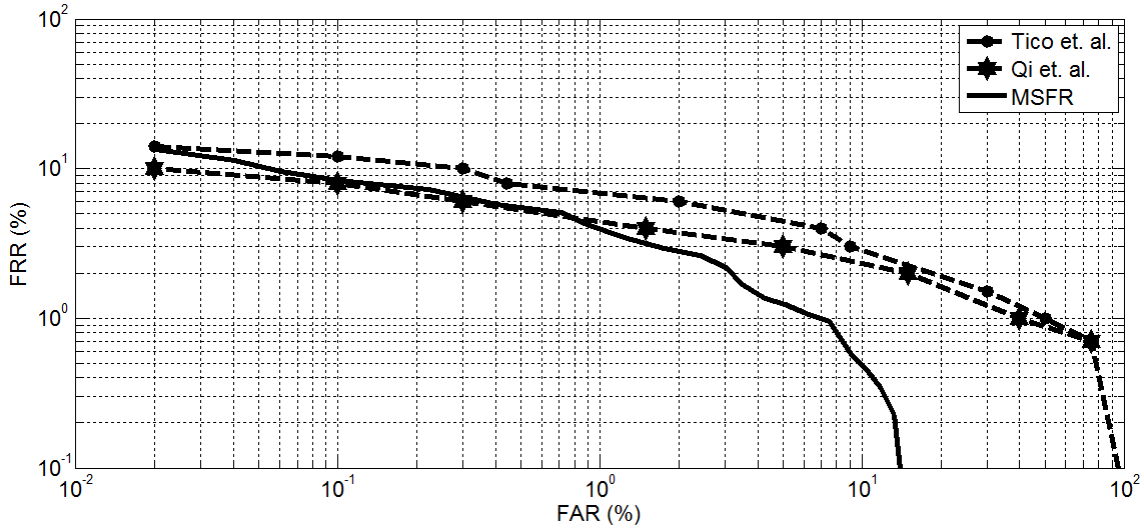

Figure 4.3: ROC curves for FVC2002 DB1 obtained by using the proposed MSFR scheme, the Tico et al. scheme [17] and Qi et al. scheme [18].

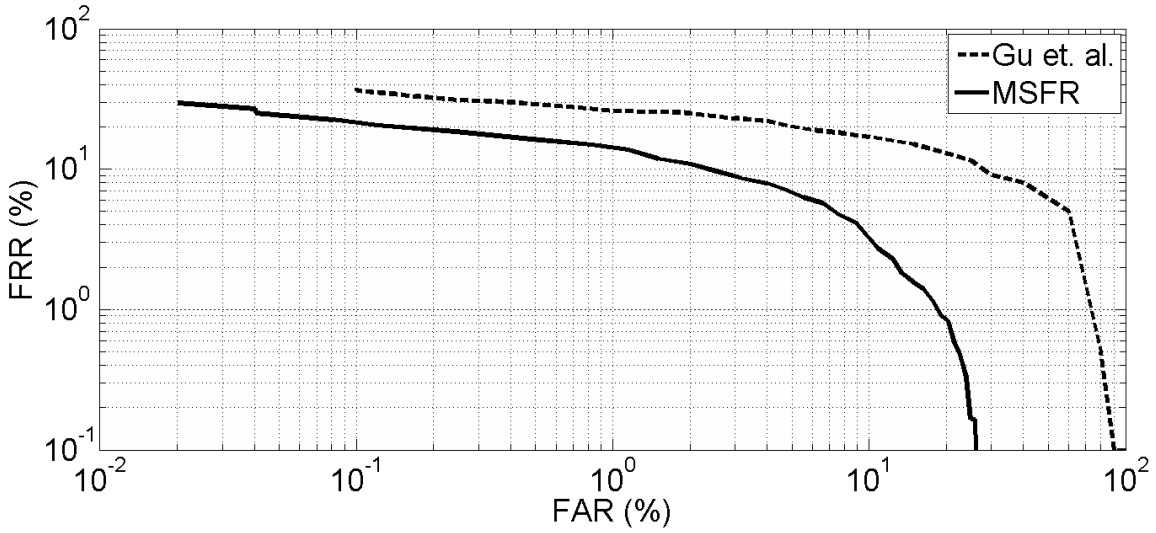

(a)

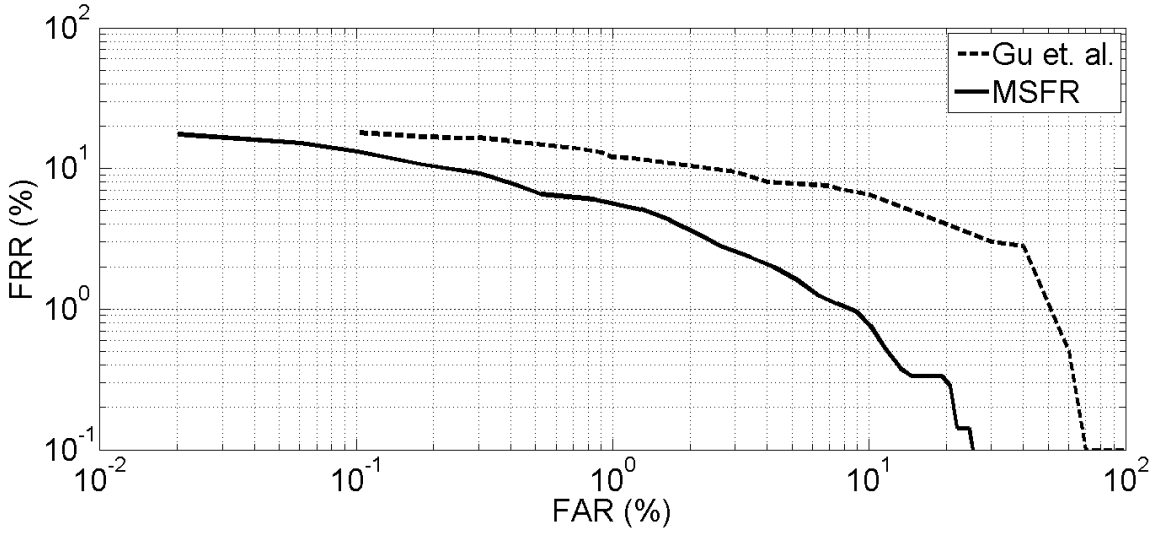

(b)

Figure 4.4: ROC curves for FVC2002 (a) DB3 and (b) DB4 obtained with the proposed MSFR scheme and Gu et al. scheme [27].

In the third scheme, Gu et al. [27] have proposed the use of a model-based fingerprint orientation field, as a global feature, in combination with the extracted minutiae set for the purpose of matching. Their so-called combination model models the real and the imagery parts of the vector field of the orientation field with two bivariate

polynomials, respectively [27]. Compared with this scheme, the proposed one uses directly the orientation field in addition to the singular points as a global feature, as explained in Section 4.2. Figure 4.4 depicts the ROC curves obtained by using the proposed scheme as well as the scheme of [27] on databases FVC2002 (DB3 and DB4). These ROC curves show that the overall accuracy of the proposed MSFR scheme is much higher than that of [27] for both the databases. In addition, for the databases DB3 and DB4, the proposed scheme provides EERs of 6% and 2.8%, respectively, which are lower than the values of 15% and 7.2% provided by the scheme of [27].

In the fourth scheme, Shi et al. [28] have proposed a fast fingerprint matching algorithm, which is based on a novel structure for fingerprint representation. They formulate a fingerprint template by combining the singular point with its neighborhood minutiae. Compared to this scheme, the proposed MSFR scheme uses singular points and orientation field in addition to all the available minutiae in the fingerprint image not just a limited number of minutiae within the neighborhood of the singular point. Therefore, the proposed scheme can be expected to be more robust than the one presented in [28]. Moreover, the scheme given in [28] would fail whenever singular points are not detected in the fingerprint. Figure 4.5 depicts the ROC curves obtained by using the proposed scheme as well as the scheme of [28] on FVC2004 DB1 database. It is seen that the accuracy of our MSFR scheme is much higher than that provided by the scheme of [28]. In addition, the proposed scheme provides an EER of 2% compared to that of 9.25% provided by the scheme of [28].

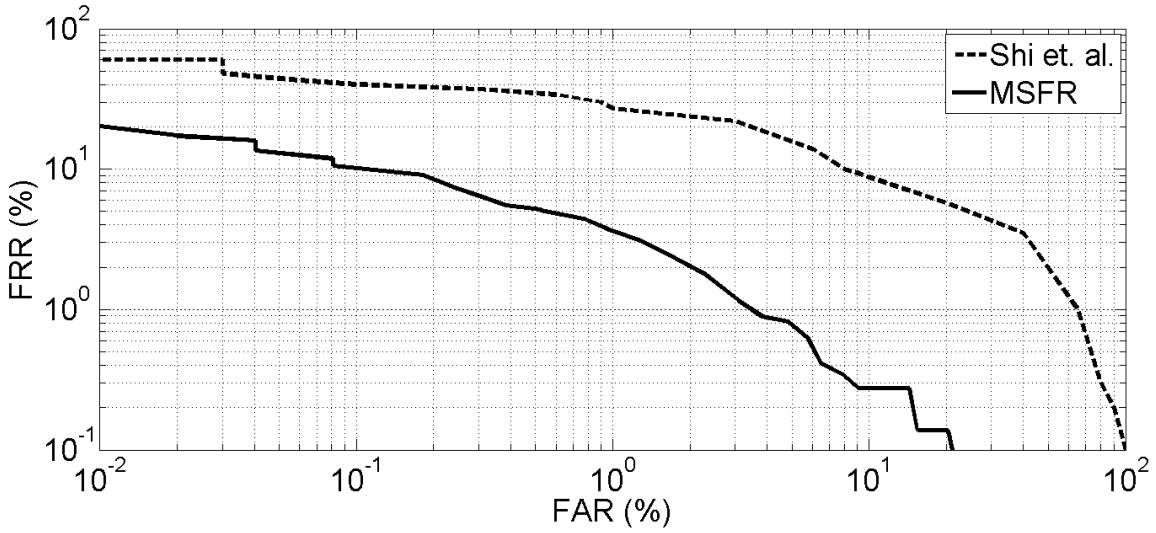

Figure 4.5: ROC curves for FVC2004 DB1 obtained with the proposed MSFR scheme and Shi et al. scheme [28].

Table 4.4 gives the template sizes, in bytes, of the proposed and the four schemes that have been used to benchmark the proposed one. The template sizes given in this table, either estimated or reported in the respective references, are based on the assumption that the average number of detected minutiae of a fingerprint is 40. Based on the formulation of the multilevel features (MFV) in Section 4.2, each of ξ, ρ_{ij} and ϕ_i need only one byte; whereas $\theta_{\Re-Core}$ and θ_{ij} need two bytes. By assuming the average number of adjacent regions Q associated with a given region to be 3, each plain region needs only 13 bytes. Based on the assumption that the average number of detected minutiae of a fingerprint is 40, the minutiae require 120 bytes. Thus, by assuming the average number of the plain regions to be 10 and number of singular regions 3, the size of MFV is 3x1 + 10x13 + 120= 253 bytes. It is seen from Table 4.4 that the proposed scheme and the one due to Gu et al. [27] require the smallest template size.

Table 4.4: Comparison with previous works in terms of template size.

	Tico et al. [17]	Qi et al. [18]	Gu et al. [27]	Shi et al. [28]	MSFR
Template size (byte)	2480	2480	337	800	253

Finally, the results of the proposed MSFR scheme are compared with those published in the FVC2004 [41] and FVC2006 competitions [46]. Depending on the template (model) size, the enrollment and the matching times, the entries to this competition were categorized as light or open category. In order for a scheme to be included in the light category of these competitions, the maximum allowable values for the template size, enrollment and the matching times were as listed in Table 4.5. In FVC2004 and FVC2006 competitions, various schemes were tested using a CPU of 1.4 GHz and 512-MB RAM and a CPU of 3.2 GHz and 1-GB RAM, respectively. Since the proposed MSFR scheme is run on a 1.8-GHz CPU, the processing times are re-scaled to correspond our results to the 1.4-GHz and 3.2-GHz CPUs of these competitions.

Table 4.5: Requirements of the light category for FVC2004 and FVC2006 competitions

Competition	Template size	Average enrollment time (s)	Average matching time (s)
FVC2004	2 Kb	0.5	0.3
FVC2006	2 Kb	0.3	0.1

Table 4.6 gives the EER results along with the template size, average enrollment time and the average matching time for the proposed MSFR scheme as well that for the best schemes in the light and open categories of the FVC2004 competition using databases DB1 and DB2. It can be seen from this table that the proposed scheme belongs to the light category. This table shows that the overall performance of the proposed scheme is better than the best schemes in the light category for both the databases. Moreover, the performance of the proposed scheme is quite impressive even in the open category. The EER results of the proposed scheme are comparable to the best scheme

using DB1 and to the fourth best one using DB2 in the open category. Table 4.7 gives the performance results of the proposed MSFR scheme along with the best schemes in the light and open categories of the FVC2006 competition using database DB1. This table shows that the overall performance of the proposed scheme is better than the best schemes in both categories for FVC2006 DB1.

Table 4.6: Comparison with FVC2004 results.

		EER(%)	Template size (byte)	Average enrollment time (s)	Average matching time (s)
DB1	MSFR	2 %	253	0.3	0.011
	Best light	3.89 %	1100	0.25	0.21
	Best open	1.97 %	1400	1.95	1.87
DB2	MSFR	3.2 %	253	0.3	0.009
	Best light	4.01 %	1000	0.23	0.23
	4th best open	3.17 %	40900	0.33	0.35

Table 4.7: Comparison with FVC2006 results.

		EER(%)	Template size (byte)	Average enrollment time (s)	Average matching time (s)
DB1	MSFR	5.2 %	253	0.070	0.001
	Best light	5.35 %	1940	0.031	0.029
	Best open	5.56 %	1220	0.038	0.039

4.5 Summary

In order to provide improved accuracy in fingerprint recognition, many researchers in recent years have proposed the use of the fingerprint information that is complementary to that contained in minutiae. The use of this additional information, however, results in a larger size fingerprint template and an increased complexity in its formulation in comparison to the traditional approaches using only minutiae. In Chapter 3, a fingerprint decomposition technique was developed to partition fingerprint images into a set of singular and plain regions by using two global features. In this chapter, by using this set

of decomposed regions, i.e. singular and plain regions, a fingerprint template has been formulated as three-level feature vectors with levels for global, neighborhood, and local features. The first two levels represent the position and ridge orientation of a region with respect to the core and its adjacent regions, respectively, whereas the third one represents the region's local features of curvature and minutiae of its ridges. The idea of using multilevel feature vectors (MFVs) ensures that the fingerprint template contains all the available useful information from the fingerprint image. In the proposed three-level representation, the features have been formulated using simple mathematical operations and thus have not resulted in a significant increase in the complexity of the template representation over these of single-level minutiae based representations. As a matter of fact, the template representation complexity of the proposed scheme has been found to be even less than that of some of the existing minutiae based schemes.

Based on the proposed MFVs, a very fast fingerprint matching scheme, referred to as multilevel matching (MLM) scheme, has been developed. In this scheme, the correspondence problem is dealt with by making use of the global feature components of the MFVs, whereas the similarity problem is taken care by employing all the three levels of features contained in the MFVs. The fast matching speed can be attributed to the following two features of the proposed scheme: 1) a significantly reduced number of comparisons required to provide the matching decision, and 2) the strategy of an early rejection that allows the MLM scheme to skip the second and/or third levels of matching. As a result, the proposed scheme could be very attractive for fingerprint identification applications involving large scale databases.

In order to study the performance of the proposed scheme, comprehensive experiments have been conducted using six benchmark databases from FVC2002, FVC2004 and FVC2006. These databases have been selected to show the robustness of the proposed scheme against a wide variety of challenges in fingerprint recognition. Experimental results have shown that the average template size in the proposed fingerprint representation scheme is 253 bytes and the average enrollment and matching time is about 0.23 s. The proposed scheme has been compared in terms of the ROC curve, the equal error rate, and the template size with the existing schemes that also use some of the global features of the fingerprint in addition to the local minutiae attributes for fingerprint representation and matching. The results of the proposed scheme have also been compared with some of the best results published from FVC2004 and FVC2006 competitions. The evaluation study has shown that the proposed scheme for fingerprint recognition and representation provides a performance superior to those of the other schemes used for an objective comparison.

CHAPTER 5

A Histogram Analysis Fuzzy C-Means Based Technique for Fingerprint Partitioning and its Application for Singular Point Detection

5.1 Introduction

The benefit of using artificial intelligence techniques for solving many pattern recognition problems or for image understanding and interpretation have been shown by many researchers [47, 68–77]. In a particular, considerable amount of research work has been devoted to the area of fingerprint recognition using artificial intelligence techniques. In these studies it has shown that the use of artificial intelligence techniques enhances the performance accuracy of the fingerprint recognition systems [10], [20], [22]. Some researchers have proposed the use of the neural networks for fingerprint classification [10, 78–81], or for minutiae filtering [82]. In addition, some other researchers have proposed the use of fuzzy neural networks for minutiae recognition [83, 84], or for fingerprint verification [85, 86]. An extensive review on the use of artificial intelligence techniques for fingerprint related research area is provided by Maltoni *et al.* [1] and Jain *et al.* [87].

As mentioned in Chapter 1, the orientation field (OF) of the fingerprint image has been used extensively for the fingerprint recognition [1, 17, 18, 27]. The idea of using the orientation field for partitioning fingerprint images into non-overlapping regions has been

proposed by many researchers [1]. Most of these OF-based partitioning schemes have been used for fingerprint classification [10–12] or for singular points detection [66, 67]. These partitioning schemes could be categorized into two groups: 1) Iterative clustering techniques that minimize some cost function, representing the non-homogeneity of the fingerprint region, with respect to its ridge orientations [10–12]. 2) Partitioning techniques for the fingerprint images based on a pre-specified number of discretization levels for the orientation field [39, 66, 67], where the number of partitioning levels is dictated by the specific application for which the partitioning is carried out. The OF-based partitioning schemes in either category are faced by challenges, such as the cuts and deformations of the fingerprint ridges or the low quality fingerprint images. In order to overcome these challenges, the use of an image enhancement technique prior to partitioning became a mandatory step [66, 67].

All the OF-based partitioning techniques in the literature provide only crisp (hard) clustering of the orientation field in that each image pixel (or block) is assigned to one and only one cluster. As mentioned in Chapter 2, the use of fuzzy-based clustering techniques has been shown to be capable of providing better results in solving many problems in pattern recognition and image processing fields [47, 50, 52–59, 72–76]. The fuzzy-based clustering techniques provide a smoother classification of a dataset by assigning each pattern to all the clusters with different degrees of membership. Therefore, these fuzzy-based clustering techniques should be able to deal more effectively with the natural patterns, in which the objects cannot be classified to belong exclusively to one cluster. In the light of above mentioned difficulties of cuts and deformations of the fingerprint ridges or the low quality fingerprint images, the use of a fuzzy-based

clustering technique would be able to assign the affected image blocks to more than one cluster. This reflects the fact that these blocks have an uncertainty problem, which can be solved using some rule-based technique [47, 61].

The most popular heuristic for solving the problem of fuzzy clustering is the so-called fuzzy c-means method (FCM) [51]. In this chapter, a novel histogram analysis based FCM (HA-FCM) technique for fingerprint partitioning is proposed [88]. Then, based on this technique a method for singular point detection is developed. Experiments using challenging benchmark databases are carried out to demonstrate the effectiveness of the proposed techniques for both fingerprint partitioning and singular points detection, and the results are compared with those of other state-of-the-art techniques.

5.2 HA-FCM Based Technique for Fingerprint Image Partitioning

In this section, a fuzzy c-means technique for fingerprint partitioning based on the ridge orientations is developed. The use of FCM allows the fingerprint image to be partitioned into overlapping homogeneous regions. The original FCM technique [51] has two main concerns. 1) It requires *a priori* knowledge of the number of clusters. In many cases, the number of clusters could be determined based on the application of the data partitioning, for example, in the image segmentation application [52–59], the partitioning is carried out using two clusters (i.e. background and foreground of the image). However, in the partitioning of a fingerprint image based on ridge orientations, the number of clusters depends on the dynamic range of the orientations, which varies for different fingerprint images. 2) Based on the initial choice of the cluster centers, the convergence rate of the FCM algorithm and the cluster quality vary. Specifically, if the FCM algorithm is to be applied to the orientation based fingerprint partitioning the homogeneity of the clusters

will depend on the initial choice of the clusters centers. Therefore, if an FCM algorithm has to be used in the orientation based homogenous fingerprint partitioning, the above two concerns, namely the number of clusters and the initial choice of clusters centers, have to be effectively dealt with. The histogram of a dataset provides information on the frequencies of occurrences of different patterns. In the proposed partitioning scheme, the histogram of the orientation field is used to deal with the above two problems of the original FCM algorithm.

5.2.1 Standard FCM algorithm

In order to classify n patterns into c clusters, the problem of FCM clustering is formulated as follows. Assume that n patterns in d-dimensional space is represented by $X = \{x_1, x_2, ..., x_n\}$, where $x_i = (x_{i1}, x_{i2}, ..., x_{id})$, $i = 1,2,...,n$. Therefore, the x_{ik} represents the k^{th} attribute (or feature) associated with pattern i. Let U be a matrix of size $n \times c$, where its item u_{ij} denotes the membership degree for the pattern i with respect to the cluster j, with the following two constraints:

$$\sum_{j=1}^{c} u_{ij} = 1, \forall i = 1,2,...,n \tag{5.1}$$

$$0 \le u_{ij} \le 1, \forall i = 1,2,...,n; \forall j = 1,2,...,c \tag{5.2}$$

The FCM algorithm is an iterative optimization that minimizes the objective function defined as follows [51]:

$$J_m = \sum_{j=1}^{c} \sum_{i=1}^{n} u_{ij}^{m} \left\| x_i - v_j \right\|^2 \tag{5.3}$$

where,

- m is a tuning parameter which controls the degree of fuzziness in the clustering process. The FCM iterative algorithm works under condition that $m > 1$, and usually $m = 2$.
- $V = \{v_1, v_2, ..., v_c\}$ is a set of the centers of the clusters, where $v_j = (v_{j1}, v_{j2}, ..., v_{jd})$ is the center of the j^{th} cluster.
- $\|\cdot\|$ is the Euclidean distance defined on R^d.

Then, the optimal fuzzy clustering structure of the set X is obtained as a solution of the non-linear programming problem in variables (U, V). Note that by fixing V the problem of the non-linear programming reduces to that of finding U and vice versa. The steps of iterative algorithm for the FCM clustering using the non-linear programming are given below.

Algorithm 5.1 : FCM Clustering

1- Let $V(0) = \{v_1, v_2, ..., v_c\}^0$ be an initial set of the centers of the clusters. Fix the values of m, ε and M, where ε is a small positive constant and M is the maximum number of iterations.

2- For $t = 1 : \text{M}$

- By using the set $V(t-1)$ calculated in iteration $(t-1)$, compute the optimal $u_{ij}^{(t)}$, $\forall i = 1,2,...,n$ and $\forall j = 1,2,...,c$ using the following equation:

$$u_{ij}(t)=\begin{cases}\dfrac{\left\|x_i-v_j(t-1)\right\|^{-2/(m-1)}}{\sum_{l=1}^{c}\left\|x_i-v_l(t-1)\right\|^{-2/(m-1)}}, & x_i \neq v_l(t-1)\ ,\ \forall l=1,2,...,c \\ 1, & x_i=v_j(t-1) \\ 0, & x_i=v_q(t-1),\ \forall q=1,2,...,c \text{ and } q\neq j\end{cases} \tag{5.4}$$

- Compute the center vectors $v_j(t)$, $\forall j=1,2,...,c$, with fixed $u_{ij}(t)$, using the following equation:

$$v_j(t)=\frac{\sum_{i=1}^{n}(u_{ij}(t))^m\ x_i}{\sum_{i=1}^{n}(u_{ij}(t))^m} \tag{5.5}$$

- If $\left\|J_m(t)-J_m(t-1)\right\|<\varepsilon$, stop.

Table 5.1 gives the centers of clusters, the values of the objective function and the number of iterations of using the FCM algorithm to classify the set of numbers $X=[1,2,3,4,5,6,7,8,9,10]$ into four clusters based on five different initial choices for the cluster centers. The table also gives the Euclidean distance between the initial and final cluster centers.

It is seen from this table that the solutions, i.e. the cluster centers and the value of the objective function, by using the FCM algorithm depend mainly on the initial choice of the cluster centers. In addition, the number of iterations required by the FCM to reach a solution depends on the distance from the initial set of cluster centers to the final set. For example, the solutions 1 and 2 provide identical cluster centers. However, solution 2 reaches the final solution faster (30 versus 41 iterations), since the choice of initial cluster centers in this case is closer (as indicated by the distances) to the final solution. It is noted

the choice of initial cluster centers in solution 2 is closer to final solution, since the initial cluster centers in solution 2 is more aligned with the distribution of the numbers in the dataset X. The same conclusions can be drawn from solutions 3 and 4. Finally, we have considered yet another solution to this clustering problem, namely solution 5. this solution is the best among all the solutions considered both in terms of the number of iterations and the minimum of the objective function achieved, since in this case the initial cluster centers is more aligned with the distribution of the data points in X. Hence, the solution 5 reinforces the importance of the distribution of the initial centers with respect to the dataset to be clustered.

Table 5.1: An illustrative numerical example

Solution	1	2	3	4	5
Initial centers	4.9818 5.5121 5.8248 5.851	3.4877 5.0594 6.0009 6.2576	5.1663 5.213 5.2586 6.6392	4.8022 5.0699 6.1672 6.6479	1.5 4.5 6.5 9.5
Centers	1.6462 4.2159 6.7972 9.3587	1.6462 4.2159 6.7972 9.3587	1.6414 4.2030 6.7843 9.3539	1.6414 4.2030 6.7843 9.3539	1.6445 4.2104 6.7896 9.3555
Objective function	3.602221	3.602221	3.602219	3.602219	3.602198
Distance	5.1045	3.7886	4.8107	4.2948	0.4577
Iterations	41	30	46	23	10

5.2.2 The proposed scheme for determining the number of clusters and their initial centers for fingerprint partitioning

As mentioned earlier, in order to apply the FCM to partition the fingerprint image, the exact number of clusters and initial choice of the cluster centers need to be known. In the

previous subsection, however, we have seen the importance of the initial choice of the cluster centers in the clustering problem of datasets. In this subsection, a new technique of determining the number of clusters and initial choice of their centers is developed for the clustering problem at hand, namely partitioning the fingerprint image based on the orientation field. Since the histogram of the orientation field of a fingerprint can provide a map of the occurrence frequencies of the orientations in the range $[0,\pi)$, it can be used rationally in deciding the number and the initial choice of the cluster centers in the FCM algorithm. To emphasize this point, consider the fingerprint images and the corresponding histograms of their orientation field shown in Figure 5.1. Figures 5.1(a) and (b) illustrate the examples of the histograms of fingerprints covering the entire range $[0,\pi)$ of the orientation field, whereas Figures 5.1(c) and (d) are the examples of partial fingerprints in which the orientation field is partially covered. On the other hand, Figure 5.1(a) is the example in which in the range of orientation field covered, there are no significant sub ranges with missing orientation values, whereas Figures 5.1(b), (c) and (d) are the examples of the fingerprints with such gaps. Therefore, one should expect a better OF-based partitioning of a fingerprint image, if the number of clusters take into consideration the significant gaps present in the histogram and the initial choice of the cluster centers is somehow synchronized with the histogram.

In the proposed technique, the entire $[0,\pi)$ range of the orientation field is considered to be circular, that is, the orientation 0 is not differentiable from orientation π. We modify the range $[0,\pi)$ as $[-\partial,\pi-\partial)$, where ∂ is a positive quantity whose value depends on the number of clusters, in order to facilitate the grouping of the orientation values in the vicinities of 0 and π. In the proposed technique, the histogram


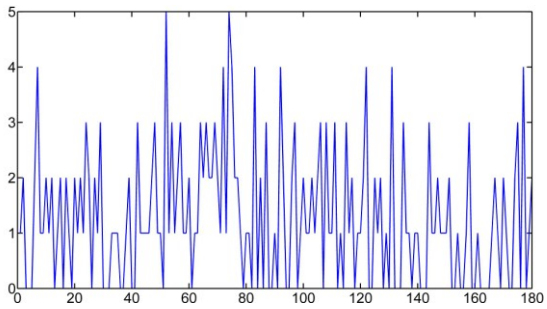

(a) A fingerprint image, with a histogram of its OF which indicates that it has all orientations with a very small number of missed orientations.


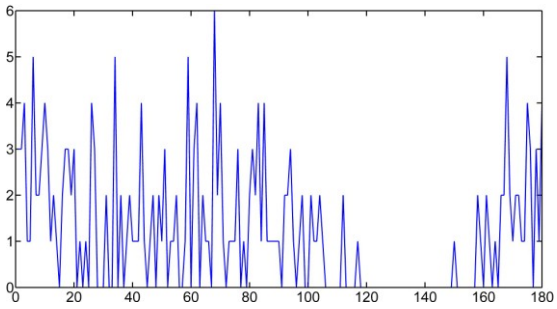

(b) A partial fingerprint image, with a histogram of its OF which indicates that it has some missed orientations.

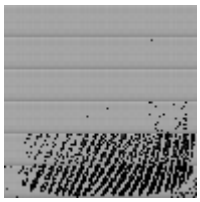
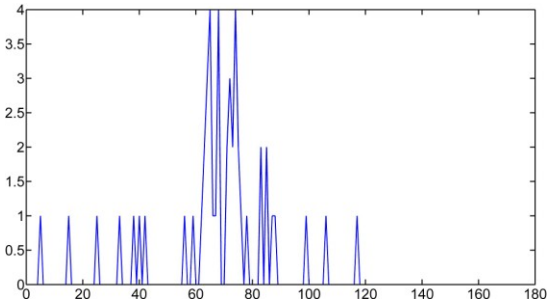

(c) A partial fingerprint image, with a histogram of its OF which indicates that the orientation field is partially covered.

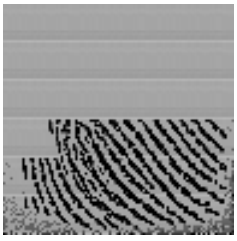
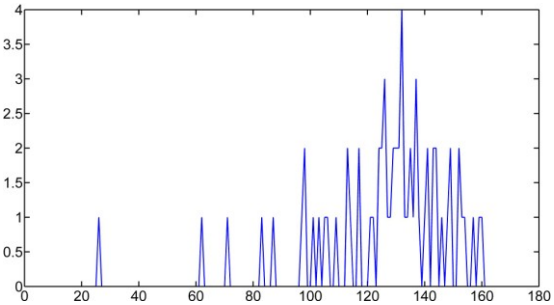

(d) Another partial fingerprint image, with a histogram of its OF which indicates that the orientation field is also partially covered, but for different ranges.

Figure 5.1.: Different examples of fingerprint images with the histograms of their OF.

of the OF of a fingerprint image with orientation values in the range $[-\partial, \pi - \partial)$ is defined as a discrete function $HOF(r_k) = n_k$, where r_k is the k[th] orientation value and n_k is the number of image blocks in the fingerprint image having the orientation value r_k.

In the proposed OF-based histogram, the number of clusters is chosen to have a pre-initial value c', which is determined based on the goal of the partitioning. For example Huang *et al.* in [67] have used 3, 4, or 5 clusters in fingerprint partitioning for the purpose of singular points detection. With this pre-initial choice of the number of clusters as c', a pre-initial set $V'(0)$ of centers is first chosen to be evenly distributed to cover the entire range of orientation, that is $V'(0) = \{v'_j \ , \ j = 0,....,c'-1\}$, where v'_j is the center of the j^{th} cluster, and each center is given as $v'_j = \frac{j\pi}{c'}$. Thus, the j^{th} cluster is considered to cover range $[\frac{(2j-1)\pi}{2c'}, \frac{(2j+1)\pi}{2c'})$ of the orientation values.

The proposed histogram based technique of determining the number of clusters c and the initial choice of the cluster centers $V(0)$ is divided into two stages. In the first stage, using the histogram of the orientation field, a set of effective sub-ranges of the orientation values $D = \{d_1, d_2,..., d_L\}$, where $d_l = [r^l_{k1}, r^l_{k2}]$ is the l^{th} sub range consisting of orientation values from r^l_{k1} to r^l_{k2} and L is the number of such sub ranges, is obtained. In the second stage, the pre-initial set $V'(0) = \left\{0, \frac{\pi}{c'}, \frac{2\pi}{c'},..., \frac{(c'-1)\pi}{c'}\right\}$ of centers and the set D are used to determine the suitable number of clusters c and the initial set of centers $V(0)$ for the FCM algorithm.

Stage 1:

By analyzing the entire range of orientations, the histogram (HOF) is represented as a set of segments $S = \{s_m \text{ , } m = 1,....,M\}$, where M is the number of segments. Each segment s_m is determined as a certain range of orientation values, such that for each orientation value in this range there exists at least one image block with this orientation, and the two orientation values just outside the two boundaries of the segment have an occurrence of zero. That is, the m^{th} segment $s_m = [r_{k1}^m, r_{k2}^m]$, where r_{k1}^m and r_{k2}^m are, respectively, the first and last orientation values of the segment, is defined as,

$$HOF(r_k^m) \begin{cases} > 0, & r_{k1}^m \le r_k^m \le r_{k2}^m \\ = 0, & r_k^m = r_{k1}^m - 1, \text{ and } r_k^m = r_{k2}^m + 1 \end{cases} \tag{5.6}$$

These segments, in general, would have different characteristics in terms of their widths and the occurrence frequencies of the orientation values covered by each segment. Based on these characteristics of the segments, the set D of effective sub-ranges is constructed. The consecutive segments of set S are considered as adjacent segments if there are small distances (gaps) between them or as isolated segments if the gaps are large. In order to consider the two consecutive segments s_m and s_{m+1} to be adjacent, the distance between their borders r_{k2}^m and r_{k1}^{m+1}, respectively, should be smaller than certain threshold. This threshold υ is chosen to be one-half of the distance between consecutive centers from the set $V'(0)$, i.e. $\upsilon = \frac{\pi}{2c'}$. From the set S of segments, the set D of effective sub-ranges are formed by combining and removing certain segments from the former set. For this purpose, we term an isolated segment or a group of adjacent segments

to be thin if its width is less than $\frac{\upsilon}{2}$. Each thin segment or thin group of segments is removed from the set S if the total occurrence frequency of its orientations is a small percentage τ of the total number of orientations of all the blocks in the fingerprint image. The final step in the construction of the set D is to combine each group of adjacent segments to form an effective sub-range d_l. Thus, the final membership of D consists of combined adjacent segments and the remaining isolated segments from the set S. It is to be noted that the set D will have only two types of effective sub-ranges, i.e. regular and irregular. A regular sub-range is the one that has a wide range of consecutive orientations from the entire range $[-\partial, \pi - \partial)$ irrespective of the frequencies of the orientation values contained within the sub-range. On the other hand, an irregular sub-range is always of a narrow width and contains significant values of its orientation frequencies. Since the former is significant by virtue of its width and the latter by virtue of its height in the orientation field histogram, both these types of sub-ranges would play an effective role in the partitioning of the fingerprint images and as such are called effective sub-ranges.

Stage 2:

The number of clusters c and the initial set of their centers $V(0)$ are determined as follows. By examining the set $D = \{d_1, d_2, ..., d_L\}$ of the effective sub-ranges and the set $V'(0) = \{v'_j \ , \ j = 0, ..., c'-1\}$ of the pre-initial centers, it is decided whether or not a pre-initial cluster center v'_j is qualified to be the center v_p for the initial set $V(0)$ of the cluster centers. A center v'_j from $V'(0)$ is chosen to be center v_p in $V(0)$, if and only if this center is either within or very close to a sub-range d_l. The location of a center v'_j is

considered to be very close to a sub-range d_l, if the distance between v'_j and one of the two extremities of d_l is smaller than $\frac{\upsilon}{3}$. For some sub-ranges, especially for the irregular ones, there may not exist a $v'_j \in V'(0)$ within or very close to a sub-range. For such a sub-range, a new center is created as the mid-point of the sub-range in question. Finally, the total number of clusters c is obviously equal to the cardinality of the set $V(0)$ of the initial cluster centers thus constructed.

The proposed orientation field histogram analysis based technique described in the preceding paragraphs can now be summarized as an algorithm.

Algorithm 5.2: The histogram analysis technique for determining the location and number of the initial cluster centers

- **Initialization**

8- With a specified orientation field OF of the fingerprint and a pre-initial number of clusters c', let the maximum distance threshold be $\upsilon = \frac{\pi}{2c'}$ and $\partial = \upsilon$.

a. Compute a uniformly-spaced set of pre-initial centers as $V'(0) = \{v'_j \ , \ j = 0,....,c'-1\}$, where v'_j is the center of the j[th] cluster calculated as $v'_j = \frac{j\pi}{c'}$.

b. Compute the histogram of OF, as $HOF(r_k) = n_k$, where $r_k \in [-\partial, \pi - \partial)$ is the k[th] orientation value, and n_k is the number of image blocks in the fingerprint image having the orientation value r_k.

- **Construction of the set** S

9- Construct the set of segments of OF as $S = \{s_m,\ m = 1,....,M\}$, where M is the total number of segments and s_m is the m^{th} segment given by $s_m = [r_{k1}^m, r_{k2}^m]$ satisfying the condition given by (5.6).

- **Construction of the set** D

10- Let $m = 1$

11- If $m \le M - 1$, then go to step 5, otherwise go to step 6.

12- If for the pair of consecutive segments s_m and s_{m+1}, $r_{k1}^{m+1} - r_{k2}^m \le \upsilon$, then combine the pair of segments as single segment $s_m = [r_{k1}^m, r_{k2}^{m+1}]$, let $M = M - 1$ and go to step 4. Otherwise let $m = m + 1$ and go to step 4.

13- Let $l = 0$ and $D = \{\phi\}$.

14- For each segment s_m, where $m = 1:M$

If $r_{k2}^m - r_{k1}^m > \dfrac{\upsilon}{2}$, then let $l = l + 1$, define a new regular sub-range $d_l = s_m$, and let $D = D \bigcup \{d_l\}$, otherwise s_m is a thin segment. For this segment check if $\sum_{r_{k1}^m}^{r_{k2}^m} HOF(r_k^m) > \tau$, then let $l = l + 1$, define a new irregular sub-range $d_l = s_m$, and let $D = D \bigcup \{d_l\}$.

- **Determination of cluster centers**

15- Let $p = 1$ and $V(0) = \{\phi\}$.

16- For each sub-range d_l, where $l = 1,..., L$,

a. For each center $v_j' \in V'(0)$, where $j = 0,..., c' - 1$, check if v_j' is a suitable center, that is, if any of the following conditions is true: $r_{k1}^l \le v_j' \le r_{k2}^l$, or

$r_{k1}^{l} - v_j' \le \frac{\upsilon}{3}$, or $v_j' - r_{k2}^{l} \le \frac{\upsilon}{3}$. Then let $v_p = v_j'$, $V(0) = V(0) \bigcup \{v_p\}$, and $p = p + 1$.

b. If $\forall j = 0,...,c' - 1$, no v_j' is found to be a suitable center centers, then let $v_p = \frac{r_{k1}^{l} + r_{k2}^{l}}{2}$, $V(0) = V(0) \bigcup \{v_p\}$, and $p = p + 1$.

In order to show the effectiveness of the proposed histogram analysis technique of determining the number of clusters and the set of initial cluster centers to be used for the FCM algorithm, we consider the following numerical example. Let us specify the number of the pre-initial clusters $c' = 6$ and the set S obtained from the histogram of the given orientation field as $S = \{[-2,28], [42,54], [70,80], [102,106], [130,164]\}$. With $c = c' = 6$ and $V(0) = \{70.32, 74.55, 77.9, 83.55, 83.74, 86.93\}$, the FCM technique provides the set of cluster centers as $V = \{11.36, 46.71, 74.83, 104.01, 137.98, 156.32\}$ in 45 iterations. On the other hand, the proposed histogram analysis technique, with $c' = 6$ and hence the pre-initial set of cluster centers given by $V'(0) = \{0, 30, 60, 90, 120, 150\}$, provides the initial set of centers as $V(0) = \{0, 30, 48, 75, 150\}$ and the number of clusters to be only 5. Based on this initialization from the histogram analysis technique, the set of cluster centers is obtained as $V = \{4.77, 21, 48.04, 75.21, 147.36\}$ in only 15 iterations.

Next, by letting the initial number of clusters $c = 5$ and $V(0) = \{70.46, 77.73, 82.63, 83.46, 84.54\}$, we apply the FCM algorithm again. In this case, the final solution of cluster centers is obtained as $V = \{11.5, 47.08, 77.68, 135.86, 155.33\}$ in 34 iterations.

This experiment thus shows the effectiveness of the proposed histogram analysis based initialization in terms of the number of iterations and the quality of the solution provided by the FCM algorithm.

5.2.3 The proposed HA-FCM fingerprint partitioning scheme

We now describe the proposed HA-FCM fingerprint partitioning scheme. First, the orientation field matrix $\mathbf{O}$ of a fingerprint image is obtained as explained in Chapter 3. By using $\mathbf{O}$, the data set $X = \{x_1, x_2, ..., x_n\}$, where n is the total number of image blocks containing ridges, is then constructed. For this purpose, we first construct the set $X' = \{x'_q, q = 1, ..., WH\}$, where $x'_q = \mathbf{O}(h, w)$, $w = 1,2,...,W$ and $h = 1,2,...,H$, such that $q = (h-1)W + w$,. Then, the data set X is obtained from X' by removing from it all the elements not containing a valid orientation value. Next, the HA technique (Algorithm 5.2) is applied on the set X to determine the number of clusters c and the set of their initial centers $V(0)$. The FCM algorithm (Algorithm 5.1) is then used to cluster the data items of the set X. This step provides a set of cluster centers V and the membership matrix U whose elements represent the degree of belonging of a data item $x_i \in X$ to each cluster $j \in \{1,2,...,c\}$. Finally, the fingerprint image is fuzzy partitioned as follows. This is done by constructing a fuzzy clustered orientation field (FCOF) set using the data set X, the final set of cluster centers V, and the membership matrix U. The i^{th} element of FCOF represents all the clusters to which the i^{th} element x_i belongs to and the degree of belonging to each of these clusters in a certain order. Thus, each element of FCOF consists of a sorted set of ordered pairs given by

$$FCOF(i) = \left\{\left(r_i(1), u_{ir_i(1)}\right), \left(r_i(2), u_{ir_i(2)}\right), ..., \left(r_i(a_i), u_{ir_i(a_i)}\right)\right\}, i = 1, ..., n \qquad (5.7)$$

where $r_i(k) = j \in \{1,2,...,c\}$, $k = 1,...,a_i$, such that $u_{ir_i(k)}$ is the k^{th} largest value in the set $\{U(i,\eta), \eta = 1,...,c\}$, and $a_i \leq c$ is a positive integer representing the number of clusters in which the total of degrees of membership of x_i is larger than a pre-specified threshold γ.

The partitioning of the fingerprint image as given by (5.7) is a fuzzy partitioning, since a data item can belong to more than one cluster (i.e. $a_i > 1$). In the specific case when $a_i = 1, \forall i$, the partitioning given by (5.7) leads to the partition of the fingerprint image into non-overlapping regions, that is, the borders between the regions get fixed similar to that in the traditional crisp partitioning techniques. However, as we will see later, this crisp partitioning carried out by the proposed scheme is different from these obtained by using the traditional techniques. The proposed HA-FCM fingerprint partitioning scheme just described is now put as an algorithm.

Algorithm 5.3: The HA-FCM fingerprint partitioning scheme

- **Construction of the set** X

1- Divide the fingerprint image into H×W blocks each of size N×N pixels.

2- Let $X' = \{\phi\}$.

3- For each block $h = 1:H$ and $w = 1:W$

   a. Compute the dominant ridge direction in the current block $\mathbf{O}(h,w)$ by using (3.1).

   b. Compute the variance σ^2 of the gray levels of image pixels within the current image block, in a direction that is perpendicular to $\mathbf{O}(h,w)$. If $\sigma^2 \leq \tau$, where τ is an empirically specified threshold, then the current image block belongs to the background, and it is removed from the orientation field. Set $\mathbf{O}(h,w) = -1$.

c. Let $q = (h-1)W + w$ and $x'_q = \mathbf{O}(h, w)$.

d. Let $X' = X' \bigcup \{x'_q\}$

4- Let $i = 0$ and $X = \{\phi\}$.

5- For each $x'_q \in X'$, where $q = 1,....,WH$, if $x'_q \neq -1$, then $i = i + 1$, $x_i = x'_q$ and $X = X \bigcup \{x_i\}$.

- **Clustering of the set X using the HA-FCM**

6- With a pre-initial c', apply the HA technique (Algorithm 5.2) on the set X to determine the initial number of clusters c with the set of initial cluster centers $V(0)$.

7- With the initial number of clusters c and the cluster centers $V(0)$, apply the FCM (Algorithm 5.1) on set X to determine the final set of cluster centers V and the membership matrix U.

- **Construction of the set *FCOF***

8- For each $x_i \in X$, where $i = 1,....,n$, construct the fuzzy clustered orientation field (FCOF) set as $FCOF(i) = \{(r_i(1), u_{ir_i(1)}), (r_i(2), u_{ir_i(2)}), ..., (r_i(a_i), u_{ir_i(a_i)})\}$, where $r_i(k) = j \in \{1,2,...,c\}$, $k = 1,..., a_i$, such that $u_{ir_i(k)}$ is the k^{th} largest value in the set $\{U(i,\eta), \eta = 1,..., c\}$, and $a_i \leq c$ is chosen to be the smallest integer υ for which $\sum_{k=1}^{\upsilon} u_{ir_i(k)} \geq \gamma$.

We now demonstrate the effectiveness of the proposed HA-FCM partitioning technique by considering several fingerprint images from FVC2002 and FVC2004 databases. Each image is partitioned into non-overlapping regions using both the

quantization technique of [39] and the proposed technique. For this set of experiments, the parameters needed for HA-FCM technique are chosen based on the following considerations.

i. The maximum number of iterations is selected as $\mathrm{M} = 200$, which is large enough to ensure that the HA-FCM algorithm does not stop prematurely before reaching the optimum solution.

ii. The minimum reduction of the objective function between two consecutive iterations is chosen as $\varepsilon = 10^{-5}$, which is small enough to ensure that the solution found is an optimum one.

iii. The tuning parameter controlling the degree of fuzziness in the clustering process is chosen to be $m = 2$, as customarily done in the use of FCM algorithm.

iv. The pre-initial number of clusters is chosen to be $c' = 8$, which consistent with the number of quantization levels used in Chapter 3.

In the first part of our experiments we have chosen eight different fingerprint images, such that their orientation field covers the entire range $[0, \pi)$ of orientations. The parameters c for FCM and c' for HA-FCM are chosen to have value 8. Since the selected images cover the entire orientation range, the HA-FCM algorithm also provides the value of c as 8. In view of the fact that both algorithms use the same number of clusters, it should be possible for them to achieve the same solution. Table 5.2 gives the number of iterations required by the proposed algorithm and the average number of iterations of 10 different runs of FCM algorithm, with randomly chosen sets of initial cluster centers, for reaching the same solution for each of the fingerprint images. It is

seen from this table that the HA-FCM algorithm for most of fingerprint provides solutions with a considerably smaller number of iterations.

Table 5.2: Comparisons between the HA-FCM and the FCM techniques.

	FVC2002 DB3					FVC2004 DB1		
	101_1	102_4	103_1	105_6	106_1	1_1	2_6	12_4
FCM	67	107	123	127	103	68	83	137
HA-FCM	39	74	96	96	85	43	56	121

In the second part of the experiment, we consider the example of a partial fingerprint image shown in Figure 5.1(b). The parameters c' and c, for HA-FCM and FCM, are chosen to be 8. As expected because of the gaps in the orientations in the fingerprint, the HA-FCM provides a lower value $c = 6$ of the number of clusters. Because of the difference in the values of c for the two algorithms, they now cannot be expected to provide the same solution. Figure 5.2 shows the images of the fingerprint, the corresponding orientation image, and the fuzzy clustered orientation images (FCOI) with a_i chosen as unity provided by the FCM and HA-FCM algorithms. A comparison of Figures 5.2(c) and (d) shows that the clustered image provided by HA-FCM is smoother and more aligned with the actual orientations shown in Figure 5.1(b) of the fingerprint image. Moreover, the number of iterations required by HA-FCM is only 51 in comparison of 83 required by FCM. From Figure 5.2 and Table 5.2, it is seen that the proposed HA-FCM technique reduces the overall computational complexity required by the original FCM and provides smoother fingerprint partitioning.

The ridge orientations are naturally almost continuous and smooth everywhere in the fingerprint, except in regions near the singular points. Therefore, it is expected from an OF-based partitioning scheme to assign an image block in the vicinity of or containing

a singular point to a larger number of different clusters. On the other hand, other image blocks should have less diversity in terms of their belonging to different clusters. In the third part of the experiment, six different fingerprint images are considered to compare the fuzzy clustered partitioning with the quantization based partitioning. Each of Figures 5.3 and 5.4 contains three different fingerprint images (first row), their orientation images (second row), the image obtained using the quantization based partitioning (third row), and the image partitioned using the proposed HA-FCM technique (fourth row). By comparing the partitioned images from the two techniques, two main observations can be made. First, the regions away from the singular points are much smoother in the case of the partitioning obtained by HA-FCM in that these regions do not have inside them many smaller regions. Many smaller regions of the quantized partitioning resulting from the noise or ridge cuts, present in the second and third images, have been more effectively resolved by the HA-FCM technique. Second, the proposed technique assigns, as desired, the singular point region to more clusters, since such regions contain larger number of ridge orientations.

In summary, the proposed HA-FCM technique, by using an image-based approach for determining the number of clusters and the set of their initial centers, provides the following benefits. 1) In comparison with the quantization (i.e. discretization) method [39], the proposed HA-FCM technique provides smoother regions. 2) The proposed HA-FCM technique is able to achieve a better or similar solution compared with the one achieved by the FCM technique at a lower computational complexity.

(a)

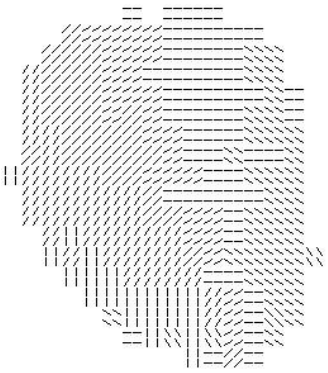

(b)

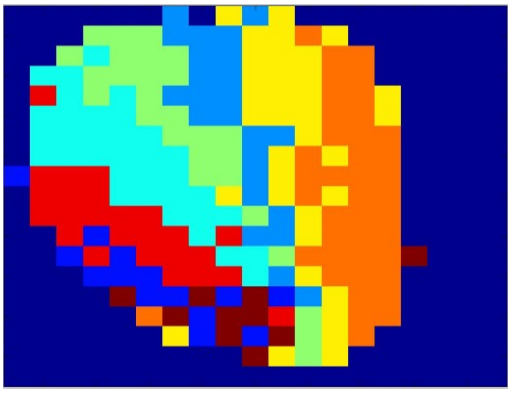

(c)

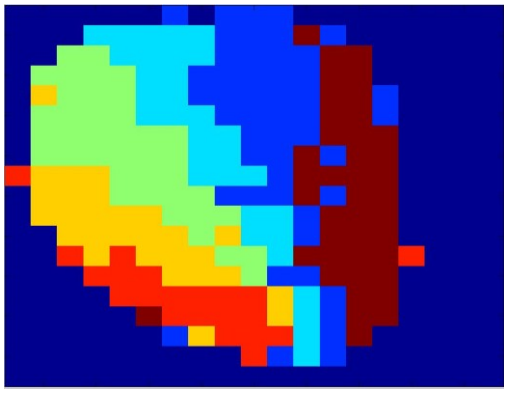

(d)

Figure 5.2: (a) the original fingerprint image, (b) the orientation image, (c) the FCOI obtained by the FCM using 8 clusters, and (d) the FCOI obtained by the proposed HA-FCM, by which the number of clusters are found to be only 6. It is clear that the proposed HA-FCM provides smoother partitions.

(a)

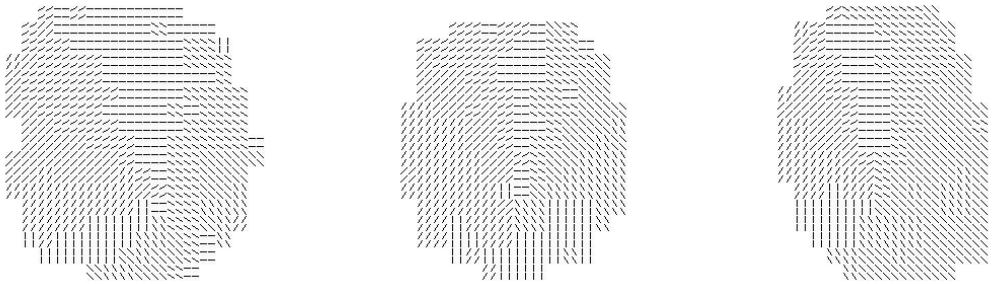

(b)

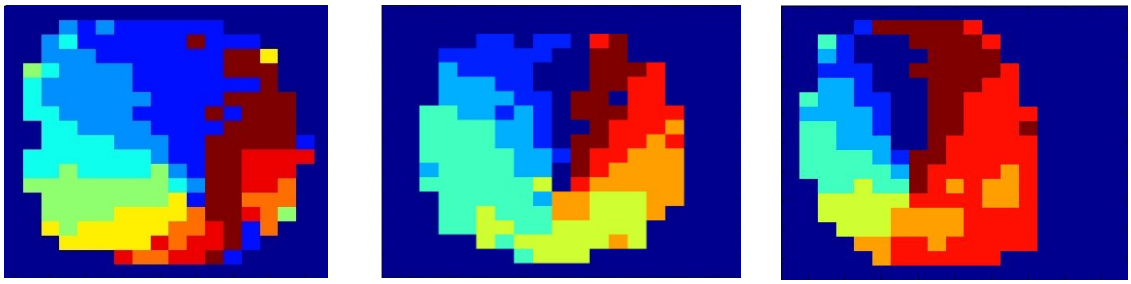

(c)

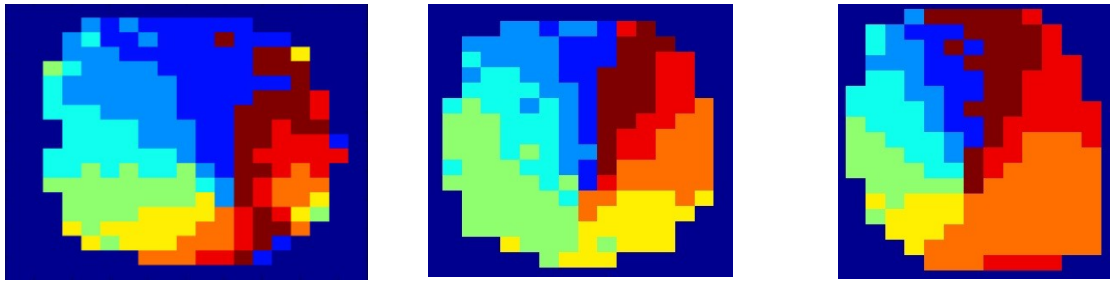

(d)

Figure 5.3: (a) A set of three fingerprint images. (b) The orientation images. (c) Images partitioned using the quantization. (d) Images partitioned using the proposed HA-FCM.

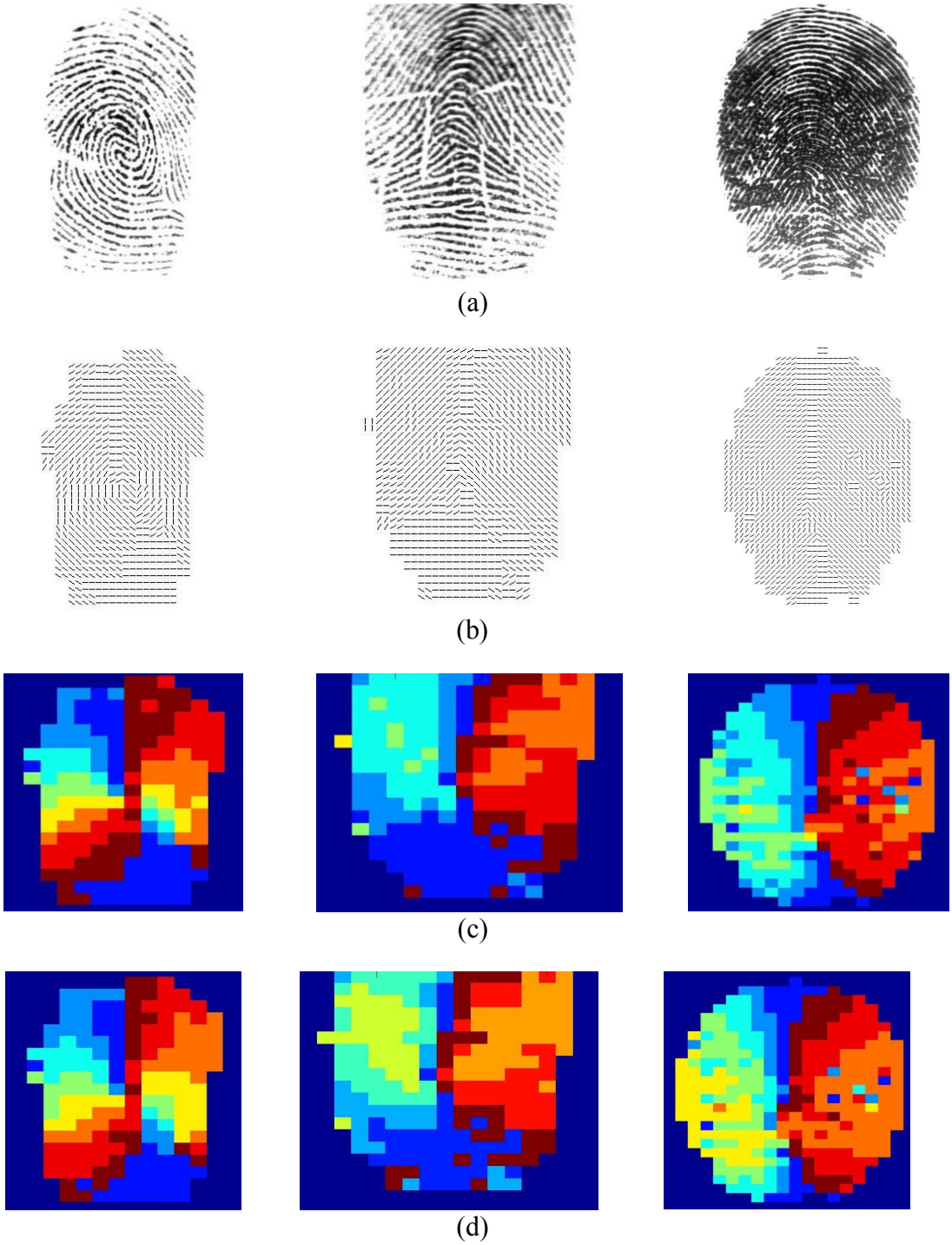

Figure 5.4: (a) Another set of three fingerprint images. (b) The orientation images. (c) Images partitioned using the quantization. (d) Images partitioned using the proposed HA-FCM.

5.3 Singular Point Detection Based on the HA-FCM Fingerprint Partitioning Scheme

The singular points (SP) of the fingerprint images, as a global feature that is invariant to rotation, translation, shrinking and enlargement, have a significant role for fingerprint pattern classification [39, 40] and fingerprint recognition [13, 14, 23, 32]. The singular points of a fingerprint represent special regions of the ridge pattern, where the orientations of the ridges are characterized by irregularities. There are two types of the singularities, namely loop and delta, which are defined based on the types of the orientation irregularities. The loop singularity is defined as the region at which the ridges are wrapped to form almost half-circled shapes. Based on this definition of loop singularity, there are four types of loop singularities as shown in Figures 5.5(a)-(d): (i) upper core, (ii) lower core, (iii) whorl and (iv) twin loops. The core point corresponds to the topmost (i.e. upper core) or bottommost (i.e. lower core) point of the innermost curving ridge [1, 39]. The delta singularity is defined as the point from which the ridges branch out in three different directions to form a delta shape as shown in Figure 5.5(e). If the fingerprint image has no singularities, such as the arch fingerprint shown in Figure 5.5(f), the core point is defined as the point of maximum ridge curvature [1, 39].

(a) (b) (c) (d) (e) (f)

Figure 5.5: The different possible types of singular points: (a) upper core, (b) lower core, (c) whorl, (d) twin loops, (e) delta, and (f) arch.

Even though there are some singular point detection approaches using directly the pixel gray values of the fingerprint images [89], most of the singular point detection techniques proposed in the literature use the orientation field of the fingerprint image. These techniques could be categorized as follows: 1) Methods based on Poincare´ index [90–96], 2) methods based on local characteristics of the orientation image [38, 39, 97–99], 3) methods based on the partitioning of the fingerprints using the orientation field [12, 66, 67, 100], and 4) methods based on the global model of the orientation image [40,101–105]. The methods based on Poincare´ index or on the local characteristics of the orientation image detect the singular points at low computational cost, but they fail to detect the singularities located near the image borders or in poor quality fingerprint images, or they falsely detect some spurious singular points. The methods based on the partitioning of the fingerprints into regions of homogeneous orientations implicitly provide the position of the singular points and provide better detection accuracy but at the expense of higher computational complexity. Since, the accuracy of detecting the singular points affects the overall performance of fingerprint classification and recognition schemes, the idea of exploiting the global model of the orientation image has been found to be more effective in improving the detection accuracy of singular points. However, the approaches for singular point detection based on the global modeling have the disadvantage of very high computational complexity because of the following reasons. First, most of the global modeling techniques require determining the candidate singular points usually by employing the Poincare´ index method. Second, the global modeling of the orientation image itself is computationally expensive. Therefore, there is a need to develop a new approach which is able to provide a high accuracy for the

detection of the singular point at a reasonable computational cost. In this section, a new singular point detection technique is proposed based on the HA-FCM fingerprint partitioning scheme developed in Section 5.2. By searching for specific cluster distributions within the fuzzy clustered orientation image (FCOI), the proposed approach for singular point detection is able not only to locate the different singular points but also to determine the types of the detected singular points as well as the orientation of the core points.

5.3.1. Cluster distributions for fingerprint ridge structures

In the proposed scheme for singular point detection, the fingerprint ridge structures are classified as singular or non-singular structures. Depending on the type of singularity, the singular structures represent the upper core, lower core or delta. In our study, four types of the non-singular structures are defined as: (i) plain region, (ii) plain region with ridge deformation, (iii) plain region with noise, and (iv) plain region with ridge cuts.

Figures 5.6 and 5.7 show the ridge flows around the image blocks contained within regions having the different types of singular and non-singular structures, respectively. They also give the corresponding cluster distributions within the 3x3 neighborhood obtained by using the HA-FCM technique with $c' = 5$, i.e. $c \leq 5$. A comparison of distributions in the two figures shows that, in general, there is a larger diversity in the number of different clusters within the set of blocks with singular points than in the set without singular points. The non-singular regions may also be characterized a large diversity in the number of different clusters, if they affected by deformation (Figure 5.7(b)), noise (Figure 5.7(c)) or cut (Figure 5.7(d)). It is to be noted, however, that the diversity in the number of clusters in singular regions are also

associated with some distinctiveness in their patterns. We now state the following three axioms based on the distinctiveness of the patterns of the clusters distributions of the neighborhood blocks associated with the three types of singular points.

α_1: Upper core:- If the upper neighborhood of 2x3 blocks contain at least $c-1$ different clusters, such that the clusters appear clockwise in a descending order of their numbers.

α_2: Lower core:- If the lower neighborhood of 2x3 blocks contain at least $c-1$ different clusters, such that the clusters appear clockwise in a descending order of their numbers.

α_3: Delta:- If the 3x3 neighborhood blocks contain a minimum of $c-2$ and a maximum of c different clusters, such that the clusters appear clockwise in a non-descending order of their numbers.

In the next subsection, the above set of axioms is used to develop the proposed technique for singular point detection.

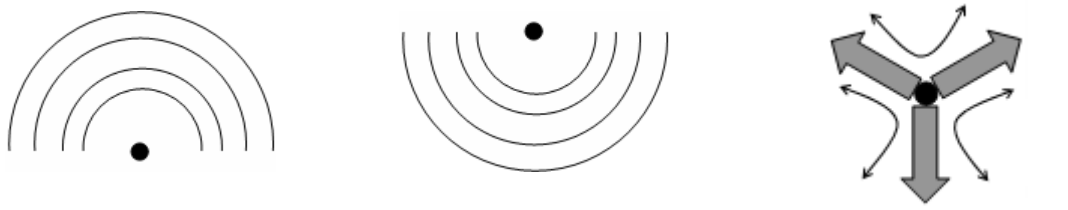

2	1	5
3	●	4
X	**X**	X

(a)

X	X	X
4	●	3
5	1	2

(b)

5	1	1
4	●	2
4	3	2

(c)

Figure 5.6: Typical ridge flows and the corresponding cluster distribution around the different types of singular points: (a) upper core, (b) lower core, and (c) delta.

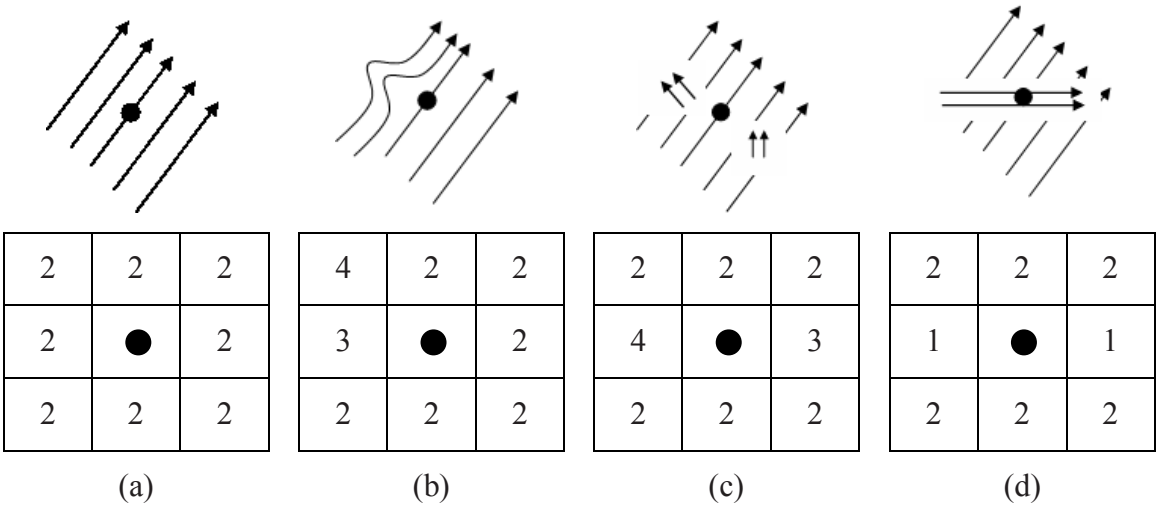

Figure 5.7: the ridge flows and the corresponding cluster distribution around: (a) a plain region, (b) a plain region with ridge deformation, (c) a plain region with noise, and (d) a plain region with ridge cut.

5.3.2. The proposed HA-FCM-based scheme for singular points detection

The proposed HA-FCM-based scheme for singular point detection is divided into two stages. In the first stage, a set of candidates corresponding to each of the three singular points are constructed. In the second stage, the consistency and relative accuracy of the detected candidate singular points are checked, to determine the actual singular points.

Stage 1:

In this stage, a fuzzy clustered orientation image (FCOI) is first constructed from the FCOF set by choosing a_i's as unity. Thus, the $(h,w)^{th}$ block of the FCOI contains an ordered pair $\left(r_i(1), u_{ir_i(1)}\right)$ of the cluster number and the membership degree corresponding to the $(h,w)^{th}$ image block. Then, the 3x3 neighborhood correspond to each block (h,w) is examined using the above axioms. If the particular block (h,w) is found to belong to one of the three types of singular points, the index (h,w) is included in the initial candidate set for that type of singular point. In addition the index (h,w) of such block is

also appended by a fuzzy-based measure of the correctness (FMC) of choosing (h, w) as a candidate to belong to that type of singular point. This measure of the degree of correctness is calculated as the average of the membership degrees of the blocks comprising the neighborhood.

Since, in our scheme, the original orientation field $\mathbf{O}$ has been estimated directly based on the computation of gradients in the fingerprint image [36], it would contain irregularities for the ridges affected by noise, cuts, deformation, or blurring. In order to overcome this problem, the idea of orientation field regularization (smoothing) has been used by many researchers in the literature [11, 39, 92]. This regularization could be implemented using a simple low-pass filtering [11, 39] or global modeling of the orientation field [92]. In the proposed HA-FCM based approach, it has been seen that the cluster distributions for fingerprint singular and non-singular structures are normally different. However, some non-singular structures, especially that of the second or third type, may have a pattern of cluster distribution similar to that of the singular structures. Accordingly, the above three initial sets of candidate blocks for the singular points may contain some spurious items. Therefore, in the proposed method, in order to remove these spurious items from the above initial candidate sets, the 3x3 neighborhood of each candidate item is first regularized by replacing the cluster number of each block $(h, w)^{nb}$ in the neighborhood of the item (h, w) with a cluster number having the maximum occurrence within the 3x3 neighborhood of $(h, w)^{nb}$. Next, the (h, w) block is rechecked for its suitability to belong to the originally determined candidate set. If (h, w) is found to not satisfy the axiom to be the originally determined candidate singular point in the context of new regularized pattern of clusters, it is then removed from the candidate set.

After the removal of the spurious blocks, the remaining candidate blocks are used to determine the candidate singular points, such that each candidate singular point is represented by a candidate block or a group of neighboring candidate blocks (Figure 5.8). Each candidate singular point is characterized by the geometrical center of the corresponding blocks and the average of their FMC. As to be seen in the description of second stage, the orientation of the core points [105–107] are utilized in determining the relative positions of delta points. In our fuzzy-based method, the orientation of a core point (upper or lower) is calculated as the average of the cluster centers of the lower or upper neighborhood of 2x3 of the image blocks corresponding to the core point.

Thus the first stage finally provides three sets of candidate singular points corresponding to the upper and lower cores and the delta. Each item in the sets contains the position of the candidate singular point and its FMC. In addition the items in the candidate sets of the upper and lower cores also have the information on the orientation of the core point. These candidate sets are used in stage 2 to determine the actual singular points.

(a) (b)

Figure 5.8: (a) An example of a fingerprint image contains upper core ($\cap$), lower core ($\cup$) and right delta (+). (b) The corresponding FCOI with the candidate blocks corresponding to the upper core (i.e. the vertical rectangle), the lower core (i.e. two small squares) and the delta (i.e. the big square).

Stage 2:

It is known that a fingerprint has at most one upper core, one lower core and two deltas. However, each of the three candidate singular point sets obtained from stage 1 may have a number of candidates that is more than these maximums. This larger number of candidate singular points arises because of the fingerprint images when affected by blurring, ridge cuts or wrapping of the ridges close to the actual core points. In this stage, these spurious singular points are removed by using the FMCs associated with the candidate singular points and verifying the typological constraints of the three different types of singular points as follows.

Figures 5.9(a) and (b) contain two examples of fingerprint images in which from stage 1 spurious (upper or lower) cores have arisen because of wrapping of the ridges close to the actual core points. In this case, the upper and lower cores with the larger FMCs are chosen as the actual core point (Figures 5.9(c) and (d)). Figure 5.10(a) is an example of the image with blurring close to the lower border of the fingerprint. In this example, stage 1 provides falsely a lower core and a left delta detected in the affected region, in addition to the actual upper core and the actual left delta. Since the upper and lower cores should exist within a certain maximum distance, the lower core is eliminated by stage 2 in view of the fact that it is within the affected region and its distance from the upper core exceeds a pre-specified threshold for the distances between the upper and lower cores. It is also seen from Figure 5.10(a) as well as from Figure 5.10(c) that two delta points have been detected by stage 1. In order to remove spurious delta points detected by stage 1, each candidate delta is first classified as either a left delta or a right delta with respect to the location and orientation of the core point. Then, if there are more

than one left (or right) deltas, stage 2 selects the one with the largest FMC value. Following this rule, the two deltas in each of the examples of Figure 5.10(a) and (c) as obtained from stage 1 are reduced by stage 2 to only one delta as shown in Figures 5.10(b) and (d), respectively.

(a) (b) (c) (d)

Figure 5.9: (a) An example of two upper ($\cap$) and two lower ($\cup$) cores obtained by stage 1, and their calculated orientations indicated by the bright lines. (b) An example of two upper ($\cap$) cores obtained by stage 1, and their calculated orientations indicated by the dark lines. (c) Correctly detected upper and lower cores in the fingerprint of (a) by stage 2. (d) Correctly detected an upper core in the fingerprint of (b) by stage 2.

(a) (b) (c) (d)

Figure 5.10: (a) An example of a spurious lower core and a left delta detected by stage 1 due to the effect of blurring. (b) Removal of the spurious singular points in (a) by stage 2. (c) An example of a spurious right delta detected by stage 1 due to the effect of ridge cuts. (d) Removal of the spurious right delta in (c) by stage 2.

5.3.3 Experimental results and comparisons

- Databases

In order to show the efficacy of the proposed HA-FCM based scheme for singular point detection, the DB1 databases of FVC 2002 [44], 2004 [41] and 2006 [45, 46] have been used. As described in Chapter 2, these databases have different image sizes and have varieties of difficulties. It has been pointed out in [1] that the databases FVC2002 DB1, FVC2004 DB1 and FVC2006 DB1 have, respectively, low, medium and high degrees of difficulties. The DB1 of FVC2002 and FVC2004 have 8 impressions each of 110 different fingers divided into 100 fingers for testing and 10 for training. On the other hand, the FVC2006 DB1 has 12 impressions of 150 different fingers divided into 140 fingers for testing and 10 for training. The FVC2006 DB1 is more heterogeneous and includes fingerprint images of manual workers and elderly people.

- Performance measures

For measuring the performance of the proposed scheme, the detected singular points and the orientations of the cores are compared with the manually decided ground truths. The three quantities of interest for the measurement of performance are the number of correct detections, the number of spurious detections and the difference between the computed orientations and the corresponding ground truth values. The detection is reported as a correct detection if its location lies within a certain number of pixels (i.e. a decision threshold) from the true singular point, otherwise it is reported as a spurious one. Since, there is no established standard in the literature for evaluating the performance of singular point detection of a scheme, we have chosen from the literature five most commonly used measurements to report and compare the performance of the proposed

scheme from different perspectives. As in [40] and [104], the performance is measured in terms of the following three quantities.

$$\text{Recall} = \frac{\text{TP}}{\text{TP} + \text{FN}} \tag{5.8}$$

$$\text{Precision} = \frac{\text{TP}}{\text{TP} + \text{FP}} \tag{5.9}$$

$$\text{F - measure} = \frac{2 \cdot \text{Recall} \cdot \text{Precision}}{\text{Recall} + \text{Precision}} \tag{5.10}$$

where TP is true positive, FP is false positive and the FN is false negative at a specified decision threshold. Therefore, Recall is the ratio of correctly detected singular points to all the true singular points. The Recall measure has also been called detection rate by some other researchers [92]. Precision is the ratio of correctly detected singular points to all detections made by the scheme. The F−measure specifies the trade-off between recall and precision, giving equal importance to both.

In [92] another important performance measure that has been used is the fingerprint correct rate (FCR), which is defined as the ratio of the correct number of fingerprints to the total number of fingerprints tested. A fingerprint is reported as "correct" if all detected singular points are correct and without any spurious or missed ones. Hence, this measure could be used to determine the usefulness of a singular point detection scheme for fingerprint classification/indexing applications. This measure takes into consideration the fingerprint images which do not contain any singular point and thus it is reported as a "correct" if no singular points have been detected. It is noted that the three measures defined earlier are not affected by such a "correct" fingerprint image. Finally, in order to report the accuracy of the calculated orientation of the core points, we use the orientation error defined as the ratio of the number of fingerprints with the

orientation difference smaller than or equal to a pre-specified value to the total number of the fingerprints tested [105].

- Results and comparisons

From the classification of the orientation-based singular point detection techniques as carried out in the introduction of Section 5.3, it is seen that the proposed scheme for singular point detection belongs to the second category. In order to compare the performance of the proposed scheme, we have chosen and implemented the shape analysis technique [39], which is considered to be one of the state of the art techniques belonging to the same category. In the implementation of the shape analysis technique, the same modules as those used in the implementation of the proposed technique for the calculation of the orientation field and fingerprint image segmentation have been used. In order to be comprehensive in examining the proposed technique, we also compare the results of our scheme with three techniques presented in [92], [67] and [40], which belong to the first, third and fourth categories, respectively. The detection technique of Zhou *et al.* [92] is based on using Poincare´ index to determine the initial set of candidate singular points followed by the development of a DORIC feature vector for these singular points. Then, a support vector machine (SVM) based classifier is designed to remove the spurious singular points. In the technique of Huang *et al.* [67] the singular points are detected at the intersection of the so called fault lines by carrying out a pixel-wise orientation based fingerprint partitioning. The technique of Jirachaweng *et al.* [40] is based on developing a residual model for the orientation field and then using Poincare´ index method to detect the singular points from this model.

Figures 5.11, 5.12 and 5.13 depict the results of the proposed scheme and the shape analysis technique [39] on the FVC2002 Db1, FVC2004 Db1 and FVC2006 Db1, respectively, where the performance measures, Recall, Precision and F-measure, are plotted as a function of the decision threshold. In addition Figure 5.12 also provides the results of the global model based technique, as reported in [40] on FVC2004 DB1. The superiority of the proposed technique to the shape analysis technique [39] on different databases, and also to [40] on FVC2004 DB1, is clearly seen.

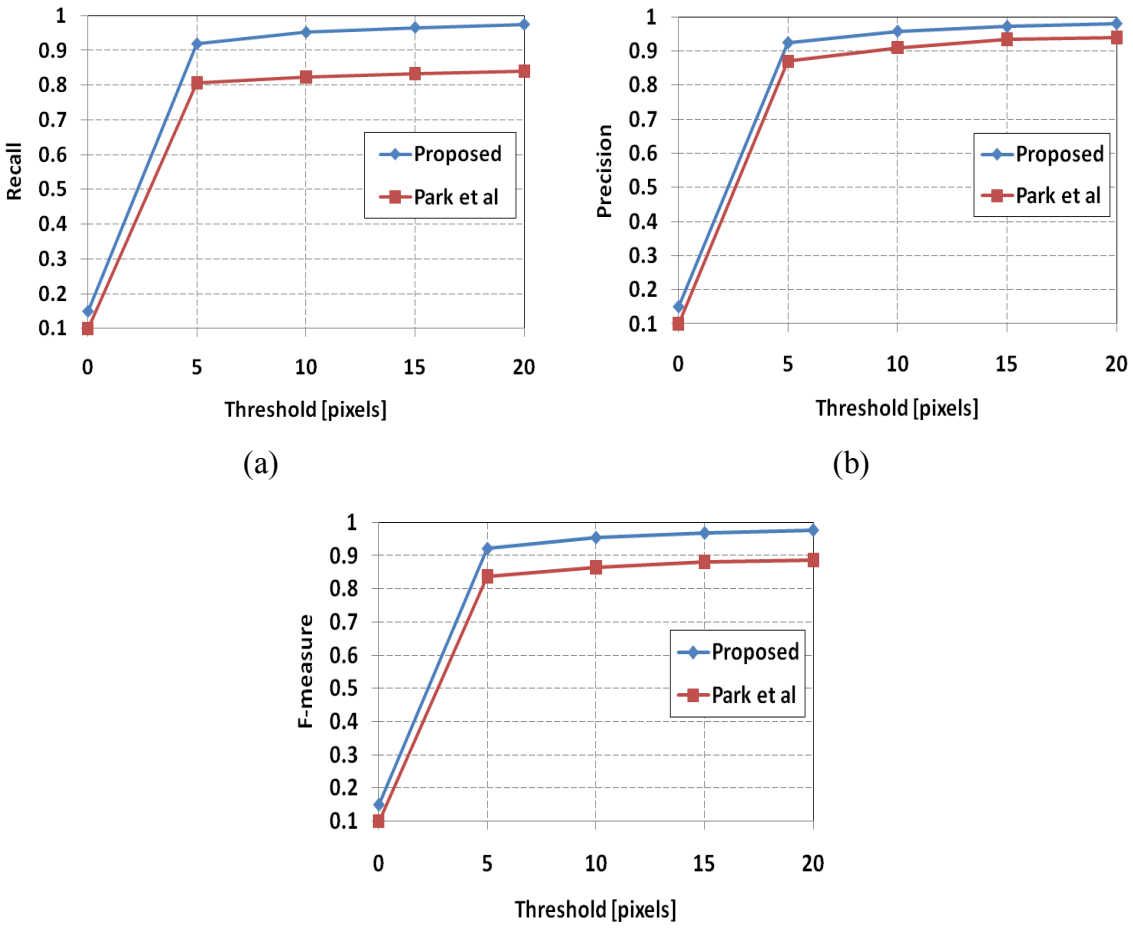

Figure 5.11: Performance measures of singular point detection using the proposed scheme and the technique of Park et al [39] on FVC2002 DB1. (a) Recall, (b) Precision and (c) F-measure.

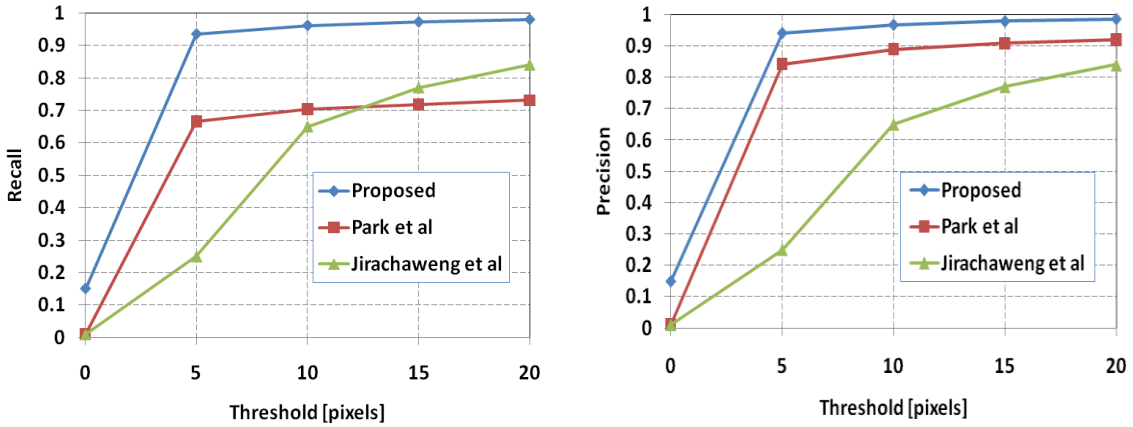

(a)

(b)

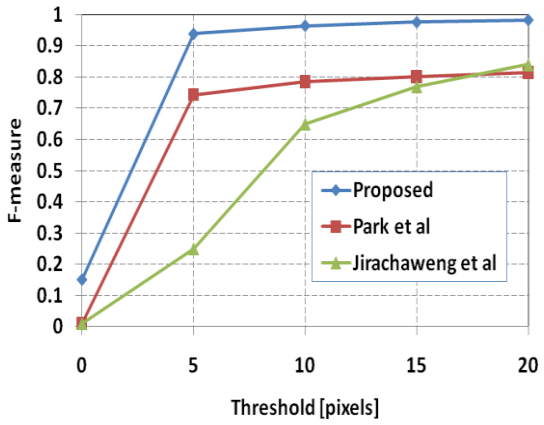

(c)

Figure 5.12: Performance measures of singular point detection using the proposed scheme and the techniques of Park *et al* [39] and Jirachaweng *et al* [40] on FVC2004 DB1. (a) Recall, (b) Precision and (c) F-measure.

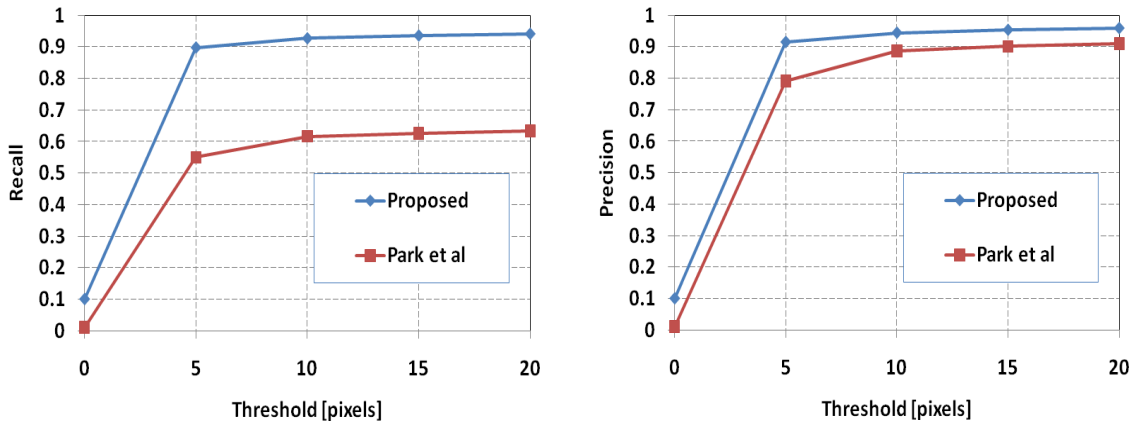

(a)

(b)

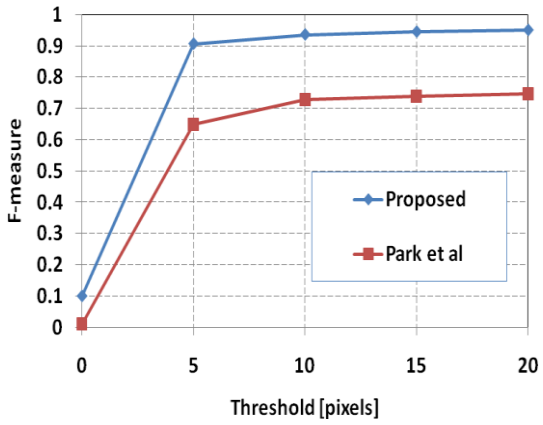

(c)

Figure 5.13: Performance measures of singular point detection using the proposed scheme and the technique of Park et al [39] on FVC2006 DB1. (a) Recall, (b) Precision and (c) F-measure.

Next, the performance measures of the proposed scheme and the schemes of [39], [92] and [67] (at decision threshold less than or equal to 20 pixels) are given in Tables 5.3, 5.4, and 5.5. These tables show that the proposed scheme has a much higher values for the performance measures FCR, Recall, Precision and F-measure for the various databases. The superiority of the proposed scheme is even more pronounced for the detection of delta points. It is to be noted that, unlike the technique of [92] the proposed technique does not perform any pre-processing on the raw fingerprint images, nor, unlike

the technique of [67], performs pixel-wise smoothing of the orientation field, in order to obtain the results given in Figures 5.11-5.13 and Tables 5.3-5.5.

Table 5.3: The performance measures of the proposed scheme and the techniques in [39] and [92] using FVC2002 DB1.

Type of measure		Proposed	[39]	[92]
FCR		94.12	75.75	88.88
Recall	Cores	97.03	86.04	95.78
	Deltas	98.3	78.92	96.98
Precision	Cores	98.24	95.02	-
	Deltas	97.57	94.2	-
F–measure	Cores	97.63	90.31	-
	Deltas	97.92	85.88	-

Table 5.4: The performance measures of the proposed scheme and the techniques in [39] and [67] using FVC2004 DB1.

Type of measure		Proposed	[39]	[67]
FCR		95.98	61.25	-
Recall	Cores	97.84	72.91	97.5
	Deltas	98.23	73.6	83
Precision	Cores	98.76	92.98	96
	Deltas	98.23	89.12	93.65
F–measure	Cores	98.3	81.74	96.74
	Deltas	98.23	80.62	88.05

Table 5.5: The performance measures of the proposed scheme and the technique in [39] using FVC2006 DB1.

Type of measure		Proposed	[39]
FCR		88	50.71
Recall	Cores	94.96	66.95
	Deltas	91.13	52
Precision	Cores	95.79	92.26
	Deltas	96.12	86.67
F–measure	Cores	95.37	77.6
	Deltas	93.56	65

Finally, Table 5.6 lists the accuracy measure of the calculated core orientation of the proposed scheme for the different databases. It is seen from this table that the proposed scheme is able to provide a very highly accurate values for core orientation, which is quite useful for the pre-alignment stage of fingerprint matching. In this regard, it may be pointed that the scheme proposed in [105] has been able to report an accuracy of only 80.7% within the orientation difference less than or equal to $\frac{\pi}{16}$ radians when this technique applied to FVC2002 DB1 in comparison to the accuracy of 94.19% achieved by the proposed scheme.

Table 5.6: Accuracy measure of the calculated core orientation.

Orientation difference (rad.) less than or equal to	FVC2002 DB1	FVC2004 DB1	FVC2006 DB1
$\frac{\pi}{16}$	94.19	94.66	94.87
$\frac{\pi}{8}$	98.63	99	98.74

From the experimental results presented in this section, it is seen that the proposed technique is quite robust in that it can deal more effectively in providing higher singular point detection accuracy in comparison to other methods. In addition, the proposed method is suitable for real-time processing, since the average processing time of each fingerprint is approximately 0.1 second, when it is implemented on a machine with a 1.8-GHz CPU and 512-MB RAM.

5.3 Summary

The idea of using the orientation field for partitioning fingerprint images into non-overlapping regions has been used effectively in various areas involving fingerprints, such as fingerprint indexing and singular point detection. In order to partition a

fingerprint image into non-overlapping regions, each fingerprint image block must be assigned to only one region, which could be achieved using a crisp clustering technique. However, the crisp clustering techniques are generally affected by the fingerprint image problems, such as ridge cuts and noise. On the other hand, the fuzzy-based clustering techniques provide a smoother classification of a dataset by assigning each pattern to all the clusters with varying degrees of memberships. Therefore, these fuzzy-based clustering techniques are able to deal more effectively with the natural patterns, in which the objects cannot be classified to belong exclusively to a specific cluster.

In this chapter a novel fuzzy c-means (FCM) technique has been proposed for partitioning fingerprint images into different regions using their orientation fields. The clustering solution in an FCM technique requires an *a priori* knowledge of the number of clusters and their initial centers. The novelty of the proposed technique is that both these input parameters to the FCM technique are determined in a rational and automated manner. In this technique, instead of pre-fixing the number of clusters and arbitrarily choosing the set of the initial cluster centers, both these parameters are made data dependent by determining them based on the analysis of the orientation field histogram of a fingerprint image. The proposed technique has been shown to lead to an optimal number of partitioning clusters that is fingerprint image adaptive. Also, the initial cluster centers thus determined has been shown to reduce the number of iterations required to obtain the optimum solution. The output of the proposed HA-FCM algorithm, which is a set of cluster centers and degrees of belonging of each data item to different clusters, has been used for partitioning the fingerprint image. The proposed technique has been experimented on a number of fingerprint images from challenging benchmark databases.

The simulation results have shown that (i) the HA-FCM technique results in smoother regions compared to that provided by the quantization technique and (ii) the proposed HA-FCM technique, in comparison to the FCM technique, is able to provide a more realistic partitioning vis-à-vis the nature of the fingerprint image under consideration at a lower computational cost.

In order to show the effectiveness of the proposed HA-FCM partitioning technique in an application, we have considered the problem of fingerprint singular point detection. For this purpose, a novel singular point fuzzy-based detection scheme has been developed by first searching for specific cluster distributions in the fuzzy clustered orientation field (FCOF) resulting from the HA-FCM partitioning technique. The set of candidate singular points corresponding to these specific cluster distributions is then examined to remove the spurious candidates using a fuzzy-based measure of correctness. The proposed scheme has been designed not only to detect the singular points but also to identify their types. Experimental results using challenging benchmark database have shown that the proposed singular point detection scheme outperforms other state of the art techniques available in the literature.

CHAPTER 6

An Enhanced HA-FCM Partitioning Scheme

6.1 Introduction

In the previous chapter, it was shown that the HA-FCM partitioning scheme provides regions that are smoother than that provided by the quantization technique at a lower computational complexity than that required by the standard FCM algorithm. In addition, it was successfully used for developing a high accuracy singular point detection scheme with a low computational complexity. However, it would be desirable to increase the smoothness of the regions even further as well as to reduce the complexity of the HA-FCM technique. In this chapter, the HA-FCM partitioning scheme proposed in Chapter 5 is enhanced in terms of the smoothness of the partitions and the computational complexity [88].

6.2 An Enhanced HA-FCM Technique for Fingerprint Image Partitioning

As pointed in Chapter 5, the ridges having large amount of noise or cuts affect the smoothness of the fingerprint partitions. The idea of regularizing the orientation field has been used, for example, in crisp partitioning schemes in order to obtain smoother partitions [11] or to have a more accurate detection of the singular points [39, 92]. In this section, the idea of regularization of the orientation field is used as a pre-processing step in the HA-FCM technique in order to obtain smoother fuzzy partitions. It is noted that the

major complexity of the proposed HA-FCM technique (or for that matter that of the original FCM algorithm) lies in the iterative process for achieving a minimum of the objective function. In this section, it is proposed to reduce the complexity of HA-FCM by reducing the amount of operations involved in the computation of the objective function as well as by increasing its convergence rate.

6.2.1 Regularization of the orientation field

The regularization step of a given data set is implemented, in general, by replacing the value of each data item with a new value that takes into consideration the values of its neighboring items. This new value could be calculated as a simple average of the values in a neighborhood including the original data item [11]. Even though the use of a simple averaging to regularize the orientation field of a fingerprint is able to smooth out the local irregularities produced by noise, it also smoothens the global irregularities (i.e. the regions contain singular points) [11, 39]. To overcome this problem the authors in [11] have proposed a three-step technique for the enhancement of the orientation field, in which they have strengthen the regions containing singularities and attenuating those without the singularities. This method, however, has a high computational complexity. The regularization can also be done more simply by replacing a data item with a linearly-weighted sum of the original data item and the average of its local neighboring data items [108]. This method was used for segmentation of MR brain images, and provides a better mechanism to control the regularization by adjusting the weights of the sum. This method is, therefore, more suitable to regularize the orientation field. We now describe this regularization step in the HA-FCM partitioning scheme giving rise to a regularized HA-FCM (RHA-FCM) scheme.

The orientation field matrix $\mathbf{O}$ of a fingerprint image is obtained as explained in Chapter 3. By using $\mathbf{O}$, the data set $X = \{x_1, x_2, ..., x_n\}$, where n is the total number of image blocks containing ridges, is then constructed as follows: we first construct the set $X' = \{x'_q, q = 1, ..., WH\}$, where $x'_q = \mathbf{O}(h, w)$, $w = 1,2,..., W$ and $h = 1,2,..., H$, such that $q = (h-1)W + w$,. Then, the data set X is obtained from X' by removing from it all the elements not containing a valid orientation value. Next, a regularized data set $\overline{X} = \{\bar{x}_1, \bar{x}_2, ..., \bar{x}_n\}$ is constructed, such that $\bar{x}_i$ is calculated as [108].

$$\bar{x}_i = \frac{1}{1+\alpha}\left(x_i + \frac{\alpha}{N_R} \sum_{j \in N_i} x_j \right) \tag{6.1}$$

where N_i denotes the set of neighboring elements falling into a local window around $x_i \in X$, and N_R represents its cardinality. The parameter α controls the effect of the average value of the neighboring elements on the value of the regularized orientation $\bar{x}_i \in \overline{X}$. The value of this parameter was empirically chosen to be unity. Then using this regularized data set the objective function of the HA-FCM algorithm is modified as.

$$J = \sum_{j=1}^{c} \sum_{i=1}^{n} u_{ij}^{m} \left\| \bar{x}_i - v_j \right\|^2 \tag{6.2}$$

$$u_{ij}(t) = \begin{cases} \dfrac{\left\| \bar{x}_i - v_j(t-1) \right\|^{-2/(m-1)}}{\sum_{l=1}^{c} \left\| \bar{x}_i - v_l(t-1) \right\|^{-2/(m-1)}}, & \bar{x}_i \neq v_l(t-1), \forall l = 1,2,...,c \\ 1, & \bar{x}_i = v_j(t-1) \\ 0, & \bar{x}_i = v_q(t-1), \forall q = 1,2,...,c \text{ and } q \neq j \end{cases} \tag{6.3}$$

$$v_j(t) = \frac{\sum_{i=1}^{n} (u_{ij}(t))^m \ \bar{x}_i}{\sum_{i=1}^{n} (u_{ij}(t))^m} \tag{6.4}$$

In order to show the effectiveness of the RHA-FCM technique in comparison to that of the HA-FCM technique, six different fingerprint images shown in Figures 6.1 and 6.2 are considered. Each figure contains three different fingerprint images in its first row, their orientation images in the second row, and the corresponding images partitioned by using the HA-FCM and RHA-FCM techniques in the third and the fourth rows, respectively.

As discussed in Chapter 5, an OF-based partitioning scheme can be expected to assign an image block in the vicinity of or containing a singular point to a larger number of different clusters, and other image blocks to have less diversity in terms of their belonging to different clusters. Even though these features are seen to be clearly present in the images of the two figures obtained by the two techniques, the following two conclusions can be drawn on the superiority of the second technique over the first one. First, the regions away from the singular points are much smoother in the case of the partitioning obtained by RHA-FCM in that these regions do not have within themselves many smaller regions. The problem of having smaller regions, which results from the noise or ridge cuts, has been more effectively resolved by the RHA-FCM technique. Second, the diversity of the singular point regions as provided by the HA-FCM technique is not compromised by the regularization step of the RHA-FCM technique.

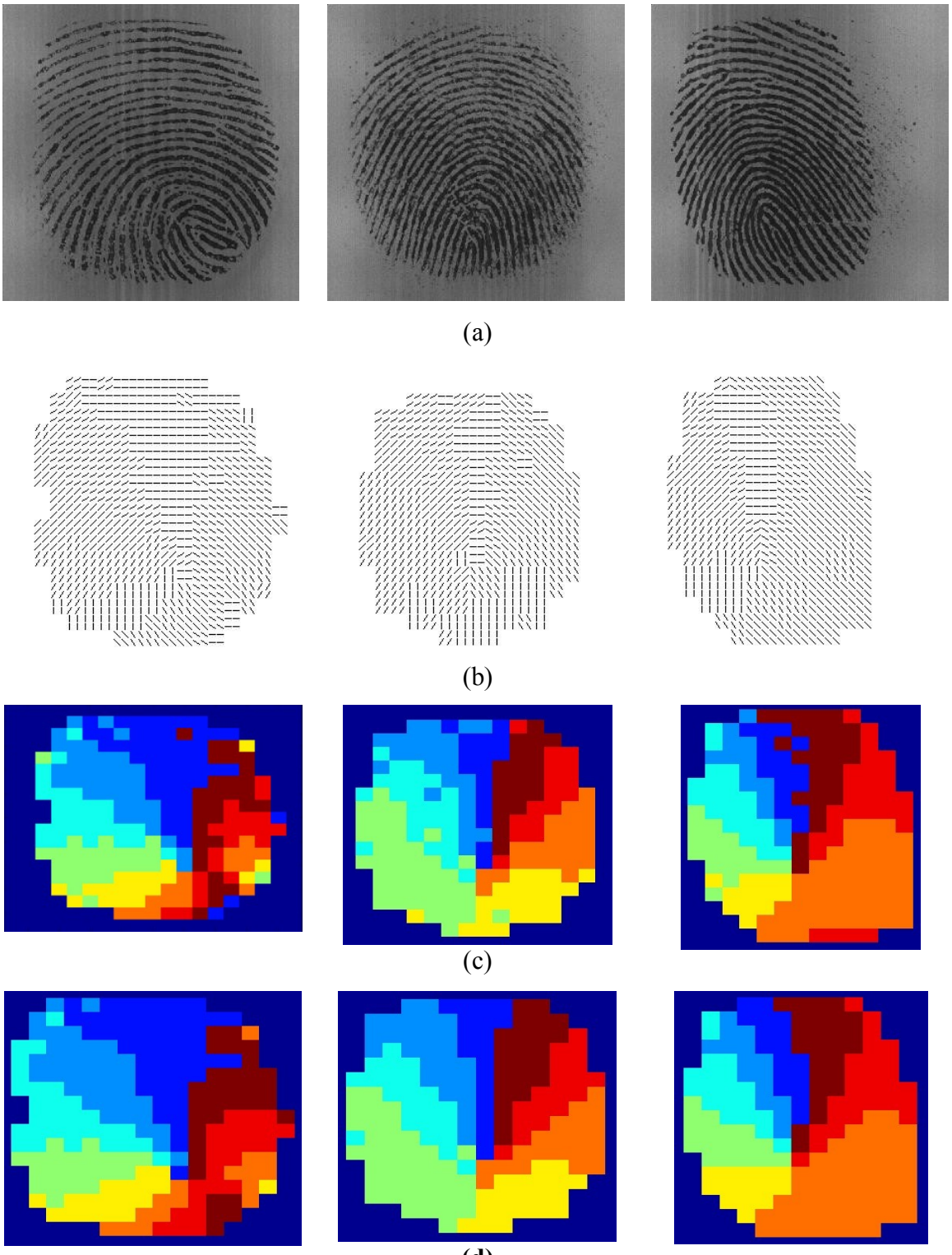

Figure 6.1: (a) A set of three fingerprint images. (b) Their orientation images. (c) Images partitioned using the HA-FCM. (d) Images partitioned using the RHA-FCM.

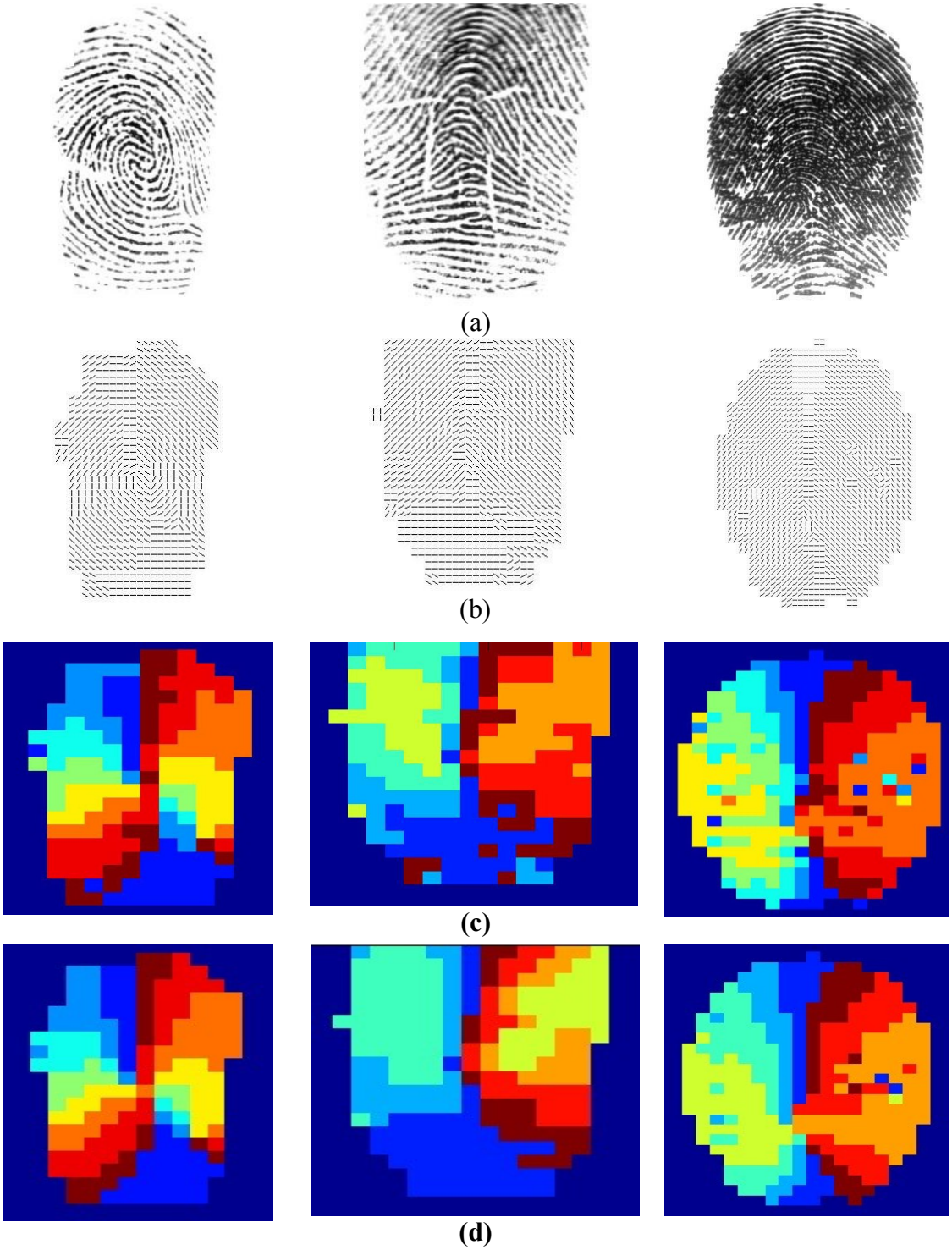

Figure 6.2: (a) Another set of three fingerprint images. (b) Their orientation images. (c) Images partitioned using the HA-FCM. (d) Images partitioned using the RHA-FCM.

6.2.2 Reduction of the computational complexity

For the purpose of segmenting MR brain images, Szilagyi *et. al*. [58] have proposed a fast FCM clustering algorithm called the EnFCM algorithm. In this algorithm, after the regularization step is carried out on the intensities of image pixels, a new data set is obtained from $\overline{X}$, as $\widetilde{X} = \{\widetilde{x}_1, \widetilde{x}_2, ..., \widetilde{x}_q\}$, where $\widetilde{x}_i$'s are the distinct intensities of the image pixels, which are arranged in $\widetilde{X}$ in an increasing order of their magnitudes, and q is the total number of the different gray levels present in the image. The number of elements in data set $\widetilde{X}$ is, in general, much smaller than n, the number of elements in $\overline{X}$. Due to this reduction in the number of elements, the amount of the calculations required in each iteration is significantly reduced. Therefore, the EnFCM algorithm has been able to provide a clustering solution with a computational complexity lower than that provided by the traditional FCM technique.

Now, we propose to reduce the overall computational complexity of the RHA-FCM technique in two stages. In the first stage, the amount of calculations involved in each iteration is reduced by adopting the approach of [58]. In the second stage, the number of iterations of the RHA-FCM algorithm is itself reduced.

(a) Reduction in the amount of computations in an iteration

The data set $\widetilde{X} = \{\widetilde{x}_1, \widetilde{x}_2, ..., \widetilde{x}_q\}$ comprising the distinct orientation values is first constructed using the regularized data set $\overline{X}$. Then using this new data set the objective function of the FCM algorithm is modified as [58].

$$J = \sum_{k=1}^{c} \sum_{l=1}^{q} \lambda_l \, u_{kl}^{m} \left\| \widetilde{x}_l - v_k \right\|^2 \tag{6.5}$$

where λ_l is the number of blocks in the image having the orientation value equal to $\tilde{x}_l$, such that $\sum_{l=1}^{q} \lambda_l = n$. Updating of the membership matrix U and that of the set of cluster centers V are carried out as [58]

$$u_{lj}(t) = \begin{cases} \dfrac{\left\| \tilde{x}_l - v_j(t-1) \right\|^{-2/(m-1)}}{\sum_{k=1}^{c} \left\| \tilde{x}_l - v_k(t-1) \right\|^{-2/(m-1)}}, & \tilde{x}_l \neq v_k(t-1)\ ,\ \forall k = 1,2,...,c \\ 1, & \tilde{x}_l = v_j(t-1) \\ 0, & \tilde{x}_l = v_r(t-1),\ \forall r = 1,2,...,c \text{ and } r \neq j \end{cases} \tag{6.6}$$

$$v_j(t) = \frac{\sum_{l=1}^{q} \lambda_l \ (u_{lj}(t))^m \ \tilde{x}_l}{\sum_{l=1}^{q} \lambda_l \ (u_{lj}(t))^m} \tag{6.7}$$

We will refer to the technique for fingerprint partitioning using this rearranged data set $\tilde{X}$ in its objective function as the reduced-data RHA-FCM (RDRHA-FCM) technique.

In order to compare the number of elements in the sets $\overline{X}$ and $\tilde{X}$, a comprehensive simulation study is carried out using the same benchmark databases as used in Chapter 4. Table 6.1 gives the average number of data items belonging to the sets $\overline{X}$ and $\tilde{X}$, i.e. n and q, respectively, for the different databases. It is seen from this table that the number of data items n has been reduced on the average by 52%. Hence, with the re-arranged expression for the objective function, the overall computational complexity of RHA-FCM is expected to be significantly reduced.

Table 6.1: Average number of data items belonging to the sets $\overline{X}$ and $\widetilde{X}$.

	FVC2002			FVC2004		FVC2006
	DB1	DB3	DB4	DB1	DB2	DB1
n	277	199	211	301	261	142
q	121	106	103	125	120	82

(b) Reduction in the number of iterations

Even though the number of operations performed in solving (6.5) in each iteration is now greatly reduced, this equation is only a re-arranged version of (6.2) representing the objective function of the RHA-FCM algorithm. Accordingly, the number of iterations and the clustering solution as provided by (6.6) and (6.7) must be the same as that provided by (6.3) and (6.4). We now propose a scheme to reduce the number of iterations without unduly affecting the clustering solution. Note that in the objective function given by (6.5), λ_l represents frequency in the set $\overline{X}$ of each distinct data item $\widetilde{x}_l$. Changing the value of each λ_l will, in general, modify the objective function given by (6.5), and therefore, the solution obtained and the number of iterations required to achieve this solution will also change. If λ_l is replaced by $\frac{\lambda_l}{n}$, the relative frequencies of the data items used in the objective function will remain unaffected. In fact, this change amounts to only increasing the value of threshold parameter ε used for terminating the iteration process by a factor n, while keeping the objective function unchanged. Note that the value of this threshold parameter ε is chosen to be very small (in our experiments $\varepsilon = 10^{-5}$) in order to ensure the convergence of the iterative process to the solution. In practice, such a small value for ε may not be necessary to ensure this convergence. Thus, increasing the value of threshold ε by a factor n would in effect reduce the number of iterations by making the stopping criterion less stringent. At the same time, with this

strategy, the stopping criterion is also made to be related to the total number of data items n in the set X or $\overline{X}$.

We now provide some simulation results in support of the proposed scheme of making the stopping criterion to be dependent on the size of the data set $\overline{X}$. Monte Carlo simulations are performed to obtain the gradient of the objective function given by (6.5) as a function of the iteration number for three values of n, namely 10, 100 and 1000. The value of parameter ε for terminating the iteration process is chosen to be a fixed value of 10^{-5}. For 100 runs of the Monte Carlo simulations, 100 independent data sets are randomly generated for a given n with their items being in the range $[0, \pi)$. Each data set is clustered using RDRHA-FCM technique with $c' = 5$. Figure 6.3 shows the results of one of the runs of the Monte Carlo simulation for each of the three values of n. We can make the following observations from the results in this figure, which are typical of the results obtained from other runs of our Monte Carlo simulation.

(i) For each n, the convergence of the iterative process toward the final solution is initially fast but slows down at higher iterations.

(ii) The initial convergence rate increases and the final convergence rate decreases as n increases.

(iii) Even though the criterion of terminating the iterations is exactly met (for $\varepsilon = 10^{-5}$) at iteration number 26, 63 and 152 for the cases of $n = 10$, 100 and 1000, respectively, an acceptable solution seems to have been obtained earlier in each case with the set having larger n providing this solution relatively even much earlier.

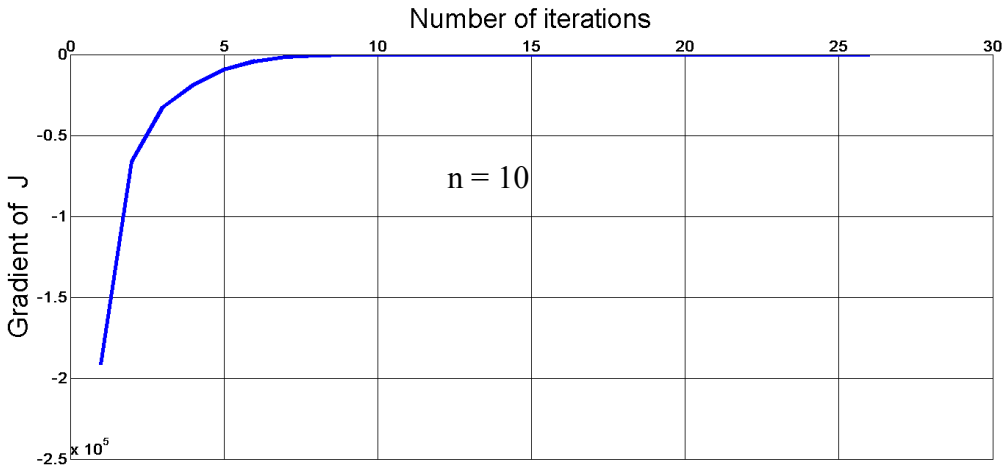

(a)

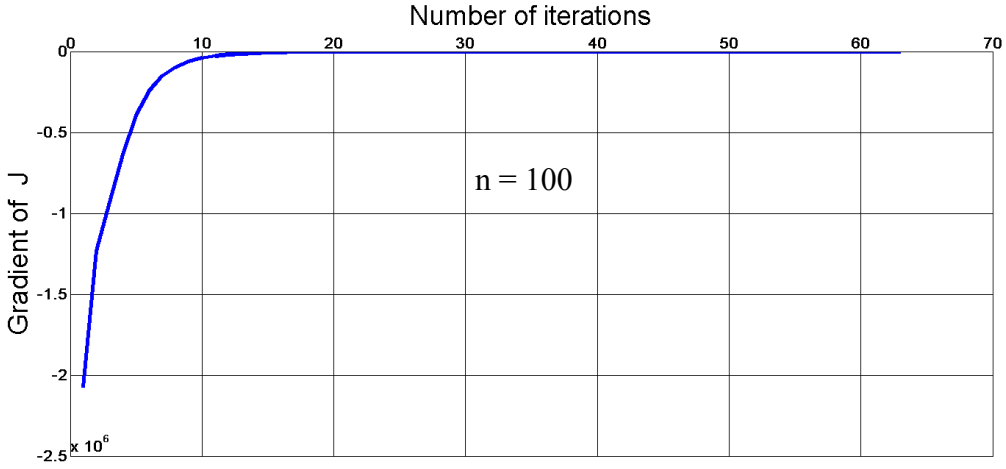

(b)

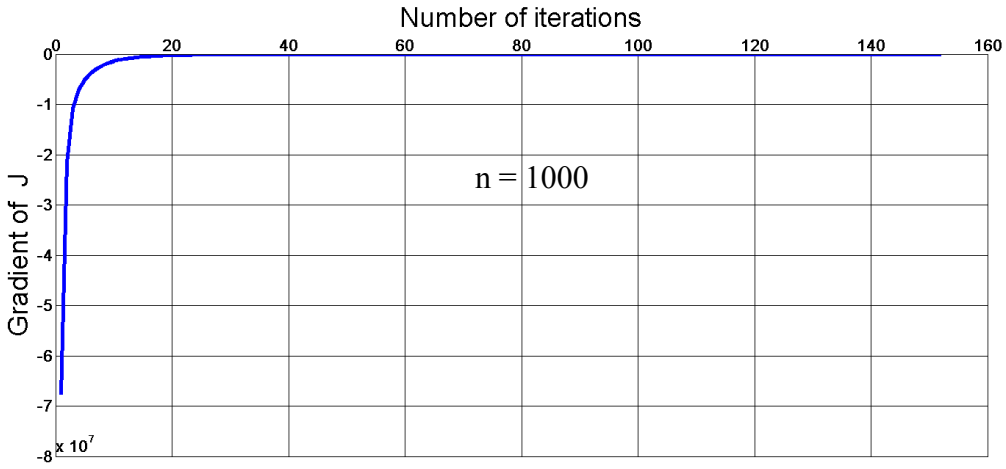

(c)

Figure 6.3: The gradient of the objective function J versus the number of iterations: (a) $n=10$, (b) $n=100$ and (c) $n=1000$ based on Monte Carlo simulation.

The above observations suggest that for each case, ε could be increased from the chosen value 10^{-5} to a higher value, in addition this value can be chosen to be larger for larger values of n without any appreciable loss in the accuracy of the solution. Thus, an effective choice of the threshold parameter can be $\varepsilon_n = n\,\varepsilon$, where ε is some very small positive number such as 10^{-5}.

The RDRHA-FCM technique with the modified threshold parameter $\varepsilon_n = n\,\varepsilon$ used in the criterion for stopping the iterations will be referred to as an enhanced HA-FCM (EHA-FCM) technique. The EHA-FCM technique should provide a solution for the fingerprint partitioning problem that is not only superior to that obtained by HA-FCM technique of Chapter 5, but also results in a smaller number of iterations and a smaller amount of computations in each iteration, that is, the overall complexity gets significantly reduced.

6.2.3 EHA-FCM fingerprint partitioning algorithm

The EHA-FCM fingerprint partitioning algorithm developed in this chapter can be summarized to have the following steps: (i) The regularized data set $\overline{X}$ is constructed from the original data set X. The data set $\widetilde{X}$ is then obtained such that its data items consist of only the distinct orientations values of $\overline{X}$. (ii) The histogram analysis (HA) technique is applied on the set $\widetilde{X}$ to determine the number of clusters c and the set of their initial centers $V(0)$. (iv) The FCM algorithm in which (5.4) and (5.5) replaced by (6.6), (6.7), respectively, and the threshold ε replaced by $\varepsilon_n = n\,\varepsilon$ is applied. This step provides the clustering solution as a set of cluster centers V, and the membership matrix U whose elements represent the degree of belonging of a data item $\widetilde{x}_l \in \widetilde{X}$ to each

cluster $j \in \{1, 2, \ldots, c\}$. (v) The fuzzy clustered orientation field (FCOF) set is constructed as described in Chapter 5.

The following algorithm gives a formal description of the EHA-FCM technique for fingerprint partitioning.

Algorithm 6.1: The EHA-FCM fingerprint partitioning scheme

- **Construction of the set $\tilde{X}$**

1- Divide the fingerprint image into H×W blocks each of size N×N pixels.

2- Let $X' = \{\phi\}$.

3- For each block $h = 1:H$ and $w = 1:W$

e. Compute the dominant ridge direction in the current block $\mathbf{O}(h,w)$ by using (3.1).

f. Compute the variance σ^2 of the gray levels of image pixels within the current image block, in a direction that is perpendicular to $\mathbf{O}(h,w)$. If $\sigma^2 \le \tau$, where τ is an empirically specified threshold, then the current image block belongs to the background, and it is removed from the orientation field. Set $\mathbf{O}(h,w) = -1$.

g. Let $q = (h-1)W + w$ and $x'_q = \mathbf{O}(h,w)$.

h. Let $X' = X' \bigcup \{x'_q\}$

4- Let $i = 0$, $X = \{\phi\}$ and $\overline{X} = \{\phi\}$.

5- For each $x'_q \in X'$, where $q = 1,....,WH$, if $x'_q \neq -1$, then $i = i+1$, $x_i = x'_q$ and $X = X \bigcup \{x_i\}$.

6- For each $x_i \in X$, where $i = 1,....,n$, calculate $\bar{x}_i$ using (6.1), then $\overline{X} = \overline{X} \bigcup \{\bar{x}_i\}$.

7- Let $l = 0$ and $\widetilde{X} = \{\phi\}$.

8- For each $\bar{x}_i \in \overline{X}$, where $i = 1,....,n$, if $\bar{x}_i \notin \widetilde{X}$, then $l = l + 1$, $\tilde{x}_l = \bar{x}_i$ and $\widetilde{X} = \widetilde{X} \bigcup \{\tilde{x}_i\}$.

- Clustering of the set $\widetilde{X}$ using the HA-FCM

9- With a pre-initial c', apply the HA technique (Algorithm 5.2) on the set $\widetilde{X}$ to determine the initial number of clusters c with the set of initial cluster centers $V(0)$.

10- With the initial number of clusters c and the cluster centers $V(0)$, apply the FCM (Algorithm 5.1) on set $\widetilde{X}$ with (5.4) and (5.5) replaced by (6.6), (6.7), respectively, and the threshold ε replaced by $\varepsilon_n = n\,\varepsilon$, to determine the final set of cluster centers V and the membership matrix U.

- **Construction of the set** *FCOF*

11- For each $x_i \in X$, where $i = 1,....,n$, construct the fuzzy clustered orientation field (FCOF) set as $FCOF(i) = \{(r_i(1), u_{ir_i(1)}), (r_i(2), u_{ir_i(2)}), ..., (r_i(a_i), u_{ir_i(a_i)})\}$, where $r_i(k) = j \in \{1,2,...,c\}$, and $k = 1,...,a_i$, such that $u_{ir_i(k)}$ is the k^{th} largest value in the set $\{U(i,\eta), \eta = 1,...,c\}$, and $a_i \le c$ is chosen to be the smallest integer υ for which $\sum_{k=1}^{\upsilon} u_{ir_i(k)} \ge \gamma$.

6.3 Experimental Results and Comparisons

In order to compare the performances of HA-FCM technique and its evolutionary versions, namely the RHA-FCM, RDRHA-FCM and the EHA-FCM techniques, a comprehensive simulation study has been undertaken using the same databases as those

chosen in Chapter 4. In the first part of this study, the computational complexities of these techniques are compared in terms of the number of iterations required and the processing times in order to obtain the clustering solutions. Tables 6.2 and 6.3 give the average number of iterations and the average processing times, respectively, of the techniques for the different databases. By comparing the results listed in these tables, the following three observations can be made. First, the computational complexity of the RHA-FCM is slightly larger than that of the HA-FCM technique, which could be the result of introducing in the histogram of $\overline{X}$ some new values of the data items by decreasing the frequencies of some of the old ones when the set X is regularized as $\overline{X}$. Second, even though, as expected, the number of iterations required by the RHA-FCM or RDRHA-FCM is the same, the processing times of the RDRHA-FCM is smaller than that of RHA-FCM. As explained previously, this is due to the reduction in the amount of calculations required in each iteration. Third, the processing time of EHA-FCM technique is significantly lower than that of RDRHA-FCM. This is because of the fact that the number of iterations required by the former is significantly lower than that required by the latter. It is also seen that the processing time of EHA-FCM technique is only about one-third of that of the RHA-FCM.

Table 6.2: Average number of iterations required by the HA-FCM, RHA-FCM, RDRHA-FCM and EHA-FCM techniques using different databases.

		HA-FCM	RHA-FCM	RDRHA-FCM	EHA-FCM
2002	DB1	85	87	87	60
	DB3	71	72	72	50
	DB4	77	84	84	59
2004	DB1	81	86	86	59
	DB2	82	88	88	61
2006	DB1	68	68	68	50

Table 6.3: Average processing times (in ms) required by the HA-FCM, RHA-FCM, RDRHA-FCM and EHA-FCM techniques using different databases.

		HA-FCM	RHA-FCM	RDRHA-FCM	EHA-FCM
2002	DB1	104.8	105.9	52.6	36.4
	DB3	65.5	65.5	37.3	25.5
	DB4	70.5	75.7	40.6	28.1
2004	DB1	101.1	106.7	51.9	35.2
	DB2	95.1	102.1	51.2	34.9
2006	DB1	43.7	42.5	22.9	16.3

The second part of the study focuses on the quality of the clustering solution obtained by the EHA-FCM technique in comparison to the one obtained by the RDRHA-FCM technique in order to show the effect of using the adaptive threshold parameter ε_n instead of ε on the accuracy of the solution obtained. In order to measure the quality of the clustering solution $(V^{(2)},U^{(2)})$ obtained by EHA-FCM technique relative to that $(V^{(1)},U^{(1)})$ obtained by RDRHA-FCM technique for the fingerprints in a given database, we define the following two metrics:

$$S_1(V^{(1)},V^{(2)}) = \frac{1}{c}\sum_{j=1}^{c}\frac{\left|v_j^{(1)} - v_j^{(2)}\right|}{v_j^{(1)}} \tag{6.8}$$

$$S_2(U^{(1)},U^{(2)}) = \frac{1}{c\,q}\sum_{l=1}^{q}\sum_{j=1}^{c}\frac{\left|u_{lj}^{(1)} - u_{lj}^{(2)}\right|}{u_{lj}^{(1)}} \tag{6.9}$$

These two metrics are computed for the fingerprints of each of the databases. Table 6.4 gives the average values of the metrics in percentages. The very small values of these metrics for each of the databases clearly show that the solution obtained by EHA-FCM using adaptive threshold parameter ε_n is almost as accurate as that obtained by RDRHA-FCM that uses a non-adaptive threshold parameter ε.

Table 6.4: Average values of the metrics (in percentage) representing the quality of the solution obtained by EHA-FCM techniques over that obtained by RDRHA-FCM for various databases.

	FVC2002			FVC2004		FVC2006
	DB1	DB3	DB4	DB1	DB2	DB1
$S_1(V^{(1)},V^{(2)})$	0.18%	0.17%	0.32%	0.2%	0.3%	0.56%
$S_2(U^{(1)},U^{(2)})$	0.17%	0.14%	0.19%	0.18%	0.55%	0.13%

In order to visually compare the solutions obtained by the RDRHA-FCM and EHA-FCM techniques, six different fingerprint images are partitioned using these two techniques. The results are shown in Figures 6.4 and 6.5. Each figure contains three different fingerprint images in the first row and the corresponding partitioned images using the RDRHA-FCM and EHA-FCM techniques in the second and third rows, respectively. It is clear from these figures that the partitioned images obtained by the two techniques are identical, thus showing that the very small difference in the solutions of the two methods, as seen from Table 6.4, has little effect on the actual partitioning of fingerprint images.

From the above comparative study, it is concluded that the performance, in terms of both the quality of the solution obtained and the overall computational complexity, of the proposed EHA-FCM technique is much superior to that of the HA-FCM technique.

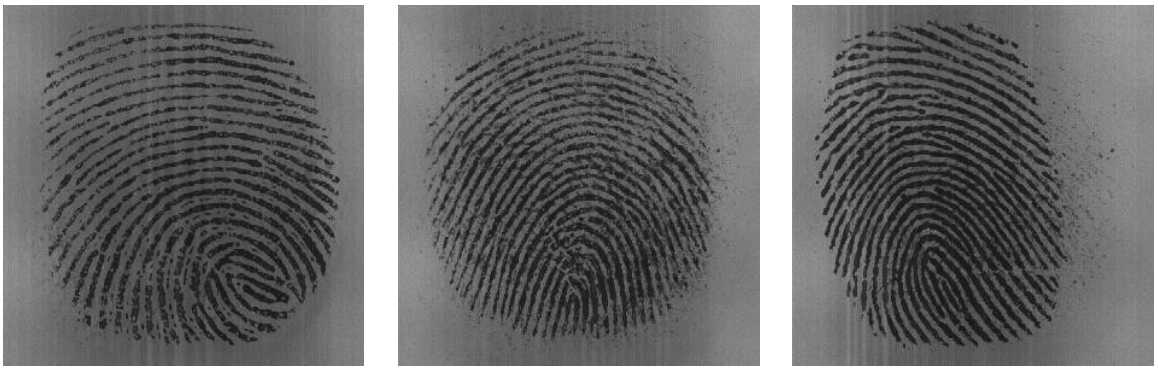

(a)

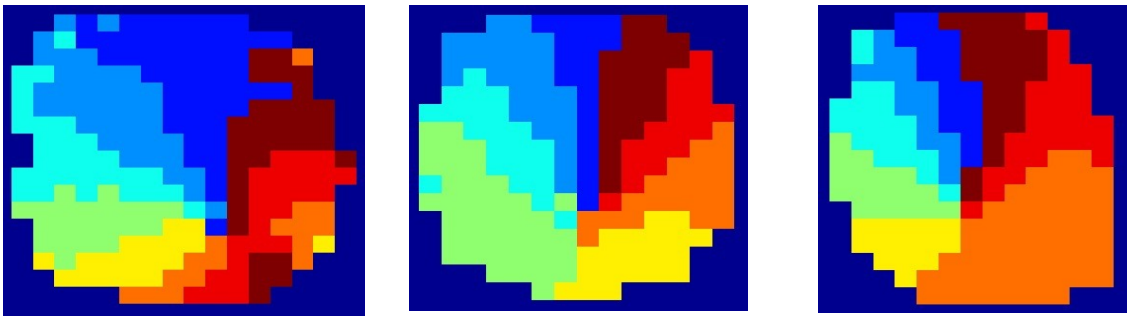

(b)

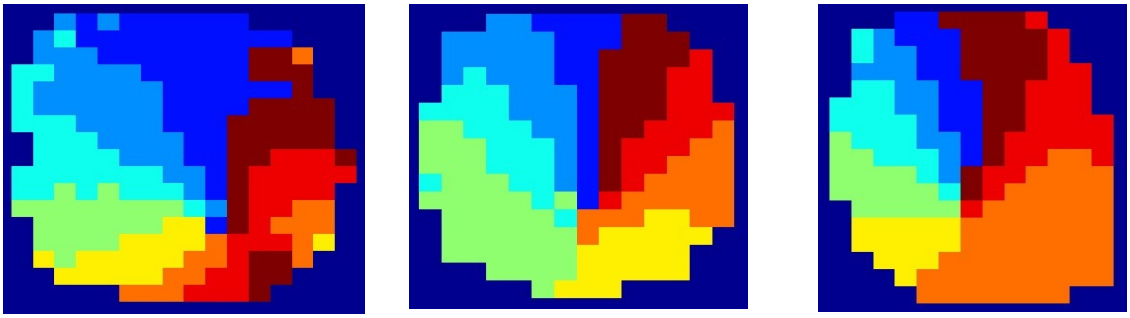

(c)

Figure 6.4: (a) A set of three fingerprint images. (b) Images partitioned using the RDRHA-FCM. (c) Images partitioned using the EHA-FCM.

(a)

(b)

(c)

Figure 6.5: (a) Another set of three fingerprint images. (b) Images partitioned using the RDRHA-FCM. (c) Images partitioned using the EHA-FCM.

6.4 Summary

In Chapter 5, a histogram analysis fuzzy c-means (HA-FCM) technique was developed for the partitioning of fingerprint images in terms of the ridge orientations of the image. The technique was shown to provide partitioned regions that are smoother than that provided by the quantization technique at a computational cost that is lower than that of using the standard FCM algorithm.

In this chapter, an enhanced HA-FCM (EHA-FCM) partitioning scheme has been proposed in order to further improve the performance in terms of the smoothness of the partitions and the computational complexity of the HA-FCM technique. In order to enhance the smoothness of the partitioned regions, the idea of data regularization has been applied on the original ridge orientation by replacing a data item by the linear combination of itself and the average of its local neighboring data items. It has been shown that through this regularization process the regions, affected by noise, are smoothened while keeping the singular regions unaffected. The problem of computational complexity has been addressed in two stages. In the first stage, the amount of computations in each iteration has been reduced by making the clustering process to depend only on the distinct orientation values rather than on all the data items. In the second stage, the number of iterations has been reduced by developing a scheme for terminating the iterative process based on the number of data items without affecting the clustering process itself.

A simulation study using challenging benchmark databases has been undertaken in order to show the effectiveness of the proposed scheme in this chapter. The simulation results have shown that, in comparison to the HA-FCM technique, the proposed EHA-

FCM technique provides a solution for the fingerprint partitioning problem that is not only superior but also results in a significant reduction of the overall computational complexity.

CHAPTER 7

A Multilevel Structural Fingerprint Recognition Based on the EHA-FCM Partitioning Scheme

7.1 Introduction

In Chapter 3, a fingerprint decomposition technique using two global features, namely singular points and ridge orientations of the fingerprint, was presented. In this technique the decomposition was carried out using a crisp clustering technique for both the determination of the singular points and the partitioning of the fingerprint orientation field. The resulting decomposed fingerprint image along with information on the local features was then used in Chapter 4 to formulate a multilevel feature representation of fingerprint image. Finally, this multilevel feature vector was used to develop a matching algorithm for fingerprint recognition. In the preceding chapter, an enhanced histogram based fuzzy c-means partitioning scheme, referred to as EHA-FCM technique, was presented. The new technique was shown to provide fingerprint partitioning that is smoother than that provided by using the HA-FCM partitioning technique at a lower computational cost.

In this chapter, using this fuzzy based partitioning along with the ideas of fingerprint decomposition, representation and matching introduced in Chapters 3 and 4, is used to develop a new fuzzy based fingerprint recognition scheme referred to as fuzzy based multilevel structural technique for fingerprint recognition (FMSFR) [109]. In Section 7.2,

a fuzzy based algorithm for fingerprint decomposition is presented. This decomposition that comprises singular points and plain orientation field regions are then used in Section 7.3 for devising a fuzzy based multilevel representation of fingerprints. In Section 7.4, a fuzzy based matching algorithm is developed for fingerprint recognition. Finally, in Section 7.5 extensive simulations are carried out to study the performance of the fuzzy based multilevel fingerprint recognition technique proposed in this chapter.

7.2 EHA-FCM Based Fingerprint Decomposition Algorithm

In Chapter 3, a fingerprint image was decomposed into regions (sub-images), such that each region has a unique global feature characteristic. In this section a fingerprint decomposition algorithm is designed based on the EHA-FCM fingerprint partitioning scheme proposed in Chapter 6. The fingerprint image is decomposed into singular and non-singular regions. A region is defined to be a singular region, if it contains a singular point (core or delta) or a plain region, if it contains only ridges having orientation values belonging to a specified cluster.

To start with, the EHA-FCM partitioning scheme of the previous chapter is used on a given fingerprint image to obtain a fuzzy clustered orientation field (*FCOF*). Such that the i^{th} element of *FCOF* represents all the clusters to which the i^{th} image block belongs to and the degree of belonging to each of these clusters in a certain order. Thus, each element of *FCOF* consists of a sorted set of ordered pairs given by

$$FCOF(i) = \left\{\left(r_i(1), u_{ir_i(1)}\right), \left(r_i(2), u_{ir_i(2)}\right), ..., \left(r_i(a_i), u_{ir_i(a_i)}\right)\right\}, i = 1, ..., n \qquad (7.1)$$

where $r_i(k) = j \in \{1,2,...,c\}$, $k = 1,...,a_i$, such that $u_{ir_i(k)}$ is the k^{th} largest value in the set $\{U(i,\eta), \eta = 1,...,c\}$, and $a_i \le c$ is a positive integer representing the number of clusters in

which the total of the degrees of membership of the i^{th} image block is larger than a pre-specified threshold γ.

Next, using $FCOF$, the singular points are detected by employing the fuzzy-based cluster distribution scheme developed in Chapter 5. As was seen in that chapter, this scheme is able to detect the singular points accurately and also determine their types, i.e., upper or lower core, or left or right delta. Moreover, this scheme is able to calculate the orientation of the cores, which will also be necessary in the next section to formulate multilevel feature vectors.

Finally, the fingerprint image is decomposed into different regions and represented as a set $\Re = \{\Re_{S_1}, \Re_{S_2}, \Re_{S_3}, \Re_{P_1}, \Re_{P_2}, ..., \Re_{P_L}\}$, where $\Re_{S_d}$ is the d^{th} singular region and $\Re_{P_l}$ is the l^{th} plain region. A singular region is defined as $\Re_{S_d} = \{B_{f,g}, f = 1,...,F, g = 1,...,G\}$, where $B_{f,g}$ is the $(f,g)^{\text{th}}$ image block corresponding to a singular point (i.e. a core or delta). In the proposed method, a singular point region $\Re_{S_d}$ could be only one of the three types: the core region $\Re_{S_1}$ (upper and/or lower core), the left delta region $\Re_{S_2}$, and the right delta region $\Re_{S_3}$. Note that if both lower and upper cores exist simultaneously, they are included in the same region $\Re_{S_1}$, since they are located in a relatively closer proximity than the left and right deltas do. In addition, the core region $\Re_{S_1}$ is associated with the orientation of the core as calculated in Chapter 5. After excluding the items corresponding to the singular regions from the $FCOF$, the remaining items are then used to form a set of overlapping plain regions. Each plain region $\Re_{P_l}$ is characterized by a cluster center v_j, which corresponds to the orientation of that region, θ_l. Hence, a plain region $\Re_{P_l} = \{B_i^j, i = 1,...,M\}$ contains M

adjacent image blocks, where B_i^j is the i^{th} image block represented as an ordered pair (j,u_{ij}) such that $j \in \{1,2,...,c\}$ and u_{ij} is the membership degree of this block to the j^{th} cluster. As explained in Chapter 3, there is a possibility to have abnormal regions in the set $\Re$, i.e., isolated regions or small regions. Therefore, an isolated region is removed from $\Re$, and the items of a small region are distributed among the neighboring regions. In order to distribute the items of a small region in this fuzzy based decomposition algorithm, an item B_i^j of a small region $\Re_{P_l}$ is first examined to determine if it has been already assigned to another region, if so, then it is removed from the small region. Otherwise, this item is assigned to a neighboring region $\Re_{P_k}$ with $\theta_k = v_q$ such that the membership degree of this item cluster number q is $u_{iq} = u_{ir_l(2)}$.

The proposed fuzzy-based fingerprint decomposition scheme described in the preceding paragraphs can be summarized as an algorithm.

Algorithm 7.1: Fuzzy-based fingerprint decomposition

1- With a pre-initial number of clusters c', apply the EHA-FCM partitioning technique (Algorithm 6.1) on a given fingerprint image to obtain the clustering solution (V,U) and thus to obtain the fuzzy clustered orientation field (*FCOF*) as in (7.1).

2- Detect the singular points in the fingerprint using the fuzzy-based cluster distribution scheme of Section 5.3.

3- Define the singular point regions $\Re_{S_d} = \{B_{f,g}, f = 1,...,F, g = 1,...,G\}$, where $B_{f,g}$ is a one-dimensional index of the $(f,g)^{\text{th}}$ image block corresponding to a singular point (i.e. a core or delta), then remove these blocks from *FCOF* .

4- Divide rest of the items of $FCOF$ into c groups. The j^{th} group represents the fingerprint image blocks belonging to cluster center v_j.

5- For each group j = 1 : c

Define the plain regions $\Re_{P_l} = \{B_i^j, i = 1,...,M\}$ by grouping the adjacent blocks into one region. The adjacent blocks are identified using the 8-connetcivity criteria [68].

6- Use the output of steps 3 and 5 to represent the decomposed image as a set of regions $\Re = \{\Re_{S_1}, \Re_{S_2}, \Re_{S_3}, \Re_{P_1}, \Re_{P_2}, ..., \Re_{P_L}\}$.

7- For each plain region l = 1 : L

- If the region is an isolated region, then remove the region from set $\Re$.
- If the region is a very small region, then each item B_i^j of a small region $\Re_{P_l}$ is first examined to determine if it has been already assigned to another region, if so, then it is removed from the small region. Otherwise, this item is assigned to a neighboring region $\Re_{P_k}$ with $\theta_k = v_q$ such that the membership degree of this item cluster number q is $u_{iq} = u_{ir_i(2)}$. Finally, remove this small region from set $\Re$.

7.3 Fuzzy-based Multilevel Fingerprint Representation

The problem of fingerprint representation is to determine a measurement (feature) space, in which fingerprint images belonging to a specific finger form a compact cluster different from those of other fingers from the stand point of these features. The objective in devising a suitable fingerprint representation is to provide high accuracy in fingerprint recognition with a reasonable computational complexity. In Chapter 4, a multilevel

structural fingerprint representation was developed that included information on both the global and local features of the fingerprint. In this scheme, a region of the fingerprint was represented using three different levels of fingerprint characteristics. The main ideas of this representation can be summarized as follows:

1) The global features of a region, which mainly represent the global structure of the fingerprint image with respect to the core region, are specified as $FV1_l = (\zeta_l, \theta_{\Re_l - Core})$, where ζ_l denotes both the relative position of the l^{th} region with respect to the core region as well as the type of the region, i.e., a singular or plain region, and $\theta_{\Re_l - Core}$ is the orientation of a plain region relative to the orientation of the core.

2) The neighborhood features of a region, which represent the region's characteristics in relation to its adjacent regions, are specified as $FV2_l = \{(\rho_{lq}, \theta_{lq}), q = 1,...,Q\}$, where ρ_{lq} is the position and θ_{lq} is the orientation of the q^{th} region relative to those of the l^{th} region. This level of characteristics is especially useful when the core point is not detectable.

3) The local characteristics of a region that include the ridge curvatures and minutiae, which vary from region to region, are specified as $FV3_l = \{\phi_l, \{(x_r, y_r, t_r)_l, r = 1,...,R\}\}$, where ϕ_l is the curvature of the ridges of the region and $\{(x_r, y_r, t_r)_l, r = 1,...,R\}$ is the minutiae inside this region.

In this section, a fuzzy-based scheme is presented for the formulation of these feature vectors. In the previous section, a preliminary representation for the fingerprint images was obtained as a set of singular regions and overlapping plain regions by using the fuzzy fingerprint decomposition technique (Algorithm 7.1). In this technique, an image block is made to belong to the plain region(s) for which the block has a

considerable degree of membership(s) (determined by γ) in its (or their) associated cluster(s). The fuzzy formulation of these three levels of characteristics is carried out using both the cluster centers and the membership belonging degrees.

(i) Formulation of Global Features (FV1)

In order to capture the global structure of the fingerprint image, we specify three global features: (i) the type of the region, in regard to whether it is a plain or a singular region, and (ii) its position and (iii) its orientation, both relative to the core point. The first feature is already determined after the application of Algorithm 7.1 on the fingerprint image. To quantify the second and third features, we first introduce a new rectangular coordinate system and split the entire fingerprint image into eight sectors based on the location and orientation of the core point (Figure 4.1, reproduced here as Figure 7.1 for convenience). The location of the core point is considered as the origin. The new coordinate system consists of the axes θ_{Core} and θ_{P-Core}, where axis θ_{Core} is the orientation of the core region $\Re_{S_1}$ as evaluated in Section 5.3, and the axis θ_{P-Core} is perpendicular to the axis θ_{Core} evaluated as.

$$\theta_{P-Core} = \begin{cases} \theta_{Core} - \dfrac{\pi}{2} & if\ \theta_{Core} \geq \dfrac{\pi}{2} \\ \theta_{Core} + \dfrac{\pi}{2} & if\ \theta_{Core} < \dfrac{\pi}{2} \end{cases} \qquad (7.2)$$

Starting from θ_{Core} axis, the entire image is divided into eight sectors, such that each sector covers 45^{o} of the space around the core point. Sectors are then labeled as 1 to 8. The second feature for each plain region is calculated by finding the sector in which the geometrical center $\Re_{P\_Center}$ of the region is located.

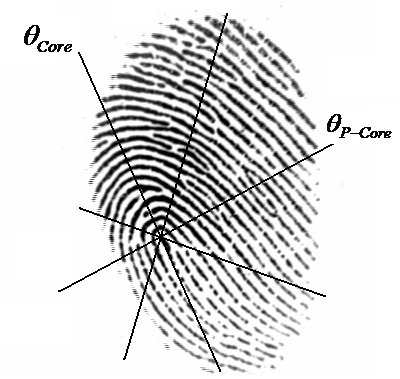

Figure 7.1: Coordinates system defined based on θ_{Core}.

The above three features are used to form the first level (FV1) of the multilevel feature vector using only two components as follows:

a- Type and position of a region (ξ)

In order to reduce the final fingerprint template size, ξ is used to represent both the relative position of a region with respect to the core point region as well as the type of the region. For a plain region $\Re_{P_l}$, ξ represents the relative position, and hence, its value is between 1 and 8, and for singular regions, the core, left delta, and right delta are represented by the digits 9, 10, and 11, respectively.

b- Relative orientation ($\theta_{\Re-Core}$) of a region

By considering θ_{Core} as reference orientation, this feature is used to represent the orientation of a plain region relative to the orientation of the core. For each plain region, this feature is calculated by subtracting θ_{Core} from the orientation θ_l of the ridges of this plain region.

With the formulation of FV1 as carried out above, it is seen that its two components are invariant to displacement and rotation, and thus a pre-alignment step,

commonly employed prior to the matching process of the fingerprint recognition, would not be required.

(ii) Formulation of Neighborhood Features (FV2)

In order to capture the characteristics of a region in relation to its adjacent regions, a pair of features for each adjacent region, the relative position ρ_{lq} and the relative orientation θ_{lq}, is used. The feature ρ_{lq} of region l is defined as the position of the geometrical center of its adjacent region q relative to that of region l. The second feature θ_{lq} is defined as the orientation of the adjacent region q relative to that of region l. In order to evaluate ρ_{lq}, a coordinate system is defined in a manner similar to that defined for the formulation of global features by using the geometrical center $\Re_{P\_Center}$ of region l as the origin and by using its ridge orientation θ_l instead of θ_{Core}. The relative orientation θ_{lq} is calculated by subtracting θ_l from θ_q. The formulation of FV2 is a set of neighborhood features of region l with the number of components equal to the number of adjacent regions.

(iii) Formulation of Local Features (FV3)

The third group of features, FV3, contains three local features: the average membership degree, the curvature of the ridges belonging to a region, and the set of minutiae contained therein.

a- Belonging degree of a region (ω_l)

This feature is a measure of correctness of a region's degree of belonging to its associated cluster. For the plain region $\Re_{P_l}$, it is calculated as the average of the membership degrees of the blocks comprising the region:

$$\omega_l = \frac{1}{M}\sum_{i=1}^{M} u_{ij} \qquad (7.3)$$

b- Curvature of a region (ϕ_l)

This feature represents the curvature ϕ_l of the ridges of a region l, which is calculated only for the plain regions $\Re_{P_l}$ as

$$\phi_l = \theta_{l\max} - \theta_{l\min} \qquad (7.4)$$

where $\theta_{l\min}$ and $\theta_{l\max}$ are, respectively, the smallest and largest orientation values of the ridges contained in region l, which are retrieved from the original orientation field $\mathbf{O}$ within $\Re_{P_l}$. Since the orientation of the region θ_l is the cluster center v_j, the lowest possible value $\theta_{l\min}$ is expected to be $\frac{v_j + v_{j-1}}{2}$ and the largest possible value $\theta_{l\max}$ is expected to be $\frac{v_j + v_{j+1}}{2}$. Therefore, the value of the curvature ϕ_l is in the range $[0, \Delta_l]$, where $\Delta_l = \frac{v_{j+1} - v_{j-1}}{2}$. Hence, this Δ_l is considered as the fuzzy-clustering step which depends on the clustering solution U and V obtained by the EHA-FCM technique.

c- Minutiae set $Minu_l = \{m_1, m_2, ..., m_R\}$

In the original MFV each minutia is represented as (x_r, y_r, t_r), where (x_r, y_r) and t_r is the minutia's type (i.e. ridge ending or ridge bifurcation). Since the EHA-FCM partitioning scheme results into overlapping regions, it is expected that the same minutia may be assigned to different regions. Therefore, another feature representing the belonging degree of the minutia ψ_r to a region under

consideration needs to be defined. The value of this feature is calculated as the membership degree of the image block, containing this minutia, to the region.

By using the features formulated as above, a fuzzy-based fingerprint representation is defined as $FMFV = \{\Re_{S_1}, \Re_{S_2}, \Re_{S_3}, \Re_1, \Re_2, ..., \Re_L\}$, in which $\Re_{S_d} = \{FV1_{S_d}\}$ corresponding to a singular region S_d, and $\Re_l = \{FV1_l, FV2_l, FV3_l\}$ corresponding to the plain region l, where $FV1_l = (\zeta_l, \theta_{\Re_l - Core})$, $FV2_l = \{(\rho_{lq}, \theta_{lq}), q = 1,...,Q\}$, and $FV3_l = \{\omega_l, \phi_l, Minu_l = \{(x_r, y_r, t_r, \psi_r)_l, r = 1,..., R\}\}$ contain, respectively, the global, neighborhood, and local features for a plain region l.

7.4 Fuzzy-based Multilevel Matching

The process of fingerprint matching is to compare the fingerprint templates of two fingerprint images and return a score between 0 and 1 representing the degree of similarity between the two fingerprint images, or a binary score of 0 or 1 indicating whether or not the fingerprint under consideration is the same as the reference fingerprint. The accuracy of the final decision and the response time are the two main concerns of a matching scheme. However, the requirements on the degree of accuracy and the response time of a matching scheme vary from one application to another. In Chapter 4, a multilevel matching (MLM) scheme using the MFVs was developed. In this scheme, a similarity measure for each feature in the MFVs was defined to provide the final matching score. The MLM algorithm was designed based on an early rejection strategy.

In this section, some of the similarity measures, as defined in Chapter 4, are modified based on the new FMFVs formulated in Section 7.3. We denote the FMFVs corresponding to the reference fingerprint template retrieved from the database as

$T = \{\Re_{S_1}, \Re_{S_2}, \Re_{S_3}, \Re_1, \Re_2, ..., \Re_M\}$ with M plain regions, and the FMFVs corresponding to the template of the input fingerprint to be matched as $I = \{\Re_{S_1}, \Re_{S_2}, \Re_{S_3}, \Re_1, \Re_2, ..., \Re_N\}$ with N plain regions. As explained in the previous section, the formulation of FV1 depends on the presence of core region; therefore, in the case when the core point does not exist or it is undetectable, in the proposed multilevel matching scheme we use only FV2 and FV3 to report the final matching result between T and I.

On the onset, the proposed multilevel matching scheme determines whether or not both T and I belong to the same category. By using $\Re_{S_1}$, $\Re_{S_2}$, and $\Re_{S_3}$ for the templates T and I, the category of the fingerprint is identified as left loop, right loop, whorl, arch, or tended arch. If T and I are found to belong to the same category, then by using FV1 the best corresponding pairs of regions from T and I are found, and the degree of similarity, referred to as elementary similarity measure, between the two fingerprints is estimated. If the value of this elementary measure is equal to zero, then the proposed scheme reports a non-match and stops the matching process. Otherwise, the matching process moves on to the next level of matching, in which the calculations of the so called secondary similarity measure is carried out by using FV2 of T and I. If the value of this secondary estimate is equal to zero, a non-match is reported and further matching of T and I is stopped. Otherwise, the matching scheme moves on to a third level and a tertiary similarity between T and I is estimated by using FV3. Finally, the three degrees of similarities are combined to obtain the final matching result.

We now derive expressions for the three similarity measures of fingerprints, which in turn depend on functions representing the similarity of the regions from the T and I templates, using FV1, FV2, and FV3.

1) Similarity measure based on FV1= $\{\xi, \theta_{\Re-Core}\}$

For a plain region, the value of the first component ξ ranges from 1 to 8; therefore, in order to find the correspondence between two plain regions belonging to T and I, respectively, we first define a spatial distance function between the two plain regions $I_{\Re_j}$ and $T_{\Re_i}$ as

$$SD(\xi(I_{\Re_j}),\xi(T_{\Re_i})) = \min\left(\left|\xi(I_{\Re_j}) - \xi(T_{\Re_i})\right|, 8 - \left|\xi(I_{\Re_j}) - \xi(T_{\Re_i})\right|\right) \qquad (7.5)$$

where $\xi(I_{\Re_j})$ and $\xi(T_{\Re_i})$ denote the values of the type and position features for the regions $I_{\Re_j}$ and $T_{\Re_i}$, respectively. An optimal similarity function between these two regions is then obtained by using the normalized difference of the orientation values $\theta_{\Re-Core}$ of the regions from T and I as [17], [27]

$$S_1(I_{\Re_j}, T_{\Re_i}) = \begin{cases} \exp\left(-\partial(I_{\Re_j}, T_{\Re_i}) \Big/ \mu\right) & \text{if } SD(\xi(I_{\Re_j}),\xi(T_{\Re_i})) \le 1 \\ 0 & \text{otherwise} \end{cases} \qquad (7.6)$$

where $\partial(I_{\Re_j}, T_{\Re_i})$ is the normalized orientation distance between the two regions $I_{\Re_j}$ and $T_{\Re_i}$ evaluated by using (4.5).

In order to find the best corresponding regions from I and T, the similarity between a region of the template I and a region of the template T is first calculated using (7.6). Then region $T_{\Re_i}$ is reported as a best corresponding region i.e. mate of $I_{\Re_j}$, if the similarity between them is greater than all other similarities between $I_{\Re_j}$ and the other regions from template T. Hence, for each region $j = 1,...,N$ from template I, its mate from regions from T can be formulated as

$$B(j)=\begin{cases}0 & if\ \ S_1(I_{\Re_j},T_{\Re_i})=0,\forall i=1,...,M\\ k & otherwise\end{cases} \qquad (7.7)$$

where k is the index of the region from template T that has maximum similarity with a region j of template I. Thus, a value $B(j)=0$ implies that a region j in template I is not mated to any region in template T; hence, $S_1(I_{\Re_j},T_{\Re_{B(j)}})=0$. Finally, the expression for the elementary similarity measure between I and T is obtained as

$$FV1(I,T)=\frac{1}{K}\sum_{j=1}^{N}S_1(I_{\Re_j},T_{\Re_{B(j)}}) \qquad (7.8)$$

where K is the number of mated regions.

2) Similarity measure based on FV2 = $\{\rho_{jq},\theta_{jq}\}$

A plain region j has a group of neighbors $q=\{1,2,...,Q\}$ each having a pair $\{\rho_{jq},\theta_{jq}\}$ to represent the neighborhood relationship. The spatial distance function $SD(\rho_{jq}(I_{\Re_j}),\rho_{ih}(T_{\Re_i}))$ between two regions h and q representing the neighbor of the region i in T and that j in I, respectively can be calculated using (7.5). In addition, the orientation distance function between these two neighboring regions h and q is defined as

$$\partial_0(\theta_{jq}(I_{\Re_j}),\theta_{ih}(T_{\Re_i}))=\begin{cases}\left|\theta_{jq}(I_{\Re_j})-\theta_{ih}(T_{\Re_i})\right| & if\ (\theta_{jq}(I_{\Re_j}).\theta_{ih}(T_{\Re_i}))\geq 0\\ \breve{\Delta} & otherwise\end{cases} \qquad (7.9)$$

where $\breve{\Delta}$ is the fuzzy threshold calculated as

$$\breve{\Delta}=\min(\Delta_j,\Delta_i) \qquad (7.10)$$

where Δ_j and Δ_i denote the values of the fuzzy-clustering steps as specified in Section 7.3 for the regions $I_{\Re_j}$ and $T_{\Re_i}$, respectively. By using the two distance measures, $SD(\bullet)$ given by (7.5) and $\partial_0(\bullet)$ given by (7.9), the neighborhood correspondence between a neighbor in T and that in I can be obtained as

$$SR(I_{\Re_j}(q), T_{\Re_i}(h)) = \begin{cases} 1 - \dfrac{\partial_0(\theta_{jq}(I_{\Re_j}), \theta_{ih}(T_{\Re_i}))}{\left|\theta_{jq}(I_{\Re_j})\right|} & \text{if } SD(\rho_{jq}(I_{\Re_j}), \rho_{ih}(T_{\Re_i})) \le 1 \\ & \text{and } \partial_0(\theta_{jq}(I_{\Re_j}), \theta_{ih}(T_{\Re_i})) < \breve{\Delta} \\ 0 & \text{otherwise} \end{cases} \tag{7.11}$$

Then, the overall similarity measure $S_2(I_{\Re_j}, T_{\Re_i})$ between two regions from T and I based on their neighborhood relationships is obtained as

$$S_2(I_{\Re_j}, T_{\Re_i}) = \frac{1}{F}\sum_{q=1}^{Q} \max\left\{ SR(I_{\Re_j}(q), T_{\Re_i}(h)),\ h = 1,...,H \right\} \tag{7.12}$$

where F is the number of mated neighborhood correspondence.

Finally, the expression for the secondary similarity measure between I and T is obtained as

$$FV2(I,T) = \frac{1}{K}\sum_{j=1}^{N} S_2(I_{\Re_j}, T_{\Re_{B(j)}}) \tag{7.13}$$

where K is the number of mated regions.

3) Similarity measure based on FV3 = $\{\omega, \phi, \{(x_r, y_r, t_r, \psi_r), r = 1,...,R\}\}$

The similarity function between the two regions $I_{\Re_j}$ and $T_{\Re_i}$ based on the first component of the feature vector FV3 is defined as

$$BD(\omega(I_{\Re_j}), \omega(T_{\Re_i})) = 1 - \frac{\left|\omega(I_{\Re_j}) - \omega(T_{\Re_i})\right|}{\omega(I_{\Re_j})} \tag{7.14}$$

where $\omega(I_{\Re_j})$ and $\omega(T_{\Re_i})$ calculated using (7.3) represent the values of the belonging degrees for the regions $I_{\Re_j}$ and $T_{\Re_i}$, respectively. The similarity function between the two regions $I_{\Re_j}$ and $T_{\Re_i}$ based on the second component of the feature vector FV3 is also defined as

$$CD(\phi(I_{\Re_j}),\phi(T_{\Re_i})) = \begin{cases} 1 & if \ \left|\phi(I_{\Re_j}) - \phi(T_{\Re_i})\right| \le \breve{\Delta}/2 \\ 0 & otherwise \end{cases} \qquad (7.15)$$

where $\phi(I_{\Re_j})$ and $\phi(T_{\Re_i})$ calculated using (7.4) represent the values of the curvature features for the regions $I_{\Re_j}$ and $T_{\Re_i}$, respectively.

As for the third component of FV3, the minutiae set $Minu = \{(x_r, y_r, t_r, \psi_r), r = 1,...,R\}$, we first compare the set in a region of I with that of T to determine the mated minutiae. The two minutiae, $m_r(I_{\Re_j})$ and $m_q(T_{\Re_i})$ having the same type, are considered a mated pair if their Euclidian spatial distance $SD(m_l(I_{\Re_j}), m_q(T_{\Re_i}))$ is smaller than a pre-specified tolerance r_0, that is,

$$MD(m_r(I_{\Re_j}), m_q(T_{\Re_i})) = \begin{cases} 1 & SD(m_r(I_{\Re_j}), m_q(T_{\Re_i})) \le r_0 \ and \ t_r(I_{\Re_j})) = t_q(T_{\Re_i}) \\ 0 & otherwise \end{cases} \qquad (7.16)$$

As mentioned in the previous section, some of the minutiae may belong to different regions; therefore, a minutia from $I_{\Re_j}$ already mated to a minutia from $T_{\Re_i}$ according to (7.16) may also belong to another region $I_{\Re_k}$. Thus such a minutia through its membership to $I_{\Re_k}$ may also mate to another minutia in $T_{\Re_l}$. In such a case, we keep only one mated pair, that is, the pair $(m_r(I_{\Re_j}), m_q(T_{\Re_i}))$ with the largest similarity measure obtained by using (7.14) with the arguments $(\omega(I_{\Re_j}), \omega(T_{\Re_i}))$ replaced by

$(\psi(m_l(I_{\Re_j})),\ \psi(m_q(T_{\Re_i})))$. Then, a similarity measure using the minutiae set of FV3 is obtained as

$$SM(Minu(I_{\Re_j}),Minu(T_{\Re_i})) = \frac{1}{R}\sum_{r=1}^{R}\max\left\{MD(m_r(I_{\Re_j}),m_q(T_{\Re_i})),\ q=1,...,Q\right\} \qquad (7.17)$$

where R is the total number of minutiae in $I_{\Re_j}$. The overall similarity measure $S_3(I_{\Re_i},T_{\Re_l})$ between two regions based on FV3 can be defined as

$$S_3(I_{\Re_j},T_{\Re_i}) = \frac{1}{3}\left(SM(Minu(I_{\Re_j}),Minu(T_{\Re_i})) + BD(\omega(I_{\Re_j}),\omega(T_{\Re_i})) + CD(I_{\Re_j}(\phi),T_{\Re_i}(\phi))\right) \quad (7.18)$$

The tertiary similarity score between I and T using the K pairs of mated regions, is given by

$$FV3(I,T) = \frac{1}{K}\sum_{j=1}^{N} S_3(I_{\Re_j},T_{\Re_{B(j)}}) \qquad (7.19)$$

The final overall similarity score between I and T is obtained as a weighted sum of the similarity measures given by (7.8), (7.13) and (7.19) as

$$S(I,T) = w_1.FV1(I,T) + w_2.FV2(I,T) + w_3.FV3(I,T) \qquad (7.20)$$

where the values of the weights w_1, w_2 and w_3 can be adjusted depending on the nature of the fingerprint images.

The proposed fingerprint multilevel matching scheme described in the preceding paragraphs can now be summarized as an algorithm.

Algorithm 7.2: Fuzzy-based multilevel fingerprint matching

1- For each region $j = 1,...,N$ of template I

   a. For each region $i = 1,...,M$ of template T

      - Compute $Similarity\_matrix(i,j) = S_1(I_{\Re_j},T_{\Re_i})$ using (7.6).

b. $mated\_score_1(j) = Max(Similarity\_matrix(1:M, j))$.

c. Compute $B(j)$ using (7.7).

2- By using the $mated\_score_1$, calculate the elementary similarity measure $FV1(I,T)$ using (7.8). If $FV1(I,T) = 0$, then report a non-match and exit; otherwise go to step 3.

3- For each region $j = 1,...,N$ of template I

a. Let $i = B(j)$.

b. Compute $mated\_score_2(j) = S_2(I_{\Re_j}, T_{\Re_i})$ using (7.12).

4- By using the $mated\_score_2$, calculate the secondary similarity measure $FV2(I,T)$ using (7.13). If $FV2(I,T) = 0$, then report a non-match and exit; otherwise go to step 5.

5- For each region $j = 1,...,N$ of template I

a. Let $i = B(j)$.

b. compute $mated\_score_3(j) = S_3(I_{\Re_j}, T_{\Re_i})$ using (7.18).

6- By using the $mated\_score_3$, calculate the tertiary similarity measure $FV3(I,T)$ using (7.19).

7- Compute the total similarity score between T and I using (7.20).

As mentioned earlier, in the case when the core point does not exist or it is undetectable, we use only FV2 and FV3. In such a case, FV2 is used to find the mated pairs of regions instead of using FV1. Thus, $S_1(I_{\Re_j}, T_{\Re_i})$ is replaced by $S_2(I_{\Re_j}, T_{\Re_i})$ in (7.7) for finding the list of mated regions B.

7.5 Experimental Results and Comparisons

In this section, with the choice of the same benchmark databases as chosen in Chapter 4, the performance of the fuzzy-based multilevel structural technique for fingerprint recognition (FMSFR) is studied. First, the parameters needed for the implementation of the proposed scheme are determined. Then, the simulation results of implementing Algorithms 7.1 and 7.2 are presented, and the performance of the FMSFR technique, in terms of its recognition accuracy, template size and computational cost, is compared with that of the MSFR technique developed in Chapters 3 and 4.

7.5.1 Selection of parameters

In this subsection, the sets B of the databases selected are used to find the values of the parameters needed for the implementation of the FMSFR technique.

For the EHA-FCM partitioning technique, the parameters N, α, c', τ, ε and γ are determined as follows:

(i) The most reasonable block size N is selected as two times the ridge width of a fingerprint to provide a compromised performance between the recognition accuracy and complexity.

(ii) The parameter α, used in (6.1), controls the effect of the neighboring elements on the value of the regularized orientation. The value of this parameter is empirically obtained to be unity to achieve the objective of smoothing the image blocks affected by noise with little or no effect on the singularity blocks.

(iii) The pre-initial number of clusters c' is chosen to be 8 to be consistent with the 8-level quantization used in Chapter 4.

(iv) Determining the optimal number of clusters c in Algorithm 6.1 requires the knowledge of the most effective sub-ranges of the orientations of the fingerprint. These sub-ranges depend on the choice of the threshold parameter τ, which is empirically obtained as 5% of the total number of data items (i.e., image blocks).

(v) For determining the adaptive threshold parameter $\varepsilon_n = n\varepsilon$ for Algorithm 6.1, the parameter ε is obtained empirically to be 10^{-5} in order to ensure the convergence of the iterative fuzzy clustering process to an optimum solution.

(vi) The threshold parameter γ is used in (7.1), and it specifies the number of clusters in which a given data item can have adequate degrees memberships. In effect, this parameter controls the overlapping between the different regions of a fingerprint. It is obtained empirically to be 85% of the total membership degrees of a given data item, to provide a compromised performance between the recognition accuracy and the computational complexity.

In the matching algorithm, Algorithm 7.2, based on the training set, the value of the parameter μ is empirically fixed to be $1/6$ for calculating the similarity measure $S_1(I_{\Re_j}, T_{\Re_i})$. The values assigned to the weights w_1, w_2 and w_3 in (7.20) are the same as those given in Table 4.2. For the sake of easy reference, this table is reproduced hereunder as Table 7.1.

Table 7.1: The values of the weights used in (7.20) for the selected databases.

Weight	FVC 2002						FVC 2004				FVC 2006	
	DB1		DB3		DB4		DB1		DB2		DB1	
	With core	w/o core	With core	w/o core	With core	w/o core	With core	w/o core	With core	w/o core	With core	w/o core
w_1	0.2	0	0.25	0	0.25	0	0.2	0	0.25	0	0.25	0
w_2	0.2	0.4	0.2	0.45	0.2	0.45	0.2	0.4	0.2	0.45	0.2	0.45
w_3	0.6		0.55		0.55		0.6		0.55		0.55	

7.5.3 Performance results and comparisons

In this subsection, the performance of the FMSFR technique, in terms of its recognition accuracy, template size and computational cost, is presented and compared with that of the MSFR technique presented in Chapter 4. First, the recognition accuracy of the FMSFR technique is presented and compared with that of the MSFR technique, in terms of the ROC (false rejection rate (FRR) versus false acceptance rate (FAR)) curves and the equal error rate (ERR). Next, the average template sizes required by the two techniques are presented and compared. Finally, the computational costs of the two techniques are compared in terms of the CPU times required for the fingerprint decomposition, representation and matching.

Table 7.2 gives the EER of the two techniques using the databases selected. By comparing the results listed in this table, the following two observations can be made. First, the FMSFR technique provides the values of the EER that are consistently smaller than that provided by the MSFR technique for the databases. Second, the improvements in the values of EER are larger for the databases FVC2002 (DB3 and DB4) and FVC2006 (DB1), in which the images are more affected by the behavioral and anatomical characteristics of the fingerprints.

Table 7.2: EER (%) of the MSFR and FMSFR techniques.

Technique	FVC 2002			FVC 2004		FVC 2006
	DB1	DB3	DB4	DB1	DB2	DB1
MSFR	2.57 %	6 %	2.81 %	2 %	3.2 %	5.21%
FMSFR	1.52 %	3.34 %	1.38 %	1.56 %	1.94 %	3.7%

Figures 7.2 to 7.7 depict the ROC curves provided by the two techniques for the various databases chosen. It is clear from these figures that the overall recognition accuracy provided by the FMSFR technique is higher than that provided by the MSFR

technique. These improvements in the recognition accuracy can be attributed to a more accurate extraction and representation of the fingerprint features using the fuzzy ideas. Specifically, a more accurate extraction of the fingerprint features, represented by the FMFV, results from: (i) the use of fuzzy clustering technique for fingerprint partitioning providing overlapping regions that are smoother than the non-overlapping regions provided by the quantization technique, and (ii) the use of fuzzy-based technique providing a higher accuracy for singular point detection.

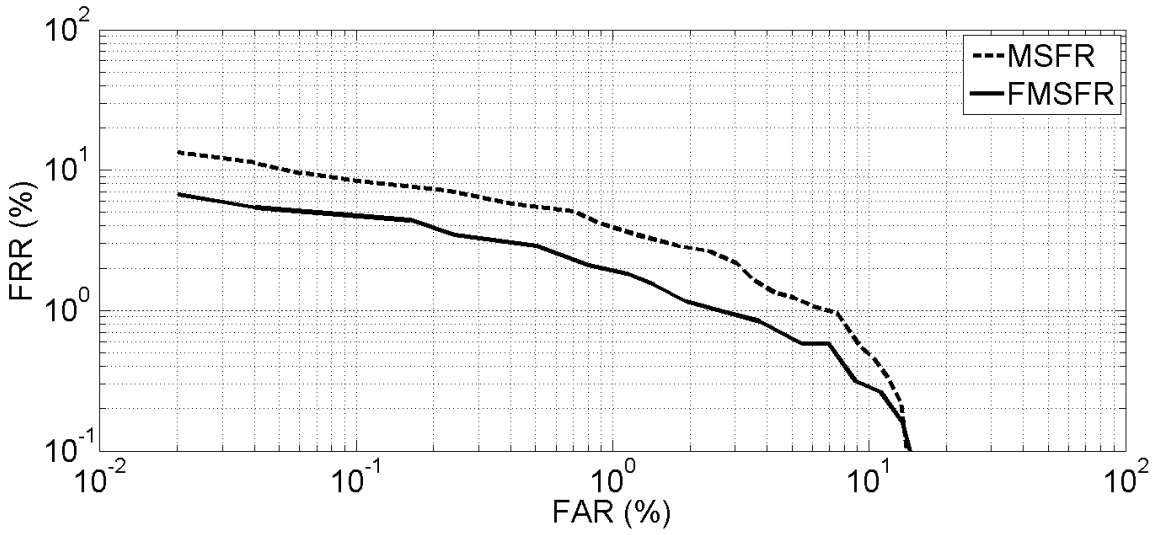

Figure 7.2: ROC curves obtained by using the FMSFR and MSFR techniques for the database FVC2002 DB1.

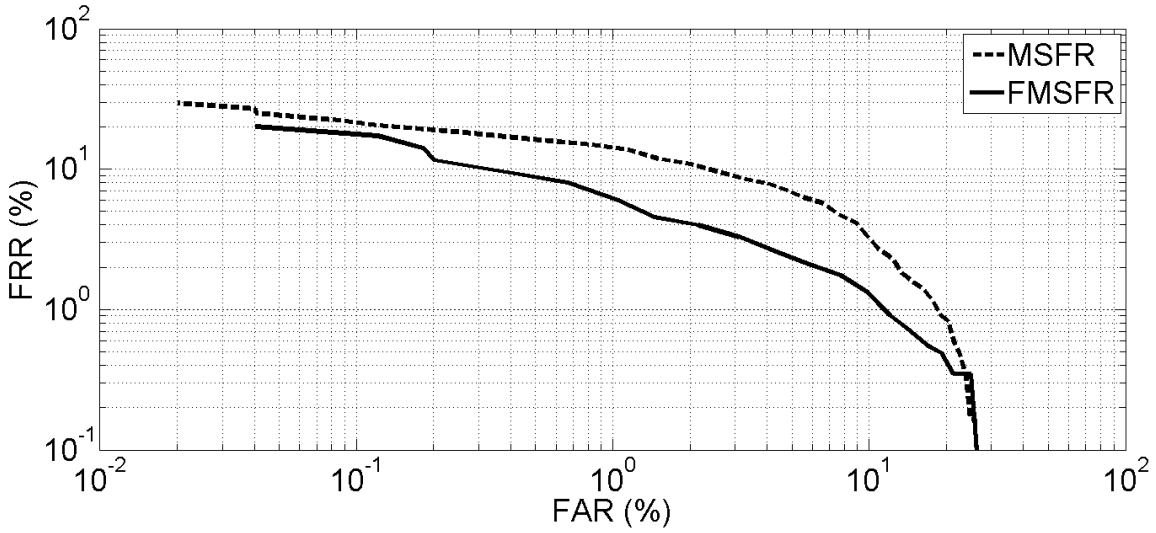

Figure 7.3: ROC curves obtained by using the FMSFR and MSFR techniques for the database FVC2002 DB3.

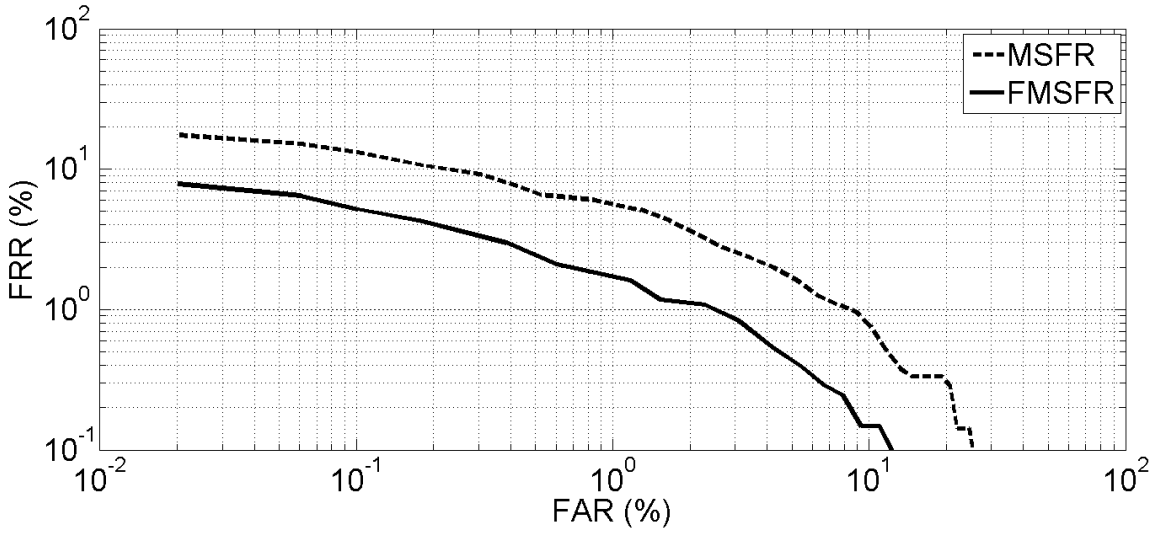

Figure 7.4: ROC curves obtained by using the FMSFR and MSFR techniques for the database FVC2002 DB4.

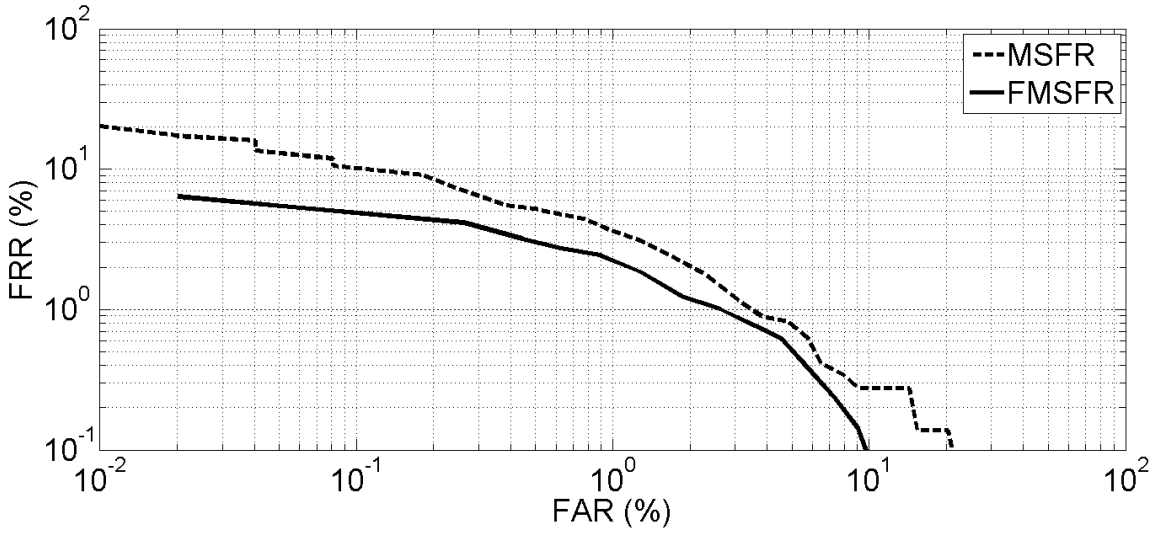

Figure 7.5: ROC curves obtained by using the FMSFR and MSFR techniques for the database FVC2004 DB1.

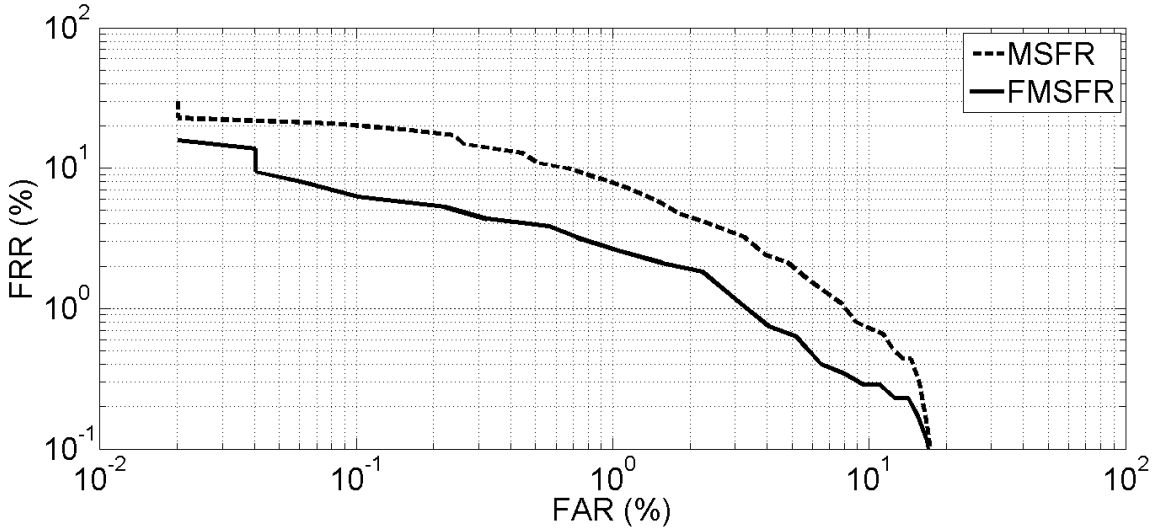

Figure 7.6: ROC curves obtained by using the FMSFR and MSFR techniques for the database FVC2004 DB2.

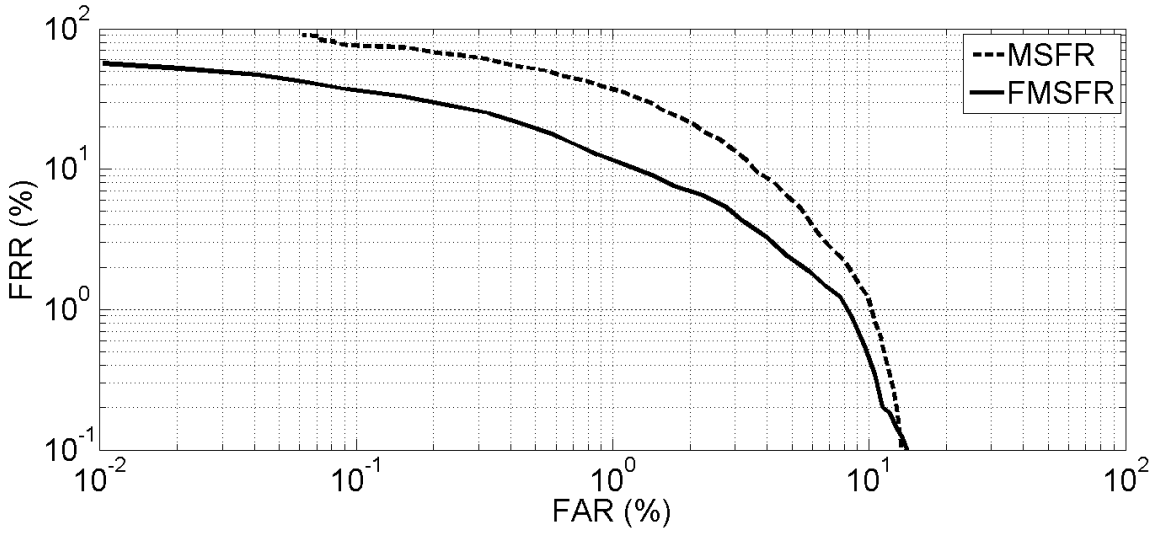

Figure 7.7: ROC curves obtained by using the FMSFR and MSFR techniques for the database FVC2006 DB1.

Table 7.3 gives the average number of regions provided and average template sizes required by the FMSFR and MSFR techniques for the databases selected. By comparing the results listed in this table, it is seen that the average template size of FMFV is always larger than that of MFV. This is expected, since FMFV contains more features in the FV3 (i.e., ω_l and ψ_r). However, it is also seen from Table 7.3 that the FMSFR technique still belongs to the light category in the FVC2004 [41] and FVC2006 [46] competitions in terms of the template size.

Table 7.3: The number of regions provided and the template sizes (in bytes) required by the FMSFR and MSFR techniques.

Technique		FVC 2002			FVC 2004		FVC 2006
		DB1	DB3	DB4	DB1	DB2	DB1
MSFR	Number of regions	11	8	9	11	10	5
	Template size	252	206	208	270	273	102
FMSFR	Number of regions	9	7	8	9	8	5
	Template size	326	264	286	355	357	145

Table 7.4 provides the CPU times of implementing the fingerprint decomposition, template formulation and matching in each of the two techniques using the same hardware as described earlier in Section 4.4. In this table, the parenthesized quantities are the parts of the total fingerprint decomposition CPU times, which result from implementing the EHA-FCM partitioning scheme in the FMSFR technique. By comparing the CPU times for the fingerprint decomposition of the two schemes, the following three observations can be made. First, the fuzzy-based fingerprint decomposition technique requires, in general, larger CPU times than that required by the fingerprint decomposition using the MSFR technique. This higher computational cost of the fuzzy-based fingerprint decomposition technique results from the use of the EHA-FCM partitioning scheme instead of using the simple quantization scheme. Second, after accounting for the fingerprint partitioning part of the decomposition time, the remaining CPU time for the decomposition in the FMSFR technique is smaller than that in the MSFR technique. This is because of the fact that the construction of the regions using already smoothened clustered orientations (FCOF) in the FMSFR technique is less time consuming. Third, even though the decomposition time in the FMSFR technique increases as the fingerprint data size becomes larger, it is not affected significantly by the difficulty of the fingerprints. This is due to the fact that the histogram analysis technique by providing the number of clusters and their initial centers brings the process of fingerprint decomposition to a stage where the process from that point on is less affected by the difficulty of the fingerprints. A comparison of the CPU times resulting from the two schemes for the fingerprint template formulation and matching shows that the FMSFR technique requires, in general, smaller CPU times than that required by the

MSFR technique. This improvement in the computational cost for template formulation and matching results from a reduced number of regions (as seen from Table 7.3) provided by the fuzzy-based fingerprint decomposition algorithm of the FMSFR technique. As for the enrollment times of the two techniques, the average enrollment time of the FMSFR technique is 0.25 s compared to 0.23 s required by the MSFR technique. Despite this increase in the enrolment time, which is of course very modest, the FMSFR technique still belongs to the light category in the FVC2004 [41] and FVC2006 [46] competitions in terms of the computational cost.

Table 7.4: CPU times (ms) for the fingerprint decomposition, template formulation and matching of the MSFR and FMSFR techniques.

Module	Technique	FVC2002			FVC2004		FVC2006
		DB1	DB3	DB4	DB1	DB2	DB1
Fingerprint decomposition	MSFR	30	25	25	34	35	37
	FMSFR	57 (36.4)	41 (25.5)	46 (28.1)	57.8 (35.2)	57.6 (34.9)	30.3 (16.3)
Template formulation	MSFR	20	18.5	16.5	27	24	8.6
	FMSFR	18.6	16.5	15.7	25.7	21.7	7
Matching	MSFR	6.2	3.9	3.6	6.24	5.3	2.5
	FMSFR	3.7	2.8	3	3.7	3.2	2.5

Finally, it is concluded that the FMSFR technique provides a higher recognition accuracy than that provided by the MSFR technique at the expense of requiring a larger template size and a slight increase in the computational cost. It is worth, however, pointing out that the technique still belongs to the light category in the FVC2004 [41] and FVC2006 [46] competitions.

7.6 Summary

In Chapters 3 and 4, a multilevel structural technique for fingerprint recognition (MSFR) was developed based on a crisp clustering of fingerprint features. In Chapters 5 and 6,

histogram based fuzzy c-means fingerprint partitioning schemes providing a fingerprint partitioning that is smoother than that provided by using the crisp technique of Chapters 3 and 4 were developed. In this chapter, using this fuzzy based partitioning along with the ideas of fingerprint decomposition, representation and matching introduced in Chapters 3 and 4, a new fuzzy based fingerprint recognition scheme (FMSFR) has been developed. First, a fingerprint decomposition scheme (Algorithm 7.1) has been developed using the fuzzy clustered orientation field provided by the EHA-FCM technique of Chapter 6. Next, a new fuzzy-based multilevel feature representation (FMFV) has been formulated using the set of regions obtained from this fuzzy decomposition algorithm. The resulting fuzzy multilevel feature vector has included in it some features in addition to those in the feature vector of the crisp technique. Finally, some fuzzy-based similarity functions have been formulated and used to compare the features of different fingerprints in the fuzzy-based multilevel matching technique.

A simulation study using some challenging benchmark databases has been undertaken in order to show the effectiveness of the scheme proposed in this chapter. In this study, the performance of the FMSFR technique, in terms of its recognition accuracy, template size and computational cost, has been presented and compared with that of the MSFR technique. The simulation results have shown that, in comparison to the MSFR technique, the proposed FMSFR technique provides higher recognition accuracy with a reasonable increase in the complexity measured in terms of the CPU time and template size.

CHAPTER 8

Conclusion

8.1 Concluding Remarks

Fingerprints are considered to be one of the best biometric measurements and are used as a universal personal identifier. There are two main phases in the recognition of personal identity using fingerprints: 1) extraction of suitable features of fingerprints, and 2) fingerprint matching making use of the extracted features in order to find the correspondence and similarity between the fingerprint images. The use of both local and global features of a fingerprint in a technique for fingerprint recognition is useful in solving the problems that arise from the behavioral and anatomical characteristics of fingerprints, such as ridge pattern deformation or distortion, translation and/or rotation, incomplete fingerprint. However, such schemes result in an increased complexity in feature extraction and representation and a larger size fingerprint template in comparison to that obtained by using the traditional minutiae-based approaches. Further, most of the fingerprint recognition schemes rely on some sort of crisp clustering of the fingerprint features. Recognition accuracies of such schemes are adversely affected due to the behavioral and anatomical characteristics of fingerprints. This research has been concerned with the development of efficient and cost-effective techniques for fingerprint recognition, that can meet not only the challenges arising from using both the local and global features of the fingerprints but also deal effectively with the problems resulting from the crisp clustering of the features specifically when the fingerprints have

behavioral or anatomical characteristics. With this objective, the work of this research has been carried out in two parts.

In the first part of the thesis, a low-complexity multilevel structural fingerprint recognition (MSFR) scheme, using both the local and global features extracted from a crisp partitioning of the fingerprint orientation field, has been developed. The main focus of the proposed scheme has been on overcoming the problems resulting from the behavioral and anatomical characteristics as well as from the crisp partitioning of fingerprint images.

Based on a study of relative merits of different global features, a fingerprint image has been first decomposed into singular and plain regions by using only the singular points and the ridge orientation field as global features. Then, by employing the structural information of local features (i.e., ridge curvature and minutiae) and global features of each region, three-level feature vectors are formulated with levels for global, neighborhood, and local features of the region. The idea of using multilevel feature vectors (MFVs) ensures that the fingerprint templates contain all the available useful information from the fingerprint image. Inclusion of the global features in the proposed MFVs makes the fingerprint representation to be less variant to the displacement, rotation and deformation of the fingerprint ridges. In the proposed MSFR technique, the features have been obtained by using some simple mathematical operations. Therefore, the complexity in obtaining the MFVs representing these features are not significantly increased over those of obtaining single-level minutiae based representations.

Finally, in the MSFR technique, a very fast fingerprint matching scheme, referred to as multilevel matching (MLM) scheme, has been devised. In this scheme, the

correspondence problem is dealt with by making use of the global feature components of the MFVs, whereas the similarity problem is taken care by employing all the three levels of features contained in the MFVs. The fast matching speed can be attributed to the following two features of the proposed scheme: 1) a significantly reduced number of comparisons required to provide the matching decision, and 2) the strategy of an early rejection that allows the MLM scheme to skip the second and/or third levels of matching. As a result, the proposed scheme could be very attractive for fingerprint identification applications involving large scale databases.

Extensive experiments have been conducted using six challenging benchmark databases to investigate the effectiveness of the proposed MSFR scheme. These benchmark databases have been selected from the FVC2002, FVC2004 and FVC2006 competitions containing a wide variety of challenges in fingerprint recognition. The proposed MSFR scheme has been compared in terms of the recognition accuracy and the template size with the existing schemes that also use some of the global features of the fingerprint in addition to the local minutiae attributes for fingerprint representation and matching. The experimental study has shown that the proposed MSFR scheme provides a performance superior to those of the other schemes used for an objective comparison.

Inspired by the ability of fuzzy-based clustering techniques in dealing with the natural patterns, in the second part of the thesis, a fuzzy based multilevel structural fingerprint recognition (FMSFR) scheme has been developed to deal more effectively than in the MSFR scheme with the problems associated with the behavioral and anatomical characteristics of fingerprints.

First, a histogram analysis fuzzy c-means (HA-FCM) clustering technique has been devised for the partitioning of fingerprints. The parameters of this partitioning technique, i.e., the number of clusters and the set of initial cluster centers, have been made to be data dependent by determining them based on the analysis of the orientation field histogram of a fingerprint image. The output of the proposed HA-FCM algorithm, which is a set of cluster centers and the degrees of belonging of each data item to different clusters, has been used to partition the fingerprint image and thus to construct a fuzzy clustered orientation field (FCOF). The proposed HA-FCM partitioning technique has been shown to provide (i) smoother regions compared to that provided by the quantization technique and (ii) a more realistic partitioning that corresponds to the ridge pattern of the fingerprint image under consideration at a lower computational cost, in comparison to the FCM technique. By using the FCOF, a novel low-complexity singular point fuzzy-based detection scheme has been developed, which has been designed not only to detect the singular points but also to identify their types. It has been shown that the proposed singular point detection scheme outperforms some of the state of the art techniques, in terms of the detection accuracy at low computational cost.

The development of the HA-FCM partitioning scheme has been further continued to devise an enhanced HA-FCM (EAH-FCM) algorithm. In this algorithm, the smoothness of the fingerprint partitioning has been further improved through a regularization process of the fingerprint orientation field, and the computational complexity has been reduced by decreasing the number of operations and by speeding up the convergence rate of the underlying iterative process of the HA-FCM technique. The EHA-FCM technique has been shown to provide a solution for the fingerprint

partitioning problem that is superior to that provided by the HA-FCM technique with a significantly lower computational complexity.

Finally, using the fingerprint partitions and singular points obtained from the EHA-FCM technique, along with the ideas developed in the MSFR scheme, a new fuzzy based fingerprint recognition scheme (FMSFR) has been devised. First, a fingerprint decomposition algorithm is developed using the fuzzy clustered orientation field, which provided by the EHA-FCM technique. Next, a new fuzzy-based multilevel feature representation (FMFV) has been formulated using the set of regions obtained from this fuzzy decomposition algorithm. The resulting fuzzy multilevel feature vector has included in it some features in addition to those in the feature vector of the crisp technique. Finally, some fuzzy-based similarity functions have been formulated and used to compare the features of different fingerprints in the fuzzy-based multilevel matching (FMLM) technique.

A simulation study using the same challenging benchmark databases as used in the first part of this work has been undertaken in order to show the effectiveness of the FMSFR scheme. The simulation results have convincingly demonstrated that the incorporation of fuzzy based schemes in the fingerprint decomposition, representation and matching has significantly improved the recognition accuracy of the multilevel structural fingerprint recognition scheme with only a modest increase in its complexity. Therefore, the FMSFR scheme proposed in this thesis could be very attractive for fingerprint identification applications involving large scale databases and/or requiring limited storage space.

8.2 Scope for Future Work

While the research work undertaken in this thesis has focused on developing efficient and cost-effective techniques for fingerprint recognition that can meet the challenges arising from using both the local and global features of the fingerprints as well as effectively deal with fingerprints' behavioral and anatomical characteristics, in the opinion of the author of this thesis, there are a number of additional studies that could be undertaken along the lines of the ideas developed in proposing a multilevel structural approach for fingerprint recognition.

1. Recently, the intra-ridge details at the very-fine-level of the fingerprint images have been identified and acquired using high-resolution scanners. These intra-ridge details may include features such as the width, shape, curvature, edge contours of the ridges. One of the most important very-fine-level details is the finger sweat pores, whose positions and shapes are considered highly distinctive. The formulation of the multilevel representation could be extended to include some of these features.
2. One could also study the effect of developing a fuzzy-based fingerprint indexing technique using the multilevel representation proposed in this thesis to reduce the matching space for fingerprint identification applications.
3. The use of the fuzzy clustered orientation field in enhancing the fingerprint images could also be studied.
4. A study could be undertaken to develop fuzzy based schemes for multimodal biometric systems by using the ideas of the multilevel structural approach developed in this thesis for fingerprint recognition.

REFERENCES

[1] Davide Maltoni, Dario Maio, Anil K. Jain, and Salil Prabhakar, *Handbook of Fingerprint Recognition*. New York: Springer-Verlag, 2009.

[2] A. Kong, D. Zhang, and M. Kamel, "A survey of palmprint recognition," *Pattern Recognition,* vol. 42, no. 7, pp. 1408-1418, July 2009.

[3] Anil K. Jain, Yi Chen, and Meltem Demirkus, "Pores and ridges: High-resolution fingerprint matching using level 3 features," *IEEE Transactions on Pattern Analysis and Machine Intelligence,* vol. 29, no. 1, pp. 15-27, January 2007.

[4] Q. Zhao, L. *Zhang*, D. Zhang, N. Luo, and J. Bao, "Adaptive pore model for fingerprint pore extraction," in *Proc. 18th Int. Conf. Pattern Recog.,* 2008, pp. 1–4.

[5] Q. Zhao, L. Zhang, D. Zhang, and N. Luo, "Direct pore matching for fingerprint recognition," *in Proc. ICB*, 2009, pp. 597–606.

[6] Q. Zhao, D. Zhang, L. Zhang, and N. Luo, "Adaptive fingerprint pore modeling and extraction," *Pattern Recognition*, vol. 43, no. 8, pp. 2833–2844, Feb. 2010.

[7] D. Zhang, F. Liu, Q. Zhao, G Lu, and N. Luo, "Selecting a reference high resolution for fingerprint recognition using minutiae and pores," *IEEE Transactions on Instrumentation and Measurement*, vol. 60, no. 3, pp. 863-871, March 2011.

[8] F. Liu, Q. Zhao, and D. Zhang, "A novel hierarchical fingerprint matching approach," *Pattern Recognition*, vol. 44, no 8, pp. 1604-13, Aug. 2011.

[9] L. Hong, Y. Wan, and A.K. Jain, "Fingerprint image enhancement: Algorithm and performance evaluation", *IEEE Transactions on Pattern Analysis and Machine Intelligence,* vol. 20, no. 8, pp. 777 – 789, 1998.

[10] Y. Yao, G.L. Marcialis, M. Pontil, P. Frasconi, and F. Roli, "Combining flat and structured representations for fingerprint classification with recursive neural networks and support vector machines," *Pattern Recognition,* vol. 36, no. 2, pp. 397 – 406, 2003.

[11] R. Cappelli, A. Lumini, D. Maio, and D. Maltoni, "Fingerprint classification by directional image partitioning," *IEEE Transactions on Pattern Analysis and Machine Intelligence,* vol. 21, no. 5, pp. 402– 421, 1999.

[12] D. Maio and D. Maltoni, "A structural approach to fingerprint classification," *Proceeding of International Conference on Pattern Recognition (ICPR)* (1996), pp. 578 – 585.

[13] Anil K. Jain, S. Prabhakar, L. Hong, and S. Pankanti, "A multichannel approach to fingerprint classification," *IEEE Transactions on Pattern Analysis and Machine Intelligence,* vol. 21, no. 4, pp. 348 – 359, 1999.

[14] A.M. Bazen and S.H. Gerez, "An intrinsic coordinate system for fingerprint matching," *Audio-and Video-Based Biometric Person Authentication Third International Conference (AVBPA),* 2001, pp. 198 – 204.

[15] A. J. Willis and L. Myers, "A cost-effective fingerprint recognition system for use with low-quality prints and damaged fingertips," *Pattern Recognition.*, vol. 34, no. 2, pp. 255–270, 2001.

[16] A. Ceguerra and I. Koprinska, "Integrating local and global features in automatic fingerprint verification," in *Proc. Int. Conf. on Pattern Recognition (16th)*, 2002, pp-347-350, vol. 3.

[17] M. Tico and P. Kuosmannen, "Fingerprint matching using an orientation-based minutia descriptor," *IEEE Transactions on Pattern Analysis and Machine Intelligence,* vol. 25, no. 8, pp. 1009–1014, Aug. 2003.

[18] Jin Qi, Mei Xie, and W. Wang, "A novel fingerprint matching method using a curvature-based minutia specifier", in *Proceedings on the International Conference on Image Processing (ICIP),* 2008, pp. 1488 – 1491.

[19] Jea, Tsai-Yang and Venu Govindaraju, "A minutia-based partial fingerprint recognition system," *Pattern Recognition*, vol. 38, no. 10, pp 1672-1684, October 2005.

[20] Jia Jia, Lianhong Cai, P. Lu, and Xuhui Liu, "Fingerprint matching based on weighting method and the SVM," *Neurocomputing*, vol. 70, no 4-6, pp. 849-58, Jan. 2007.

[21] J. Feng, "Combining minutiae descriptors for fingerprint matching," *Pattern Recognition,* vol. 41, no. 1, pp. 342 – 352, 2008.

[22] Thai Hoang Le and Hoang Thien Van, "Combining global features and local minutiae descriptors in genetic algorithms for fingerprint matching," *ACM International Conference Proceeding Series Proceedings of Symposium on Information and Communication Technology, SoICT2010,* 2010, pp. 100-107.

[23] Jain A. K., S. Prabhakar, L. Hong, and S. Pankanti, "Filterbank-based fingerprint matching," *IEEE Transaction on Image Processing*, vol. 9, no. 5, pp. 846–859, May 2000.

[24] A. Ross, A. K. Jain, and J. Reisman, "A hybrid fingerprint matcher", *Proc.* of *lnrernarionnl Conference on Pattern Recognition (ICPR),* vo1.3, August 2002, pp. 795-798.

[25] A. Ross, A. K. Jain. and J. Reisman, "A Hybrid Fingerprint Matcher", *Pattern Recognition*, vol. 36, no. 7, pp. 1661-73, July 2003.

[26] V. Krivec, J.A. Birchbauer, W. Marius, and H. Bischof, "A hybrid fingerprint matcher in memory constrained environments," in *Proc. ISPA 2004. (3rd)*, 2003, pt. 2, pp 617-20, vol. 2.

[27] Jinwei Gu, Jie Zhou, and Chunyu Yang, **"**Fingerprint recognition by combining global structure and local cues". *IEEE Transaction on Image Processing*, vol.15, no. 7, pp. 1952 – 1964, July 2006.

[28] P. Shi, J. Tian, W. Xie, and X. Yang, "Fast fingerprint matching based on the novel structure combining the singular point with its neighborhood minutiae," *Lecture Notes in Computer Science, Progress in Pattern Recognition, Image Analysis and Applications* 4225, 2006, pp. 804 – 813.

[29] L. Nanni, and A. Lumini, "A hybrid wavelet-based fingerprint matcher," *Pattern Recognition,* vol. 40, no. 11, pp. 3146-3151, Nov. 2007.

[30] F. Benhammadi, M.N. Amirouche, H. Hentous, K.B. Beghdad, and M. Aissani, "Fingerprint matching from minutiae texture maps," *Pattern Recognition*, vol. 40, no. 1, pp. 189-97, Jan. 2007.

[31] X. Wang, J. Li, and Y. Niu, "Fingerprint matching using orientationcodes and polylines," *Pattern Recognition,* vol. 40, no. 11, pp. 3164 – 3177, 2007.

[32] Ju Cheng Yang and Dong Sun Park, "A fingerprint verification algorithm using tessellated invariant moment features," *Neurocomputing,* vol. 71, no. 10-12, pp. 1939-46, June 2008.

[33] L. Nanni and A. Lumini, "Descriptors for image-based fingerprint matchers" *Expert Systems with Applications*, vol. 36, no. 10, pp. 12414-22, Dec. 2009.

[34] Kai Cao, Xin Yang, Xunqiang Tao, Peng Li, Yali Zang, and Jie Tian, "Combining features for distorted fingerprint matching," *Journal of Network and Computer Applications*, vol. 33, no. 3, pp. 258-267, May 2010.

[35] Fanglin Chen and Jie Zhou, "A comparative study of combining multiple features for fingerprint recognition," *Emerging Techniques and Challenges for Hand-Based Biometrics, ETCHB 2010*, 2010.

[36] N.K. Ratha, C. Shaoyun, and A.K. Jain, "Adaptive flow orientation-based feature extraction in fingerprint images," *Pattern Recognition,* vol. 28, no. 11, pp. 1657 – 1672, 1995.

[37] D. Maio and D. Maltoni, "Ridge-line density estimation in digital images," *in Proc. Fourteenth International Conference Pattern Recognition,* vol.1, 1998. pp 534 – 538.

[38] Jin Qi and Mei Xie, "A robust algorithm for fingerprint singular point detection and image reference direction determination based on the analysis of curvature map," *IEEE International Conference on Cybernetics and Intelligent Systems*, CIS 2008, pp. 1051 –1054.

[39] C. Park, J. Lee, M.J.T. Smith, and K. Park, "Singular point detection by shape analysis of directional fields in fingerprints," *Pattern Recognition*, vol. 39, no. 5, pp. 839 – 855, 2006.

[40] S. Jirachaweng, Z. Hou, W. Yau, and V. Areekul, "Residual orientation modeling for fingerprint enhancement and singular point detection," *Pattern Recognition,* vol. 44, no. 2, pp. 431 – 42, 2011.

[41] http://bias.csr.unibo.it/fvc2004/default.asp.

[42] D. Maio, D. Maltoni, R. Cappelli, J.L. Wayman, and A.K. Jian, "FVC2000: fingerprint verification competition," *IEEE Transactions on Pattern Recognition and Machine Intelligence*, vol. 24, no. 3, pp. 402 – 412, 2002.

[43] http://bias.csr.unibo.it/fvc2000.

[44] http://bias.csr.unibo.it/fvc2002.

[45] J. Fierrez, J. Ortega-Garcia, D. Torre-Toledano and J. Gonzalez-Rodriguez, "BioSec baseline corpus: A multimodal biometric database", *Pattern Recognition,* vol. 40, no. 4, pp. 1389-1392, April 2007.

[46] http://bias.csr.unibo.it/fvc2006.

[47] James C. Bezdek, James Keller, Raghu Krisnapuram and Nikhil R. Pal, *Fuzzy Models and Algorithms for Pattern Recognition and Image Processing*, New York: Springer-Verlag, 2005.

[48] R.E. Bellman, R.A. Kalaba, and L.A. Zadeh, "Abstraction and pattern classification", *J. Math. Anal. Appl.*, vol. 13, pp. 1–7, 1966.

[49] E.H. Ruspini, "A new approach to clustering", *Inf. Control*, vol. 15, no. 1, pp. 22–32, 1969.

[50] N. Belacel, P. Hansen, and N. Mladenovic, "Fuzzy J-Means: a new heuristic for fuzzy clustering," *Pattern Recognition,* vol. 35, no. 10, pp. 2193-200, Oct. 2002.

[51] J.C. Bezdek, *Pattern Recognition with Fuzzy Objective Function Algorithms,* Plenum Press, New York, 1981.

[52] Jiayin Kang Cheng-Long Gong and Wen-Juan Zhang, **"**Fingerprint image segmentation using modified fuzzy c-means algorithm," *Journal of Biomedical Science & Engineering,* vol. 2, no. 8, pp. 656-60, Dec. 2009

[53] Jiayin Kang Cheng-Long Gong and Wen-Juan Zhang, **"**Fingerprint image segmentation using modified fuzzy c-means algorithm," *3rd International Conference on Bioinformatics and Biomedical Engineering (iCBBE 2009),* pp. 1-4, 2009.

[54] D. Zhang and Y. Wang, "Medical image segmentation based on FCM clustering and rough set," *Chinese Journal of Scientific Instrument,* vol. 27, pp. 1683–1687, 2006.

[55] W. J. Chen, M. L. GIGER, and U. BICK, "A fuzzy c-means (FCM)-based approach for computerized segmentation of breast lesions in dynamic contrast-enhanced MR images," *Academic Radiology,* vol. 13, pp. 63–72, 2006.

[56] K. S. Chuang, H. L. Tzeng, S. and W. Chen, "Fuzzy c-means clustering with spatial information for image segmentation," *Computerized Medical Imaging and Graphics,* vol. 30, pp. 9-15, 2006.

[57] S. C. Chen and D. Q. Zhang, "Robust image segmentation using FCM with spatial constraints based on new kernel-induced distance measure," *IEEE Trans. Systems Man Cybernet, B,* vol. 34, pp. 1907-1916, 2004.

[58] L. Szilagyi, Z. Benyo, and S. M. Szilagyii, "MR brain image segmentation using an enhanced fuzzy c-means algorithm," *25th Annual International Conference of IEEE EMBS,* Piscataway: USA, pp. 17-21, 2003.

[59] Tianming Zhan, Zhihui Wei, Qi Ge, Liang Xiao, and Jun Zhang, "Brain MR image segmentation and bias field correction using adaptive fuzzy C-means model," *2010 International Conference on Computer, Mechatronics, Control and Electronic Engineering (CMCE 2010),* pp. 151-4, 2010.

[60] L.A. zadeh, "Fuzzy sets", *Information and Control*, vol. 8, pp. 338-353, 1965.

[61] Kwang H. Lee, *First Course on Fuzzy Theory and applications,* Springer-Verlag Berlin Heidelberg, 2005.

[62] J.C. Bezdek, "A convergence theorem for the fuzzy ISODATA clustering algorithms," *IEEE Transactions on Pattern Analysis Machine Intelligence,* vol. 2, pp. 1–8, 1980.

[63] M.A.Wahby Shalaby and M.Omair Ahmad, "A multilevel structural technique for fingerprint representation and matching," under review.

[64] A. Ross, S. Dass, and A. Jain, "A deformable model for fingerprint matching," *Pattern* Recognition*,* vol. 38, no. 1, pp. 95-103, Jan. 2005.

[65] A. Ross, S. Dass, A. Jain, "Fingerprint warping using ridge curve correspondences," *IEEE Transactions on Pattern Analysis Machine Intelligence,* vol. 28, no. 1, pp. 19–30, 2006.

[66] D.C.D Hung and Ching-Yu Huang, "A model for detecting singular points of a fingerprint," *Proceedings of the Ninth Florida Artificial Intelligence Research Symposium, FLAIRS-96,* pp. 444-8, 1996.

[67] Ching-Yu Huang, Li-min Liu, and D.C. Douglas Hung, "Fingerprint analysis and singular point detection," *Pattern Recognition Letters,* vol. 28, no. 15, pp. 1937-1945, Nov. 2007.

[68] R.C. Gonzalez and R.E. Woods, *Digital Image Processing,* second ed., Prentice Hall, Upper Saddle River, New Jersey, 2002.

[69] Sven Behenke, *Hierarchical Neural Networks for Image Interpretation,* Berlin Heidelberg New York: Springer-Verlag, 2003.

[70] B.A. Gross and D.M. Hanna, "Artificial neural networks capable of learning spatiotemporal chemical diffusion in the cortical brain", *Pattern Recognition,* vol. 43, no. 11, pp. 3910-21, Nov. 2010.

[71] S. Cote and A.R.L. Tatnall, "The use of the Hopfield neural network to measure sea-surface velocities from satellite images," *IEEE Geoscience and Remote Sensing Letters,* vol. 4, no. 4, pp. 624-8, Oct. 2007.

[72] Qin Li and You, J. "Robust human motion detection via fuzzy set based image understanding" *Proceedings of the SPIE - The International Society for Optical Engineering,* vol. 6064, pp. 60640L-1-9, Feb. 2006.

[73] G. Schaefer and T. Nakashima, "Application of cost-sensitive fuzzy classifiers to image understanding problems," *IEEE International Conference on Fuzzy Systems (FUZZ-IEEE),* pp. 1364-8, 2009.

[74] W. Tarnawski, G. Schaefer, T. Nakashima, and L. Miroslaw, "Fuzzy rule-based classification systems in medical image understanding," *Proceedings of the 2009 International Conference on Image Processing, Computer Vision, & Pattern Recognition. IPCV 2009,* pp. 859-63, 2009.

[75] A.R. Varkonyi-Koczy, and A. Rovid, "Fuzzy logic supported primary edge extraction in image understanding", *IEEE 16th International Conference on Fuzzy Systems (FUZZ-IEEE),* pp. 2177-81, 2008.

[76] Feng Yue, Wangmeng Zuo, D. Zhang, and Kuanquan Wang, "Orientation selection using modified FCM for competitive code-based palmprint recognition," *Pattern Recognition,* vol. 42, no. 11, pp. 2841-9, Nov. 2009.

[77] Y.L. Li, K.Q. Wang, and D. Zhang, "Palmprint recognition based on translation invariant Zernike moments and modular Neural network," In *Proceedings of International Symposium on Neural Networks,* 2005, pp. 177–182.

[78] P. Huges and A.D.P Green, "The use of neural networks for fingerprint classification," *Second International Conference on Artificial Neural Networks,* 1991, pp. 79-81.

[79] M. Kamijo, H. Mieno, and K. Kojima, "Classification of fingerprint images using a neural network," *Systems and Computers in Japan,* vol. 23, no. 3, pp. 89-101, 1992.

[80] M. Kamijo, "Classifying fingerprint images using neural network: deriving the classification state," *IEEE International Conference on Neural Networks,* vol. 3, 1993, pp. 1932-7.

[81] K. Moscinska, and G. Tyma, "Neural network based fingerprint classification," *Third International Conference on Artificial Neural Networks,* 1993, pp. 229-232.

[82] D. Maio, and D. Maltoni, "Neural network based minutiae filtering in fingerprints": Proceedings. *Fourteenth International Conference on Pattern Recognition,* vol. 2, 1998, pt. 2, pp. 1654-8.

[83] Guang Yang, Darning Shi and Chai Quek, "Fingerprint minutia recognition with fuzzy neural network", *Advances in Neural Networks* - ISNN 2005. vol. 2, 2005, pt. 2, pp. 165-70.

[84] Sagar Vijay Kumar, Koh, and Jit Beng Alex, "Hybrid fuzzy logic and neural network model for fingerprint minutiae extraction", *Proceedings of the International Joint Conference on Neural Networks,* vol. 5, 1999, pp. 3255-3259.

[85] C. Quek, K.B. Tan, and V.K. Sagar, "Pseudo-outer product based fuzzy neural network fingerprint verification system", *Neural Networks,* vol. 14, no 3, pp. 305-23, April 2001.

[86] Luo Jing, Lin Shu-zhong, and Zhan Xiang-lin, " EBF neural network based on fingerprint recognition," *Computer Engineering and Applications,* vol. 44, no. 34, pp. 219-22, 1 Dec. 2008.

[87] L.C. Jain, U. Halici, I. Hayashi, S.B. Lee, and S. Tsutsui, *Intelligent biometric techniques in fingerprint and face recognition,* CRC Press, Boca Raton FL, 1999.

[88] M.A.Wahby Shalaby and M.Omair Ahmad, "A histogram analysis fuzzy c-means technique for fingerprint partitioning and its application to singular point detection," under review.

[89] Liu Yong-xia, Qi Jin, and Xie Rui, "A new detection method of singular points of fingerprints based on neural network," *3rd IEEE International Conference on Computer Science and Information Technology (ICCSIT 2010),* pp. 301-5, 2010

[90] M. Kawagoe and A. Tojo, "Fingerprint pattern classification," *Pattern Recognition,* vol. 17, pp. 295–303, 1984.

[91] Jie Zhou, Gu Jinwei, and D. Zhang, "Singular points analysis in fingerprints based on topological structure and orientation field," *Advances in Biometrics. Proceedings International Conference, ICB 2007*, vol. 4642, pp. 261-70, 2007.

[92] Jie Zhou, Fanglin Chen, and Jinwei Gu, "A novel algorithm for detecting singular points from fingerprint images," *IEEE Transactions on Pattern Analysis and Machine Intelligence,* vol. 31, no. 7, pp. 1239-50, July 2009.

[93] F. Magalhaes, H.P. Oliveira, and A.C Campilho, "A new method for the detection of singular points in fingerprint images," *Workshop on Applications of Computer Vision (WACV 2009),* p 6 pp., 2009.

[94] Cheng Xin-Ming, Xu Dong-Cheng, and Xu Cheng, "A new algorithm for detecting singular points in fingerprint images," *Proceedings of the 2009 Third International Conference on Genetic and Evolutionary Computing (WGEC 2009),* pp. 822-6, 2009.

[95] Wang Feng, Chen Yun, Wang Hao, and Wang Xiu-You, "Fingerprint classification based on improved singular points detection and central symmetrical axis," *International Conference on Artificial Intelligence and Computational Intelligence, AICI 2009,* vol. 3, pp. 508-512, 2009.

[96] Z. Saquib, N. Salam, R. Nair, and N. Pandey, "An enhanced method for singular points detection in fingerprint images," *International Conference on Computer and Communication Technology (ICCCT 2010),* pp. 206-9, 2010.

[97] V.S. Srinivasan and N.N. Murthy, "Detection of singular points in fingerprint images," *Pattern Recognition,* vol. 25, no. 2, pp. 139-153, Feb 1992.

[98] T. Liu, C. Zhang, and P. Hao, "Fingerprint Reference Point Detection Based on Local Axial Symmetry," *In Proceedings of International Conference on Pattern Recognition (18th),* vol. 1, pp.1050–1053, 2006.

[99] X. Wang, J. Li, and Y. Niu, "Definition and extraction of stable points from fingerprint images," *Pattern Recognition,* vol. 40, no. 6, pp. 1804–1815, 2007.

[100] K. Kryszczuk and A. Drygajlo, "Singular Point Detection in Fingerprints Using Quadrant Change Information," *In Proceedings of International Conference on Pattern Recognition* (18th), vol. 4, pp. 594–597, 2006.

[101] Yi Wang, Jiankun Hu, and D. Phillips, "A fingerprint orientation model based on 2D Fourier expansion (FOMFE) and its application to singular-point detection and fingerprint indexing," *IEEE Transactions on Pattern Analysis and Machine Intelligence,* vol. 29, no. 4, pp. 573-85, April 2007

[102] Fan Lingling, Wang Shuguang, Wang Hongfa, and Guo Tiande, "Singular points detection based on zero-pole model in fingerprint images," *IEEE Transactions on Pattern Analysis and Machine Intelligence,* vol. 30, no. 6, pp. 929-940, June 2008.

[103] Gao Hengzhen, Mandal Mrinal K., Guo Gencheng, and Wan Jianwei, "Singular point detection using Discrete Hodge Helmholtz Decomposition in fingerprint images," *IEEE International Conference on Acoustics, Speech and Signal Processing (ICASSP) Proceedings,* pp. 1094-1097, 2010.

[104] S. Ram, H. Bischof, and J. Birchbauer, "Modeling fingerprint ridge orientation using Legendre polynomials," *Pattern Recognition,* vol. 43, no. 1, pp. 342-57, Jan. 2010.

[105] S. Fei, Sun Peng, Wang Bo-Tao, and Cai An-Ni, "Fingerprint singular points extraction based on the properties of orientation model," *Journal of China Universities of Posts and Telecommunications,* vol. 18, no. 1, pp. 98-104, Feb. 2011.

[106] A. M. Bazen, and S. H. Gerez, "Systematic methods for the computation of the directional fields and singular points of fingerprints" *IEEE Transactions on Pattern Analysis and Machine Intelligence,* vol. 24, no. 7, pp. 905−919, 2002.

[107] M. H. Liu, X. D. Jiang, and A. C. Kot, "Fingerprint reference-point detection". *EURASIP Journal on Applied Signal Processing,* no. 4, pp. 498−509, 2005.

[108] Mohamed N. Ahmed, Sameh M. Yamany, Nevin Mohamed, Aly A. Farag and Thomas Moriarty, "A modified fuzzy c-means algorithm for bias field estimation

and segmentation of MRI data," *IEEE Transactions on Medical Imaging,* vol. 21, no. 3, March 2002.

[109] M.A.Wahby Shalaby and M.Omair Ahmad, "A multilevel structural fingerprint recognition based on the EHA-FCM partitioning scheme," To be submitted for publication in a special issue of *Information Sciences* "New Sensing and Processing Technologies for Hand-based Biometrics Authentication".